PhD thesis

Characterization of the alpha7 nicotinic receptor and Lynx proteins and their relation to Alzheimer's disease - a translational neurobiology study

Majbrit Myrup Jensen, M.Sc.

Neurobiology Research Unit
Copenhagen University Hospital, Rigshospitalet

Faculty of Health Sciences
University of Copenhagen

Title: Characterization of the alpha7 nicotinic receptor and Lynx proteins and their relation to Alzheimer's disease - a translational neurobiology study

Author: Majbrit Myrup Jensen, M.Sc. Human Biology

Department: Neurobiology Research Unit, Neuroscience Center, Copenhagen University Hospital, Rigshospitalet, Denmark
Institution: Faculty of Health and Medical Sciences, University of Copenhagen, Denmark
Date of submission: January 4th, 2015
Date of defence: March 26th, 2015

Supervisors:
Professor Jens D. Mikkelsen, Neurobiology Research Unit, Neuroscience Center, Copenhagen University Hospital, Rigshospitalet, Denmark

Associate Professor Morten S. Thomsen, Systems Pharmacology, Department of Drug Design and Pharmacology, University of Copenhagen, Denmark

Evaluating Committee:
Associate Professor Anders A. Jensen (Chairperson), Medicinal Chemistry Research, Department of Drug Design and Pharmacology, University of Copenhagen, Denmark

Professor Poul Henning Jensen, Department of Biomedicine, University of Aarhus, Denmark

Professor Neil S. Millar, Department of Neuroscience, Physiology and Pharmacology, University College London, UK

This thesis has been submitted to the Graduate School at the Faculty of Health and Medical Sciences, University of Copenhagen.

Contents

Preface

The thesis is the result of a three year PhD programme at the Faculty of Health and Medical Sciences, University of Copenhagen. The work was primarily conducted at Neurobiology Research Unit, Copenhagen University Hospital, Rigshospitalet.

The thesis is based on the following original manuscripts, which in the text are referred to by their Roman numerals:

I. **Jensen MM**, Dyrvig M, Bertelsen B, Tümer Z, Christiansen SH, Pinborg LH, Thomsen MS, Lichota J, Mikkelsen JD. Expression and binding profiles of the α7 nicotinic acetylcholine receptor in human cortical tissue. *Manuscript in preparation for Mol. Pharmacol*.

II. Thomsen MS, Cinar B, **Jensen MM**, Lyukmanova EN, Shulepko MA, Tsetlin V, Klein AB, Mikkelsen JD (2014). Expression of the Ly-6 family proteins Lynx1 and Ly6H in the rat brain is compartmentalized, cell-type specific, and developmentally regulated. *Brain Struct Funct, 219(6):1923-34.*

III. **Jensen MM**, Arvaniti M, Mikkelsen JD, Michalski D, Pinborg LH, Härtig W, Thomsen MS (2015). Prostate stem cell antigen interacts with nicotinic acetylcholine receptors and is affected in Alzheimer's disease. *Neurobiol Aging, in press*.

The following original manuscripts are related to the work described in the thesis but not included in the thesis, although data from the manuscripts are presented in the section *Results and Discussion*. They are referred to by their Roman numerals:

IV. Thomsen MS, **Jensen MM**, Arvaniti M, Wang H, Klein AB, Thiriet N, Pinborg LH, Muldoon PP, Wienecke J, Damaj MI, Gondré-Lewis MC, Mikkelsen JD. Functional interaction between Lypd6 and nicotinic acetylcholine receptors. *Manuscript*.

V. Thomsen MS, Arvaniti M, **Jensen MM**, Lyukmanova EN, Shulepko MA, Dolgikh DA, Pinborg LH, Härtig W, Tsetlin V, Mikkelsen JD. Lynx1 and Aβ1-42 bind competitively to multiple nAChR subtypes in the brain. *Manuscript*.

Acknowledgments

First of all, I would like to thank my principal supervisor Jens D. Mikkelsen for scientific guidance and encouragement during this three-year period. Also a special thank to my co-supervisor Morten S. Thomsen for excellent advice, and inspiration, and for always taking the time, when I came by with a long list of questions.

I would also like to thank Jacek Lichota and Mads Dyrvig Johannesen, Aalborg University, for their great engagement and collaboration on the project studying human α7 nAChR, where Mads performed the DNA methylation analysis. Also thanks to Bettina Laursen and Jesper F. Bastlund from H. Lundbeck A/S for letting me perform experiments on the brain tissue from their transgenic AD mouse model. In addition, thank you to Professor Wolfgang Härtig for warmly welcoming me in his lab, collaboration on the manuscript, and for giving me a full guided tour around Leipzig.

A special thank to all my colleagues at Neurobiology Research Unit for creating a professional yet warm and pleasant work environment. Also thanks to Maria Arvaniti for fruitful discussions on Lynx proteins, to Hans Jørgen Jensen, Louise Nielsen, and Maria Nørnberg for skilled technical assistance, and to Dorthe Givard and Birgit Tang for administrative support.

The project was funded by the Danish Strategic Research Council (COGNITO) and the Lundbeck Foundation.

Finally, I would like to thank my family and friends for all your encouragement and support. But the biggest thanks of all to you Nikolai - you are the world's greatest to me.

Majbrit Myrup Jensen
Copenhagen, January 2015

Summary

Several disorders of the central nervous system such as schizophrenia and Alzheimer's disease (AD) are characterized by cognitive impairments, which are not sufficiently treated with the current therapies. It is well-known that nicotine has pro-cognitive effects and thus the interest for the nicotinic acetylcholine receptors (nAChRs) as possible drug targets for diseases with cognitive deficits has been immense. Several proteins and peptides have been demonstrated to interact with the nAChRs. One of the most interesting groups of proteins is the Ly-6/neurotoxins (Lynx) protein family from which members have recently been demonstrated to regulate the function of the nAChR with an important impact on cognition and synaptic plasticity.

The aims of the PhD thesis were 1) To investigate the α7 nAChR in human cortical tissue with respect to mRNA expression and binding properties when displacing with a selective α7 nAChR agonist, 2) To study α7 nAChR binding in a transgenic mouse model of AD with and without partial basal forebrain cholinergic degeneration, and 3) To characterize Lynx proteins in rodent and human brain tissue as well as in pathological tissue from AD patients and in transgenic animal models of AD.

We found that the mRNA levels of the gene encoding the α7 nAChR, *CHRNA7*, is 3.4 times more expressed in human cortical tissue than the partial duplication of the *CHRNA7* gene (*CHRFAM7A*). The latter has been demonstrated to be unique to humans, and its gene product suggested to be a negative modulator of the α7 nAChR function. We also demonstrated that the α7 nAChR agonist encenicline (EVP-6124), currently in clinical phase III trials, displaces the binding of the selective α7 nAChR antagonist [^{125}I]-α-bungarotoxin in human cortex. We found that displacement with encenicline resulted in different IC_{50} displacement profiles in the human individuals, suggesting that the efficacy of the compound may differ between the individuals.

Degeneration of basal forebrain cholinergic neurons is a neuropathological hallmark of AD besides β-amyloid (Aβ) deposition and hyperphosphorylated tau proteins. In a transgenic mouse model of AD, Tg2576, harbouring both excessive Aβ deposition and cholinergic degeneration induced by the immunotoxin mu p-75 saporin, we found reduced [^{125}I]-α-bungarotoxin binding in temporal cortex and hippocampus, which suggests that the combination of Aβ overload and cholinergic degeneration can alter α7 nAChR levels.

We further found that the Lynx proteins Ly6H, Lynx1, and Lypd6 were localized in synaptic compartments and that short-term nicotine exposure did not alter the protein levels of these proteins

in young and adult rats, indicating that Lynx proteins have a synaptic function and that they are not regulated by nicotine. Another Lynx protein, prostate stem cell antigen (PSCA), was found to form stable complex with the α4 nAChR subunit, but not the α7 nAChR subunit. Interestingly, we observed an up-regulation of PSCA protein in the frontal cortex of patients suffering from AD and in a transgenic mouse model displaying both Aβ and tau pathology. This animal model also showed decreased Lynx1 levels in frontal cortex, indicating that Lynx proteins may be involved in AD pathology.

Collectively, the results of this work elucidate important aspects of α7 nAChR regulation in human tissue and in an AD animal model. In addition, the work contributes to new understanding of Lynx proteins in human and animal brain tissue in both healthy and diseased states as well as their interaction with nAChRs.

Summary in Danish

Adskillige sygdomme i centralnervesystemet, såsom skizofreni og Alzheimers sygdom (AD), er kendetegnet ved kognitive dysfunktioner, som ikke er tilstrækkeligt behandlet med de nuværende behandlingsformer. Det er velkendt, at nikotin har prokognitive effekter og derfor har der været stor interesse for nikotinreceptorer (nAChRs) som mulige *drug-targets* for nye lægemidler i behandlingen af sygdomme med kognitive forstyrrelser. Adskillige proteiner og peptider har vist sig at interagere med nAChRs. En af de mest interessante proteinfamilier er Ly-6/neurotoxin (Lynx) proteinfamilien, hvor visse medlemmer for nylig er blevet påvist at regulere funktionen af nAChR med en betydelig påvirkning af kognition og synaptisk plasticitet.

Formålet med denne ph.d-afhandling er, at 1) at undersøge α7 nAChR i humant cortexvæv med henblik på at måle mRNA ekspression og bindingsegenskaber, når der displaceres med en selektiv α7 nAChR agonist, 2) at studere α7 nAChR binding i en transgen musemodel for AD med og uden cholinerg degeneration i den basale forhjerne, og 3) at karakterisere Lynx proteiner i hjernevæv fra mus, rotter og mennesker såvel som i patologisk væv fra patienter med AD og i transgene dyremodeller for AD.

Vi fandt, at mRNA-niveauet af *CHRNA7* genet, der koder for α7 nAChR, er 3,4 gange mere udtrykt i humant cortexvæv end den partielle duplikering af *CHRNA7* genet (*CHRFAM7A*). Sidstnævnte duplikation har vist sig kun at være udtrykt i mennesker, og dets genprodukt foreslåes at fungere som en modulator af funktionen af α7 nAChR. Vi påviste også, at α7 nAChR agonisten encenicline (EVP-6124), som i øjeblikket er i klinisk fase III studier, displacerer bindingen af den selektive α7 nAChR antagonist [^{125}I]-α-bungarotoxin i humant cortexvæv. Vi fandt, at displaceringen med encenicline resulterede i forskelige IC_{50} displaceringskurver i de forskellige individer, hvilket tyder på, at effektiviteten af encenicline kan variere mellem individer.

Degenerering af cholinerge neuroner i den basale forhjerne er en af de neuropatologiske kendetegn for AD foruden β-amyloid (Aβ) deponering og hyperfosforylerede tau-proteiner. I en transgen musemodel for AD, Tg2576, med både overekspression af Aβ og cholinerg degeneration induceret af immunotoxinet mu p-75 saporin, fandt vi reduceret [^{125}I]-α-bungarotoxin binding i temporal cortex og hippocampus, hvilket tyder på, at kombinationen af Aβ overekspression og cholinerg degeneration kan ændre α7 nAChR niveauer.

Vi fandt endvidere, at Lynx proteinerne Ly6H, Lynx1 og Lypd6 var lokaliseret i synaptiske segmenter, og at eksponering med nikotin over kort tid ikke ændrede deres proteinniveauer, hvilket

viser, at Lynx proteiner kunne have en synaptisk funktion, og at de ikke reguleres af nikotin. Et andet Lynx protein, prostate stem cell antigen (PSCA), blev vist at danne et stabilt kompleks med α4 nAChR-enheden, men ikke α7 nAChR-enheden. Vi observerede en opregulering af PSCA proteinet i frontal cortex hos patienter med AD og i en transgen musemodel med både Aβ- og tau-patologi. Denne dyremodel viste også at have reduceret Lynx1 niveauer i frontal cortex, hvilket indikerer, at Lynx-proteiner kan være involveret i AD patologi.

Samlet set understreger resultaterne i dette arbejde vigtige aspekter af α7 nAChR regulering i humant væv og i en AD dyremodel. Derudover bidrager dette arbejde til ny viden angående Lynx proteiner udtrykt i humant såvel som dyrehjernevæv ved både raske og syge tilstande samt deres interaktion med nAChRs.

Abbreviations

5-HT	5-hydroxytryptamine
Aβ	β-amyloid
α-Bgt	α-bungarotoxin
ACh	Acetylcholine
AD	Alzheimer's disease
ADAS-Cog	Assessment Scale-Cognitive Subscale
APP	Amyloid precursor protein
BDNF	Brain-derived neurotrophic factor
cDNA	Complementary deoxyribonucleic acid
ChAT	Choline acetyltransferase
C_T	Cycle threshold
ER	Endoplasmatic reticulum
ERK	Extracellular-signal-regulated kinase
FC	Frontal cortex
GABA	Gamma-aminobutyric acid
GPI	Glycosylphosphatidylinositol
hAPPSwe	Swedish double-mutation of human amyloid precursor protein
HIP	Hippocampus
kg	Kilogram
KO	Knock-out
Lynx	Ly-6/neurotoxin
MAPK	Mitogen-activated protein kinase
mg	Milligram
mM	Millimolar
MLA	Methyllycaconitine
mRNA	Messenger ribonucleic acid
n	Number of separate samples
nAChR	Nicotinic acetylcholine receptor
nM	Nanomolar
NMDA	N-methyl-D-aspartate
NSB	Non-specific binding
PET	Positron emission tomography
PS1	Presenilin 1
PSCA	Prostate stem cell antigen
ROI	Region of interest
RT-qPCR	Reverse-transcription quantitative polymerase chain reaction
SB	Specific binding
SCZ	Schizophrenia
SEM	Standard error of mean
SLURP	Secreted mammalian Ly-6/uPAR-related protein
TB	Total binding
TBS	Tris-buffered saline
TE	Tissue equivalent
WT	Wild-type

Introduction

"*To what extent can we stave off Alzheimer's disease?*" and "*What causes schizophrenia*?" were among the top hundred scientific questions almost ten years ago (Science, 2005). Today, the questions are still unanswered, even though the fields of research have been extensively studied. With estimated ~50 millions suffering from these diseases worldwide, there are great demands to solve the mechanisms behind these devastating diseases, where the medical treatments are currently symptomatic. Even though Alzheimer's disease (AD) and schizophrenia (SCZ) are significantly different in terms of etiology, neuropathology and symptoms at onset, they are both characterized by cognitive impairment. Since nicotine was demonstrated to have pro-cognitive effects, nicotinic acetylcholine receptors (nAChRs) have been promising drug targets in the treatment of the cognitive deficits in AD and SCZ. Most research in drug development so far has focused on a direct activation of nAChRs; however, members of the Ly-6/neurotoxin (Lynx) protein family have been shown to modulate nAChR function and be involved in cognition and synaptic plasticity. These proteins could thus be a novel target in the current research.

Nicotinic receptors, especially the α7 nAChR, have been the focus of research in the scientific work of Jens D. Mikkelsen and Morten S. Thomsen for almost a decade with over 20 peer-reviewed publications. The main findings have been α7 nAChR-dependent activation of rat brain regions involved in working memory and attention e.g., prefrontal cortex (Kristensen et al., 2007; Thomsen et al., 2010c; Thomsen et al., 2008), and that activation of α7 nAChR reversed behavioral deficits and prevented molecular changes in a rodent SCZ model, supporting the potential of α7 nAChR in treatment of SCZ (Thomsen et al., 2009; Thomsen et al., 2010a). Moreover, when investigating the function of α7 nAChR activation in rodents, an α7 nAChR agonist was shown to increase the level of α7 nAChRs both *in vitro* (Thomsen and Mikkelsen, 2012b) and *in vivo* (Christensen et al., 2010), and repeated administration of another α7 nAChR agonist induced memory enhancing effects in rats (Thomsen et al., 2011a). Studies of the α7 nAChR were primarily carried out in animals as most studies within the research field, however, one study showed up-regulation of α7 nAChR in postmortem hippocampus of patients with bipolar disorder (Thomsen et al., 2011b). Although the nAChRs have been extensively studied for decades, several questions are still unanswered. Particularly, due to lack of effects with several nAChR compounds in clinical trials for AD and SCZ, which showed cognitive benefits in preclinical studies, further investigations of the regulation of nAChRs in human tissue are needed and especially how endogenous modulators such as the Lynx proteins may affect the function of the nAChRs in both healthy and diseased states.

This chapter contains a short introduction to the field of research including a description of nAChRs and their potential involvement in diseases of the brain, particularly AD and SCZ, as well as the Lynx proteins and their relation to nAChRs.

Nicotinic acetylcholine receptors

Neuronal nAChRs are widely distributed in the nervous system as well as in non-neuronal tissue such as muscle, skin, and lung cells (Gotti and Clementi, 2004). The nAChR belong to the Cys-loop superfamily of ligand-gated ion channels, which are pentameric receptors that also include $GABA_A$, glycine, and 5-HT_3 receptors, and they are selective for the cations Na^+, K^+, and Ca^{2+} (Jensen et al., 2005). To date, 11 nAChR subunits (α2-7, α9-10, and β2-4) have been cloned from neuronal tissue. Each nAChR subunit consists of a large N-terminal extracellular domain, four transmembrane domains with a cytoplasmic loop between the third and the fourth, and a short extracellular C-terminal (Albuquerque et al., 2009). The subunits can either form heteromeric receptors or homomeric receptors (see Figure 1). However, only the α7 and α9 subunits are able to form homopentamers (Gotti and Clementi, 2004; Jensen et al., 2005).

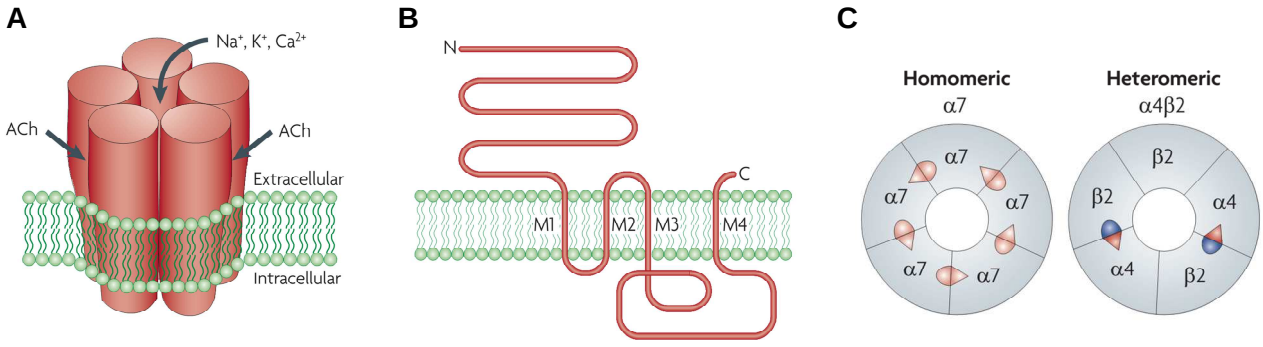

Figure 1. Structure of nicotinic acetylcholine receptors. (A) Schematic view of nicotinic acetylcholine receptors (nAChRs) consisting of five transmembrane subunits with the extracellular acetylcholine (ACh) binding sites. **(B)** Each subunit consists of an extracellular N-terminal domain, four transmembrane domains (M1-4), a cytoplamic loop, and a short extracellular C terminal. **(C)** The homomeric α7 nAChR with five orthosteric binding sites and the heteromeric $(α4)_2(β2)_3$ with two orthosteric binding sites. Modified from (Changeux, 2010).

The nAChRs are activated by the endogenous neurotransmitter ACh or exogenous ligands such as nicotine. The orthosteric binding sites are in the interface between two subunits i.e., between α- and β-subunits in the heteromeric receptor complex and between two α-subunits in the homomeric receptor (see Figure 1C). The α7 and α4β2 nAChRs are the most abundant in the brain, where the homomeric α7 nAChR displays lower affinity to ACh and nicotine compared to the α4β2 nAChR (Dani and Bertrand, 2007; Gotti et al., 2006b). Although α7 nAChR subunits are mostly described to assemble as homopentamers, there is evidence that it can form functional heteromeric receptor

assemblies with β-subunits, which have significantly different pharmacological properties compared to the homomeric receptor when expressed heterologously in *Xenopus* oocytes (Criado et al., 2012; Khiroug et al., 2002; Liu et al., 2009; Murray et al., 2012; Palma et al., 1999; Zwart et al., 2014). Recent studies demonstrate that α7β2 heteromers are present in the mammalian brain, where α7 and β2 subunits were found to form stable complexes using co-immunoprecipitation in distinct rodent brain regions (Liu et al., 2012; Liu et al., 2009) and affinity purification in mouse and human forebrain tissue extracts (Moretti et al., 2014).

The α7 nAChR differs from other nAChRs in various ways besides the formation of homomers and low-affinity binding. Upon activation, the α7 nAChR opens and activates extremely fast followed by a rapid closing within <100 milliseconds due to receptor desensitization (Castro and Albuquerque, 1993). Unlike other nAChRs, the α7 nAChR also has a high permeability to Ca^{2+}, whereby activation of α7 nAChRs alone can trigger several Ca^{2+}-dependent signaling pathways including activation of the mitogen-activated protein kinase (MAPK) pathway and induction of gene transcription (Albuquerque et al., 2009). Furthermore, the α7 nAChR is the only nAChR activated by choline, the precursor/metabolite of acetylcholine (ACh), suggesting that choline can function as an endogenous neurotransmitter (Alkondon et al., 1997).

The gene encoding the human α7 nAChR subunit, *CHRNA7*, located at chromosome 15q13.3 contains 10 exons, differing from the other nAChR subunits, which are constituted of six exons (Albuquerque et al., 2009). The N-terminal is encoded by exons 1-6, the first three transmembrane domains are encoded by exons 7-8, and exons 9-10 correspond to the intracellular cytoplasmic loop, the fourth transmembrane domain, and the C-terminal. The *CHRNA7* gene is partially duplicated (see Figure 2), where exons 5-10 of *CHRNA7* along with additional DNA (~200 Kbp) are duplicated upstream of the *CHRNA7* and interrupting a second partial duplication of the *ULK4* gene (Gault et al., 1998). The partially duplicated, chimeric gene, *CHRFAM7A*, maps centromeric and is oriented opposite to the full-length *CHRNA7* by 1.6 Mb and contains, besides three exons of the *ULK4* gene, an exon of unknown origin (Gault et al., 1998; Riley et al., 2002). Interestingly, the duplication seems to be a recent evolutionary event, since it is not present in closely related primates (Locke et al., 2003).

Individuals can have copy variations with *CHRFAM7A* gene with one, two, or three copies reported, and in a few individuals the gene is lacking completely (Flomen et al., 2006; Sinkus et al., 2009). A two base pair deletion polymorphism has been found in exon 6 of the *CHRFAM7A* gene,

which causes a frame-shift and is associated with a gene inversion resulting in the same orientation as the full-length *CHRNA7* gene (Flomen et al., 2008; Gault et al., 2003).

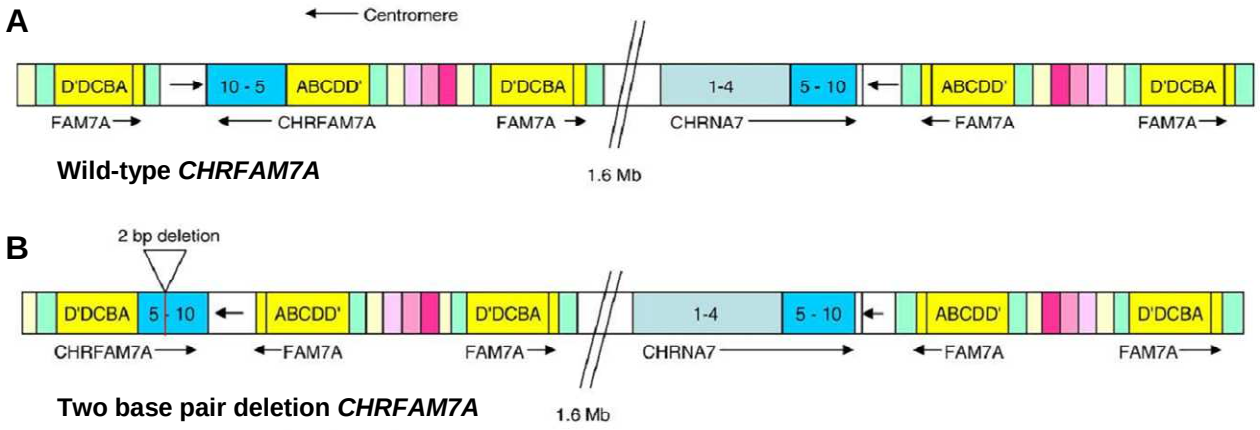

Figure 2. Genomic map of *CHRNA7* and its partial duplication *CHRFAM7A* on chromosome 15q13.3. (A) Wild-type allele of *CHRFAM7A*. The sequence *FAM7A* is duplicated from the gene *ULK4* on chromosome 3. (B) The two base pair deletion polymorphism results in inversion of *CHRFAM7A*. Modified from (Sinkus et al., 2009).

The gene product of *CHRFAM7A*, dupα7, is lacking a large part of the N terminal of the α7 nAChR subunit containing the signal peptide and part of the binding domain (Gault et al., 1998). With the frame shift in the two base pair deletion variation, this results in an even smaller gene product, dupΔα7, lacking nearly the entire ligand binding domain (Araud et al., 2011). Currently, it is not known, whether the gene products are translated and what functional role they might have. Both the dupα7 and dupΔα7 have so far only been studied in heterologous expression systems (Araud et al., 2011; de Lucas-Cerrillo et al., 2011; Wang et al., 2014). When co-expressed with α7 nAChR subunit in *Xenopus* oocytes, dupα7 and dupΔα7 was found to reduce the amplitude of ACh-evoked currents, suggesting they have dominant negative effects on the α7 nAChR function (Araud et al., 2011; de Lucas-Cerrillo et al., 2011). In contrast, this was not found in a recent study in transfected mammalian cells, where the α7 nAChR subunit was demonstrated to co-assemble with dupα7 and dupΔα7 (Wang et al., 2014). The presence of dupα7 or dupΔα7 with the α7 nAChR subunit was instead shown to alter the sensitivity to the α7 nAChR agonists choline and varenicline, respectively (Wang et al., 2014).

Cognition and nicotinic receptors

For decades it has been known that the cholinergic system is involved in cognitive processes such as memory and attention, since the first studies revealed that lesions of cholinergic neurons in the

basal forebrain of rats led to memory deficits (Bartus et al., 1985). Since then, several studies, both in animals and humans, have demonstrated that nicotine has pro-cognitive effects (Levin et al., 2006; Newhouse et al., 2004; Sacco et al., 2004). The cholinergic neurons of the basal forebrain project to the prefrontal cortex and hippocampus, which are highly associated with cognitive functions such as working memory, attention, and executive function (Dalley et al., 2004; Sweatt, 2004).

The nAChRs, especially the α7 and α4β2 nAChR, have been extensively studied in the frontal cortex and hippocampus for their role in cognitive performance (Bloem et al., 2014; Levin, 2013; Wallace and Bertrand, 2013). Activation of the α7 nAChR has been shown to improve cognitive performance such as short-term, long-term, and working memory in animal studies (reviewed in (Thomsen et al., 2010b)). The α7 nAChR partial agonist A-582941 improved short-term memory in the rat social recognition test, memory retention in mice by the inhibitory avoidance test, and working memory in non-human primates (Bitner et al., 2007). Administration of other partial agonists of the α7 nAChR, SSR180711 and ABBF, showed improvements in long-term memory in rodents by novel object recognition test, which was abolished by co-administration of the selective α7-nAChR antagonist methyllycaconitine (MLA) suggesting that the effect was dependent on α7 nAChR activation and not the desensitization of the receptors (Boess et al., 2007; Pichat et al., 2007). In addition, the effect of SSR180711 was present only in wild-type (WT) mice but not in α7 nAChR knock-out (KO) mice (Pichat et al., 2007), indicating that the effect was specific to α7 nAChR activation. Remarkably, repeated administration of the α7 nAChR agonist TC-5619 enhanced long-term memory, while acute doses had no effect (Hauser et al., 2009). The same was observed with short-term memory by repeated administration of A-582941 in a social discrimination test (Thomsen et al., 2011a), suggesting that repeated administration produce sustained memory-enhancing effects.

In contrast to animal studies, nicotine and α7 nAChR ligands improve attentional parameters in human studies rather than short- and long-term memory (Levin et al., 2006; Newhouse et al., 2004; Sacco et al., 2004). The α7 nAChR partial agonist GTS-121 was found to improve performance regarding attentional function and working memory in healthy volunteers (Kitagawa et al., 2003). The discrepancy between the effects of α7 nAChR ligands on cognitive parameters in animal and human studies might be due to different testing methods and/or a lower expression of α7 nAChR in prefrontal cortex and hippocampus in humans compared to rodents (Thomsen et al., 2010b). In relation to drug development, the differences in cognitive effects are of high relevance

since animal studies are part of the preclinical studies to verify whether a specific compound can proceed to clinical trials.

Agonists of the α4β2 nAChR have also shown cognitive effects, particularly related to attentional performance in animal and human studies (Sarter et al., 2009). In the prefrontal cortex, a study suggested that α4β2 and α7 nAChRs have different roles in attentional processes, where activation of the α4β2 nAChR in the prefrontal cortex increased release of the neurotransmitter glutamate resulting in enhanced cholinergic tone, while activation of the α7 nAChR was involved in controlling the duration of ACh release (Parikh et al., 2010). Furthermore, the β2 nAChR subunit was shown to be essential for attentional performance in mice, where re-expression of β2 subunits by a lentiviral vector in the prefrontal cortex of β2 KO mice restored their attentional deficits (Guillem et al., 2011). Activation of α4β2 and α7 nAChRs has also improved working memory in rats (Levin et al., 2002) and in non-human primates (Buccafusco et al., 2007).

Despite that many studies in the last decades have found that activation of α7 and α4β2 nAChR led to improvements in cognitive function, recent studies have found that antagonists of the nAChRs are also able to improve cognitive function (reviewed in (Levin, 2013)), which questions whether the effects of nicotinic agonists are due to stimulation or desensitization of the receptor. Further research are needed to determine exactly how the nicotinic compounds cause pro-cognitive effects, which will be important knowledge in the therapeutic treatment of diseases with cognitive impairments, such as AD and SCZ.

Alzheimer's disease and nicotinic receptors

Alzheimer's disease (AD) is a devastating neurodegenerative disorder and the most common form of dementia. Even though it was first described by Alois Alzheimer over 100 years ago (Alzheimer, 1907), there are still an ongoing debate regarding the role of neuropathological hallmarks and their contribution to the progression of the disease.

AD is characterized by the formation of plaques containing aggregated β-amyloid (Aβ) and neurofibrillary tangles of hyperphosphorylated tau protein (Querfurth and LaFerla, 2010). Amyloid plaques consist of the peptide $A\beta_{1-42}$, which is produced by abnormal cleavage of the amyloid precursor protein (APP). The plaque formation is suggested to be caused by an imbalance between the production and clearance of $A\beta_{1-42}$ and was early on thought to be neurotoxic and the initiating factor of AD in the so-called amyloid hypothesis (Hardy and Selkoe, 2002). However, in more recent studies it became evident that soluble oligomers of particularly the $A\beta_{1-42}$ form, and not

insoluble plaques, were the most neurotoxic form of Aβ and that they correlated with the cognitive decline (Walsh and Selkoe, 2007) and synaptic loss in AD patients (Shankar et al., 2008).

Several findings have demonstrated interactions between Aβ levels and nAChR, which suggest that these interactions serve a role in both non-diseased and diseased conditions in relation to synaptic plasticity and Aβ toxicity in the progression of AD, respectively (Parri and Dineley, 2010). Interestingly, soluble $A\beta_{1-42}$ was shown to bind and activate α7 nAChR with a high affinity in the low picomolar range, whereas the affinity of $A\beta_{1-42}$ binding to α4β2 nAChR was 5,000 times lower (Dougherty et al., 2003; Wang et al., 2000).

Although $A\beta_{1-42}$ has been shown to modulate the function of nAChRs in various studies, the exact effects of these interactions are inconclusive, since both inhibition and activation of nAChR function have been reported (Dougherty et al., 2003; Lamb et al., 2005; Pettit et al., 2001; Wu et al., 2004). However, reviews of recent studies agree that $A\beta_{1-42}$ is activating nAChRs at low (picomolar) concentrations and short incubation while inhibiting at high (nanomolar) concentrations and longer incubation time (Lombardo and Maskos, 2014; Parihar and Brewer, 2010). Interestingly, α7β2 nAChR heteromers were highly sensitive to blockade by $A\beta_{1-42}$ in heterologous expression systems and hippocampal interneurons, when compared to the homomeric α7 nAChR, suggesting that α7β2 nAChRs may play a unique role in the neuropathology of AD (Liu et al., 2012; Liu et al., 2009).

It has been demonstrated that α7 nAChR agonists may modulate $A\beta_{1-42}$ accumulation. Reducing the interaction between $A\beta_{1-42}$ and α7 nAChR with a partial α7 nAChR agonist was shown to enhance the clearance of $A\beta_{1-42}$ in mice that had been administered intracerebroventricular infusion of $A\beta_{1-42}$ (Wang et al., 2010). It has further been demonstrated that α7 and α4 nAChR mRNA are found in neurons that accumulate Aβ but not hyperphosphorylated tau protein (Wevers et al., 1999). Intracellular $A\beta_{1-42}$ also correlated with high expression of α7 nAChR in postmortem AD brains, and α7 nAChR was reported to be involved in the internalization of $A\beta_{1-42}$ using transfected neuroblastoma cells (Nagele et al., 2002). However, crossing APP-overexpressing mice with mice deficient of the α7 nAChR resulted in contradicting results (Dziewczapolski et al., 2009; Hernandez et al., 2010). These APP-α7KO mice showed in one of the studies no memory deficits and rescued the levels of synaptic markers with no changes in Aβ pathology, suggesting that the absence of the α7 nAChR was preventing the behavioral deficits and neuropathology (Dziewczapolski et al., 2009). In contrast, the other study with APP-α7KO mice, although with a different APP mutation profile, observed that the cognitive deficits worsen, when α7 nAChR was

absent, and that the levels of $A\beta_{1-42}$ and Aβ plaques were lowered when compared to the APP mice, indicating a protective role of α7 nAChR (Hernandez et al., 2010). Thus, it seems that α7 nAChR might have both protective and non-protective effects.

Another field of AD research is focusing on the cholinergic neurotransmitter system formulating a cholinergic hypothesis of AD, suggesting that the cognitive impairment in AD patients is associated to cholinergic hypofunction (Bartus et al., 1982; Contestabile, 2011). Several studies have shown that an early event in the pathology of AD is cholinergic degeneration and dysfunction in the basal forebrain, which correlate with the cognitive deficits in AD (Auld et al., 2002; Kim et al., 2013). The cholinergic nuclei in the basal forebrain, that project to the neocortex and hippocampus, are involved in attention and memory storage processes (Sarter and Bruno, 1997; Woolf, 1998). Thus, pharmacological blockade of the cholinergic system was demonstrated to have negative impacts on memory function in humans (Drachman and Leavitt, 1974) and rodents (Huang et al., 2011; Janas et al., 2005). Moreover, the activity of the enzyme involved in the synthesis of ACh, choline acetyltransferase (ChAT), is decreased in AD (Bierer et al., 1995). The current pharmacological therapies available to AD patients are largely acetylcholinesterase inhibitors which maintain cholinergic transmission by preventing the degradation of ACh. However, they have shown limited success in halting the progression of AD, and therefore new drug targets in the treatment of AD are needed (Buckingham et al., 2009).

Although loss of cholinergic neurons in the basal forebrain is well-recognized phenomenon in AD, it is still widely debated, whether the cholinergic degeneration is an early and initial stage of AD progression or it is merely a consequence of other pathophysiological hallmarks. Furthermore, it is questioned how and if the expression of different nAChR subtypes are altered in AD. Using *in vivo* techniques such as PET imaging, a study showed that reduced ^{11}C-nicotine binding in frontal and parietal cortices of patients with mild AD correlated with poorer cognitive performance in attention tests (Kadir et al., 2006), which was further confirmed in a recent study with the selective α4β2 nAChR PET tracer ^{18}F-2FA-85380 (Okada et al., 2013). Interestingly, in the latter study ^{18}F-2FA-85380 binding was shown to negatively correlate with Aβ deposition in the medial prefrontal cortex of AD patients, suggesting that interactions between Aβ and the α4β2 nAChR are affecting cognitive function in AD patients. *In vitro* receptor autoradiography using [^{3}H]-nicotine has also demonstrated reduced α4β2 nAChR binding in frontal cortex of AD patients, when compared to age-matched non-demented controls (Marutle et al., 2013) and cortical loss of α4β2 was shown by reduced [^{3}H]-epibatidine membrane binding in AD brains (Gotti et al., 2006a).

There have been reported rather inconsistent findings when investigating the α7 nAChR levels in AD patients, where both reduction and no change have been observed. Using [^{125}I]-α-bungarotoxin ([^{125}I]-α-Bgt), α7 nAChR binding was shown to be decreased in temporal cortex of AD patients, while there was no change in α7 nAChR binding in the frontal cortex (Davies and Feisullin, 1981; Marutle et al., 2013). However, the loss of α7 nAChR in temporal cortex was not replicated in a later study showing decreased α7 nAChR binding in hippocampus with no changes in the temporal cortex (Hellstrom-Lindahl et al., 1999). Similarly, the hippocampal reduction in α7 nAChR was not able to be replicated in another [^{125}I]-α-Bgt binding study (Court et al., 2001), which however reported a high variability in [^{125}I]-α-Bgt binding among the AD patients, which could cause the inconsistent findings and suggest that α7 nAChR may only be altered in a subgroup of AD patients. The loss of nAChRs in AD is shown not to be caused by alterations in mRNA expression (Buckingham et al., 2009; Hellstrom-Lindahl et al., 1999; Wevers et al., 1999).

Genetic studies have demonstrated that variations in genes encoding nAChR subunits may be associated to AD pathology. Thus, it was shown that single nucleotide polymorphisms in *CHRNA7* were associated to both AD itself and to the delusional symptoms in AD (Carson et al., 2008a; Carson et al., 2008b). Furthermore, the *CHRFAM7A* genotype without the two base pair deletion was significantly over-represented in AD and other dementias, suggesting that the presence of the *CHRFAM7A* with the two base pair deletion may protect against AD (Feher et al., 2009). Single nucleotide polymorphisms in the genes encoding the α4, *CHRNA4* (Dorszewska et al., 2005; Kawamata and Shimohama, 2002) and β2, *CHRNB2*, nAChR subunits (Cook et al., 2004; Laumet et al., 2010) have also shown associations with AD.

Compounds targeting both the α7 and α4β2 nAChRs have been developed in the treatment of cognitive deficits in AD. The therapeutic potential of α4β2 nAChR activation in AD has not been as well-studied as the α7 nAChR. Thus, a recent phase II study with the α4β2 nAChR agonist AZD3480 was considered to be inconclusive, since it was demonstrated to have no effects on the Assessment Scale-Cognitive Subscale (ADAS-Cog), although several secondary outcomes measures were improved (Frolich et al., 2011). More promising results have been obtained with the α7 nAChR agonists (reviewed in (Valles et al., 2014; Wallace and Porter, 2011)). Preclinical studies with the α7 nAChR agonist A-582941 showed that cognition was restored in an AD mouse model, 3×Tg-AD mice, with both Aβ and tau pathology, while the AD pathology was unaltered in these treated mice (Medeiros et al., 2014). In addition, the α7 nAChR partial agonist SSR-180711 rescued $A\beta_{1-42}$-induced impairments of long-term potentiation in rat hippocampal slices, while the

acetylcholinesterease inhibitor, donepezil, and the α4β2 nAChR agonist TC-1827 had no effects (Kroker et al., 2013). Several α7 nAChR agonists have reached advanced clinical. The α7 nAChR agonist TC-5619 showed promising results in treating cognitive impairments in preclinical and clinical phase II trials (Hauser et al., 2009; Lieberman et al., 2013). Currently, the most promising α7 nAChR compounds in the treatment of AD are encenicline (EVP-6124), which showed pro-cognitive effects in animals and is now in phase III trials for AD and SCZ (Preskorn, 2014; Prickaerts et al., 2012), and ABT-126 demonstrating improved ADAS-Cog scores similar to donepezil in a phase IIb study in patients with mild to moderate AD (Gault et al., 2013).

Degeneration of cholinergic neurons and decreased levels of nAChRs in AD combined with the interaction between nAChRs and Aβ as described above, suggest that nAChRs are implicated in cognitive function and may be involved in the pathophysiology of AD.

Schizophrenia and nicotinic receptors

Schizophrenia (SCZ) is a chronic psychiatric disorder affecting approximately 1% of the population worldwide. The onset of SCZ is typically in late adolescence or early adulthood and the symptoms are divided in three categories referred as positive (psychotic), negative, and cognitive symptoms. The positive symptoms include delusions, hallucinations, and bizarre behavior, while negative symptoms are characterized by apathy, blunted emotional responses, and social withdrawal. The cognitive symptoms comprise impairments in attention, learning and memory, executive function, and working memory (Mueser and McGurk, 2004). Although the current medical treatment of SCZ with antipsychotics has high efficacy in alleviating positive symptoms, they are poorly effective in reducing the negative symptoms and especially the cognitive impairments (Hill et al., 2010; Woodward et al., 2005). Currently, the cause of SCZ is unknown; however, genetic, early environmental, and social factors are suggested to contribute to the etiology of SCZ (Fox, 1990; Stefansson et al., 2008).

Combining the pro-cognitive effects of nicotine and the observation that the prevalence of smoking in patients with SCZ is very high compared to the general population, smoking has been suggested to be a form of self-medication to improve the cognitive impairments in SCZ (Kumari and Postma, 2005). Involvement of nAChR in SCZ was first suggested, when reduced expression of nAChRs in the hippocampus of SCZ patients was demonstrated using [^{125}I]-α-Bgt and [^{3}H]-cytisine binding to identify α7 nAChRs and high-affinity nAChRs such as α4β2, respectively (Freedman et al., 1995). The hippocampal α7 nAChR binding was decreased with ~50% in the study, which was not reproduced in a more recent study with a larger sample size (Thomsen et al., 2011b), indicating

that altered expression in hippocampus only occur in a subgroup of SCZ individuals. However, reduced [^{125}I]-α-Bgt binding was also found in cingulate cortex in postmortem brains of SCZ patients, while the level of α7 nAChRs was unaltered in orbitofrontal and temporal cortices (Marutle et al., 2001). Remarkably, the latter study showed contradicting results with [^{3}H]-cytisine binding, which was increased in cortical regions of SCZ subjects. Several studies of α4β2 nAChR expression in SCZ have since then demonstrated inconclusive findings, and given that nAChRs were not upregulated in SCZ patients in response to cigarette smoking as observed in control smokers, it has been suggested that possibly dysfunction of the high-affinity nAChRs is a more common feature of SCZ rather than altered expression levels (reviewed in (Adams and Stevens, 2007)).

Genetic alterations in the *CHRNA7* gene encoding α7 nAChR have been proposed to associate with attentional deficits in SCZ. Thus, the chromosomal location of *CHRNA7* (Freedman et al., 1997) and genetic polymorphisms in the promoter region of *CHRNA7* (Leonard et al., 2002) have been demonstrated to be linked to SCZ and the P50 sensory gating deficit, which is associated to attentional performance. Interestingly, several of the mutations in the promoter region decreased transcription in an *in vitro* reporter gene assay (Leonard et al., 2002). More recently, a specific single nucleotide polymorphism, rs3087454, in a regulatory region upstream of *CHRNA7* (Stephens et al., 2009) as well as large deletions of 15q13.3, the locus of both *CHRNA7* and *CHRFAM7A*, are shown to be associated with SCZ (International Schizophrenia Consortium, 2008; Stefansson et al., 2008). In many of the individuals the *CHRNA7* gene was deleted, while the *CHRFAM7A* gene remained. In addition, the two base pair deletion in exon 6 of *CHRFAM7A*, but not in *CHRNA7*, was significantly associated with both SCZ and P50 sensory gating deficit (Flomen et al., 2013; Gault et al., 2003; Sinkus et al., 2009). Combining the above results, that mutations in both the *CHRNA7* and *CHRFAM7A* are linked to SCZ, and the demonstrations that the gene products of *CHRFAM7A*, dupα7 and dupΔα7, could be dominant negative regulators of α7 nAChR function (Araud et al., 2011; de Lucas-Cerrillo et al., 2011), suggest that targeting the expression of *CHRFAM7A* and/or the function of α7 nAChR may be beneficial in the treatment of SCZ. So far only the α7 nAChR has been investigated as a drug target in SCZ research.

The genes encoding the α4 and β2 nAChR subunits, *CHRNA4* and *CHRNB2*, have not been as intensively studied in relation to SCZ as the α7 nAChR-associated genes. However, it was shown that *CHRNB2* was significantly linked to smoking in SCZ (Faraone et al., 2004), and that combination of three mutations in *CHRNA4* with one mutation in *CHRNB2* resulted in increased

susceptibility to SCZ, while the mutations in the two genes alone were not sufficient to be risk factors for SCZ (De Luca et al., 2006b).

Pharmacological animal models have been used to mimic the symptoms observed in SCZ. Mostly, NMDA antagonists such as phencyclidine and ketamine have been administrated in these animal models, since they produce psychosis-like behavior in healthy adults resembling what is observed in patients with SCZ, and in addition exacerbate positive and negative symptoms in SCZ patients (Malhotra et al., 1997; Malhotra et al., 1996; Mouri et al., 2007). Several agonists of the α7 nAChR improved cognitive impairments in these animal models such as deficits in short- and long-term memory, working memory, and attention. Furthermore, α7 nAChR agonists restored auditory gating deficits in impaired animals, which can be comparable to the sensory gating deficits in SCZ patients (reviewed in (Thomsen et al., 2010b)).

Drugs targeting both α7 and α4β2 nAChRs have been developed for the treatment of cognitive deficits in SCZ (Freedman et al., 2008; Olincy and Stevens, 2007; Ripoll et al., 2004). Although there have been mixed results with α4β2 nAChR agonists, α7 nAChR agonists have in several studies been demonstrated to improve attentional function in patients with SCZ. The α7 nAChR partial agonist GTS-121 was the first to show improvements in cognitive performance in non-smoking schizophrenic patients in proof of concept studies linking nAChRs to SCZ (Freedman et al., 2008; Olincy et al., 2006; Tregellas et al., 2011). In addition, a recent study demonstrated effects with the TC-5619 in executive function and Scale for Assessment of Negative Symptoms in patients with SCZ as well as positive effects in working memory in smokers (Lieberman et al., 2013). The antipsychotic and cognitive effects of TC-5619 had previously been validated in a preclinical study in rodents (Hauser et al., 2009). Interestingly, the α7 nAChR partial agonist, encenicline also showed improvements in cognitive impairments associated with SCZ in a clinical phase IIb study (Preskorn, 2014).

Lynx proteins

The Ly-6/neurotoxin (Lynx) proteins belong to the Ly-6/uPAR superfamily, which share a characteristic cysteine-rich motif determining a tertiary three-finger loop structure similar to snake venom toxins, such as the α7 nAChR antagonist α-Bgt, indicating evolutionary and structural homology (Bamezai, 2004; Tsetlin, 1999). The Lynx proteins have originally been used as differentiation markers for lymphocytes (Bamezai, 2004), but are widely expressed in the brain as well as in peripheral tissue, where members of the Lynx protein family present in the brain include Lynx1, Lynx2, Lypd6, Lypd6B, prostate stem cell antigen (PSCA), Ly6H, and PATE-M (reviewed

in (Miwa et al., 2012)). Primarily, the Lynx proteins are tethered to the lipid membrane via a glycosylphosphatidylinositol (GPI) anchor (see Figure 3), but some are expressed as soluble proteins and thereby can be secreted like the venom toxins (Adermann et al., 1999).

Several members of Lynx proteins have been demonstrated to modulate nAChR function (reviewed in (Miwa et al., 2011; Thomsen and Mikkelsen, 2012a). The first Lynx protein to be associated to nAChRs was the Lynx1 protein (Miwa et al., 1999), and both Lynx1 and Lynx2 have been shown to form stable complexes and negatively modulate α7 and α4β2 nAChRs using co-immunoprecipitation and electrophysiology, respectively (Fu et al., 2012; Ibanez-Tallon et al., 2002; Miwa et al., 2006; Tekinay et al., 2009). The results were all obtained using heterologous expression systems, and thus it has not been studied so far, whether the Lynx proteins are binding and modulating nAChRs in native brain tissue.

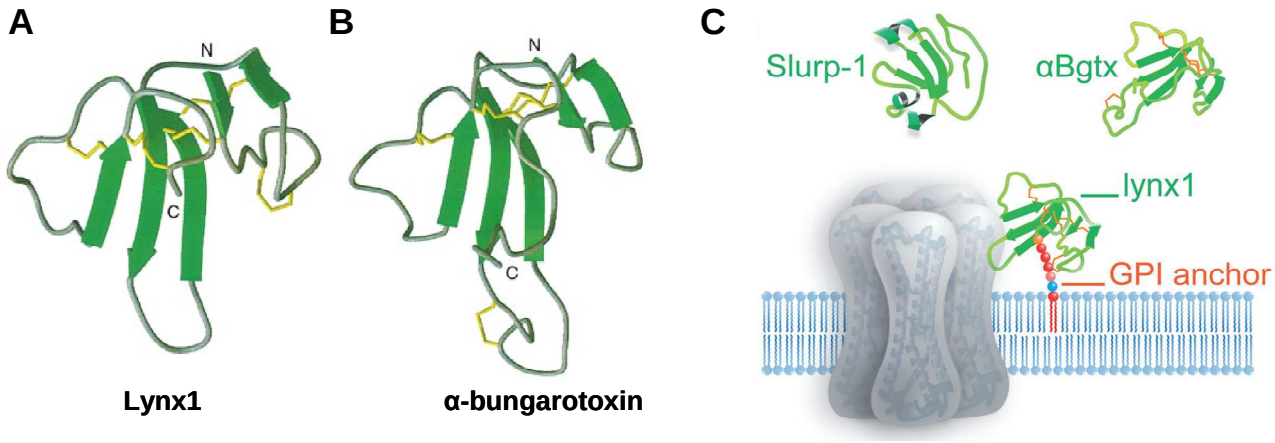

Figure 3. Schematic models of Lynx1 and α-bungarotoxin. Three-dimensional models of Lynx1 **(A)** and α-bungarotoxin (α-Bgt) **(B)**. β strands are shown as green arrows and disulfide bridges indicated with yellow. **(C)** Lynx1 is tethered to the cell membrane by the glycosylphosphatidylinositol (GPI)-anchor, whereas SLURP-1 is soluble. Modified from (Holford et al., 2009; Miwa et al., 1999).

Heterologous expression of α4β2 nAChR was less sensitive to ACh and nicotine in the presence of Lynx1 and Lynx2 i.e., the EC_{50} for activation was increased, and both Lynx proteins was shown to increase the rate and extend the recovery of desensitization (Ibanez-Tallon et al., 2002; Tekinay et al., 2009). The activity of Lynx1 on α7 nAChRs have been reported to be concentration-dependent, where a soluble form of 1 µM Lynx1 increased ACh-induced currents in oocytes expressing α7 nAChRs, whereas 10 µM was shown to inhibit the response to ACh in oocytes expressing either α7, α4β2, or α3β2 nAChRs (Lyukmanova et al., 2011). Soluble Lynx1 was also shown to enhance the amplitude of ACh-induced currents in *Xenopus* oocytes expressing either α7 or α4β2 nAChRs (Ibanez-Tallon et al., 2002; Miwa et al., 1999), suggesting that at low concentrations Lynx1 may

enhance the ACh-induced currents through α7 nAChRs. Soluble forms of Lynx proteins can be advantageous, when investigating the function of these proteins, however it has been shown that there were major differences in the effects of tethered Lynx1 and soluble Lynx1 in transgenic mouse models in a motor learning paradigm (Miwa and Walz, 2012), indicating that the association to the membrane is important for the function of Lynx1.

Although Lynx1 competed with ^{125}I-Bgt binding to ACh binding proteins and muscle-type *Torpedo californica* nAChRs with IC_{50} values of 10 and 30 µM, respectively, it was first proposed that Lynx1 binds outside the orthosteric binding site, since 30 µm Lynx1 was shown neither to inhibit ^{125}I-Bgt binding to α7 nAChR nor ^{3}H-epibatidine binding to α4β2 nAChR expressed in GH_4C_1 and SH-EP1 cells, respectively (Lyukmanova et al., 2011). However, in a more recent study, site-directed mutagenesis and computer modeling indicated that the binding site of Lynx1 might be close to the orthosteric binding site of the α7 nAChR (Lyukmanova et al., 2013).

GPI-anchored Lynx proteins have been suggested to be involved in chaperoning of nAChRs, where the interactions between Lynx proteins and nAChRs could be altering the trafficking, maturation and surface number of the receptors (Lester et al., 2009). Indeed, a recent study demonstrated the localization of Lynx1 to be both in the endoplasmatic reticulum (ER) in addition to the plasma membrane in transfected cultured mouse neurons using fluorescent tags (Nichols et al., 2014). Lynx1 was further shown to alter the assembly of α4β2 nAChR within the cell by stabilizing α4-α4 subunit dimerization, but not β2-β2 subunit dimers in the ER, thereby changing the stoichiometry towards low sensitivity α4β2, $(\alpha4)_3(\beta2)_2$, nAChRs instead of the high sensitivity α4β2, $(\alpha4)_2(\beta2)_3$, nAChRs (Nichols et al., 2014). Interestingly, nicotine is suggested to have the opposite effect of Lynx1, since it is demonstrated that upon chronic exposure to nicotine, nicotine binding within the ER results in up-regulation of α4β2 by stabilizing high sensitivity α4β2, $(\alpha4)_2(\beta2)_3$, nAChRs (Lester et al., 2009).

Other Lynx proteins that are shown to modulate nAChR function include PSCA, which was first identified to be highly expressed in prostate cancer (Reiter et al., 1998). PSCA was found to be highly expressed and to correlate with α7 nAChR expression in brain tissue from chicken and mouse. Moreover, retroviral expression of PSCA in dissociated chicken ciliary ganglion neurons suppressed nicotine-induced Ca^{2+} influx possibly via α7 nAChR suggesting that PSCA acts as a negative modulator of α7 nAChR function (Hruska et al., 2009). Contrarily, transgenic over-expression of another Lynx protein, Lypd6, was found to increase the cholinergic tone shown by enhancement of Ca^{2+} influx in dissociated trigeminal ganglion neurons, increased locomotor

arousal, and hypoalgesia (Darvas et al., 2009). The Lynx proteins, secreted mammalian Ly-6/uPAR-related protein 1 and 2 (SLURP-1 and -2), which are found to be expressed peripherally and implicated in skin disorders, have also been demonstrated to modulate nAChR function (Arredondo et al., 2006; Arredondo et al., 2005; Chimienti et al., 2003). These proteins are, as their names imply, not tethered to the membrane via a GPI-anchor. SLURP-1 increased the amplitude of ACh-induced currents in oocytes transfected with α7 nAChR without changes in desensitization and had no effect alone (Chimienti et al., 2003). Hence, it was suggested that SLURP-1 function as a type I positive allosteric modulator of the α7 nAChR (Thomsen and Mikkelsen, 2012a) although it has been demonstrated to compete with [^{3}H]-nicotine binding indicating binding to the orthosteric binding site (Arredondo et al., 2005). SLURP-2 showed a higher affinity for heteromeric nAChRs and anti-apoptotic effects in keratinocytes, which were opposite to SLURP-1 (Arredondo et al., 2006).

Lynx1 is suggested to act as an endogenous allosteric modulator of nAChR *in vivo*. Lynx1 KO mice showed higher sensitivity to nicotine with marked reduction in EC_{50} for nicotine and in receptor desensitization. Furthermore, the absence of Lynx1 resulted in enhanced nicotine-mediated Ca^{2+} influx and synaptic activity (Miwa et al., 2006). It was therefore proposed that Lynx1 endogenously regulates nAChRs to maintain low ACh affinity and avoid potentially critical overstimulation of the receptors. In addition, the Lynx1 KO mice displayed age-dependent degeneration with intracellular vacuolation and disordered myelin sheaths (Kobayashi et al., 2014; Miwa et al., 2006). The degeneration was worsened by administration of nicotine and rescued by crossing the Lynx1 KO mice with α7 or α4β2 KO mice (Miwa et al., 2006), indicating that nAChRs are involved in the neurodegeneration.

Interestingly, Lynx1 has been shown to regulate synaptic plasticity in primary visual cortex. Lynx1 expression was shown to be increased after a critical period for amplyopia, and Lynx1 KO mice displayed recovery from amblyopia, which is normally restricted to the early critical development period. Hence, it was suggested that Lynx1 is critical for the loss of synaptic plasticity in visual cortex seen in adulthood (Morishita et al., 2010).

Lynx proteins have also been associated to regulation of development. Thus, it was shown that Lypd6 plays an essential role in regulating embryogenesis in zebrafish via enhancement of the Wnt/β-catenin signaling pathway (Ozhan et al., 2013). Furthermore, transgenic mice expressing siRNA directed against Lypd6 showed that the knockdown of Lypd6 resulted in inability to procreate, suggesting that Lypd6 is involved in germ cell and/or embryonic development (Darvas et

al., 2009). PSCA has also been proposed to have a modulating role during development. Hence, premature overexpression of PSCA in chicken embryos prevented α7 nAChR signaling-induced cell death of neurons in ciliary ganglion, and an association was suggested between expression and activation of nAChRs and PSCA levels, since exposure to α-Bgt was shown to reduce PSCA expression in the developing ciliary ganglion neurons (Hruska et al., 2009).

As mentioned above, animal behavioral studies have linked nAChRs to cognitive function, but only a few studies have focused on the behavioral characteristics of Lynx proteins. Interestingly, Lynx1 KO mice displayed improved associative learning and memory in a fear-conditioning paradigm (Miwa et al., 2006), and Lynx2 KO mice showed elevated fear- and anxiety-related behaviors suggested to be caused by alterations in glutamatergic signaling in the prefrontal cortex (Tekinay et al., 2009). In addition, in transgenic mice overexpressing Lypd6 there were indications on improved working memory, and these mice showed enhanced pre-pulse inhibition of startle response to acoustic stimuli, which is a measure of pre-attentional processing (Darvas et al., 2009). These studies indicate that Lynx proteins might be involved in cognitive function, and thus could have a potential role in diseases associated to dysregulation of nAChRs and/or cognitive impairment such as AD and SCZ.

Aims

The overall aim of the thesis is to characterize the α7 nAChR and Lynx proteins and their relation to AD.

Specifically, the aims are to:

- Compare mRNA levels of the α7 nAChR gene, *CHRNA7*, with its partially duplicated gene *CHRFAM7A*
- Study α7 nAChR binding in the presence of the α7 nAChR agonist encenicline in human cortex
- Study α7 nAChR binding in a transgenic mouse model of AD with and without basal forebrain cholinergic degeneration
- Characterize Lynx proteins in rodents and humans
- Study expression levels of Lynx proteins in AD patients and in transgenic mouse models of AD

Experimental Methods

In vitro receptor autoradiography

Investigation of receptor binding *in vitro* is most often done with autoradiography. This technique employs radioactive labeled ligands which bind specifically to selective receptors and are applied to thin tissue sections to determine the level of binding sites and localization of the particular receptors. *In vitro* receptor autoradiography has the benefits of anatomical resolution and sensitivity when compared to protein detection methods such as Western blot analysis. However, the receptors are detected in their native folded structure, and thus high affinity ligands with incubation concentration in the nanomolar range, which availability can be limited, as well as high specific activity of the radiochemical synthesis are required to obtain high quality of the autoradiograms. Furthermore, proper optimization of the protocol is essential to ensure optimal condition for the binding of the ligands to the receptors.

A broad variety of isotopes can be used when labeling ligands for autoradiography. The most common used for receptor autoradiography are ^{3}H and ^{125}I. Both have the advantages of relative low energies and long half-lives with 12.3 years for ^{3}H and 59.4 days for ^{125}I, which enables long-term storage and use. Tritium displays high spatial resolution due to low-energy β-emission, whereas ^{125}I has the advantage of very high specific activity. Here, we employed the classical nAChR radioligands [^{125}I]Tyr-54-mono-iodo-α-bungarotoxin ([^{125}I]-α-Bgt; 2,200 Ci/mmol; Perkin Elmer, Skovlunde, Denmark) and [5,6-Bicycloheptyl-^{3}H]-(+/-)epibatidine ([^{3}H]-epibatidine; 56,3 Ci/mmol, Perkin Elmer) to detect α7 and α4β2 nAChRs, respectively.

The autoradiography was carried out in brain tissue from human temporal cortex obtained from neurosurgical resection (Paper I) as well as brains of Tg2576 mice (see p. 33) and age-matched WT mice. After resection, the tissue was immediately frozen on dry ice to preserve the tissue and avoid protein degradation and stored at -80°C until sectioning. The brain tissue was sectioned into 12 µm thickness, thaw-mounted on Super Frost Plus glass slides, and stored at -80°C until use. Sections from the mice were collected in parallel series with both the frontal cortex (1.7–2.0 mm anterior to Bregma) and the dorsal hippocampal region (2.0–2.3 mm posterior to Bregma) (Paxinos and Franklin, 2001).

The autoradiographic procedure consisted of four steps: Hydration, incubation, washing, and drying. The slides were thawed at room temperature for 30 minutes prior to the hydration. In the [^{3}H]-epibatidine binding protocol, the hydration step consisted of light pre-fixation with 0.2%

paraformaldehyde in phosphate-buffered saline (0.1 M, pH 7.4) for 5 min to preserve the tissue and enhance the anatomical resolution (Tribollet et al., 2004), followed by a dip in the binding buffer containing 50 mM Tris buffer (pH 7.4) with 120 mM NaCl, 5 mM KCl, 2.5 mM $CaCl_2$ and 1 mM $MgCl_2$. A binding buffer consisting of 50 mM Tris buffer with 0.1% BSA (pH 7.3) was used to hydrate the sections for 30 minutes in the [^{125}I]-α-Bgt binding protocol. Incubation was then carried out at room temperature in the respective binding buffers containing the radioactive ligands in the concentrations: [^{125}I]-α-Bgt mixed 1:10 with non-radioactive α-Bgt yielding a total of 5 nM and 0.46 nM [^{3}H]-epibatidine for 2 hours and 1 hour, respectively, to determine the total binding (TB). Non-specific binding (NSB) was determined in adjacent slides with the addition of 1 mM or 300 µM (-)-nicotine for [^{125}I]-α-Bgt and [^{3}H]-epibatidine binding, respectively. Another ligand for the receptor is used to avoid the same off-target binding. Subsequently, the slides were washed several times in ice-cold binding buffers to separate the bound radioactive ligands from the unbound, followed by a quick dip in ice-cold distilled water to remove excess buffer salts. Prior to exposure, the slides were dried under an air stream to avoid dissociation of the radioactive ligand and fixated overnight at 4°C in a sealed chamber containing paraformaldehyde vapor.

Visualization of the binding was done with the use of phosphor-image plates, which can store the energy from the isotopes and later release it as luminescence, when scanned in a phosphoimager (Kanekal et al., 1995). From the autoradiographies regions of interest (ROIs) were hand-drawn for each brain region (see Figure 4) and the mean optical density in the ROIs were quantified using a computer image analysis system (Quantity One®, Bio-Rad, CA, USA). Specific binding (SB) was calculated as TB subtracted NSB.

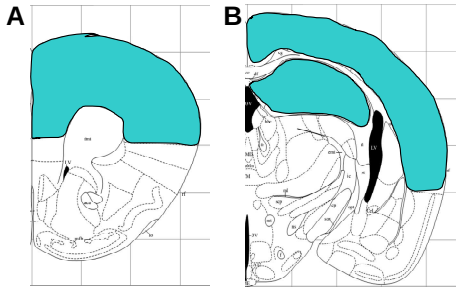

Figure 4. Graphic representation of the densitometric analysis. The mean optical density was measured in frontal cortex **(A)**, temporal cortex, and hippocampus **(B)** Modified from (Paxinos and Franklin, 2001).

In Paper I, competitive binding studies were performed to determine whether α7 nAChR compounds have affinity for the [^{125}I]-α-Bgt binding site. Here, it was investigated if the partial α7 nAChR agonist encenicline (EVP-6124, kindly provided by Dr. Dan Peters, Neurosearch, Ballerup, Denmark) displaced [^{125}I]-α-Bgt in human cortical tissue. This was done by measuring the binding of a fixed concentration of [^{125}I]-α-Bgt in the presence of increasing concentrations of encenicline. The IC_{50} could then be determined, which is defined as the concentration of the compound, which inhibits 50% of total SB.

Western blotting

Western blotting or immunoblotting is a widely used technique for detection of proteins and has been used for over three decades with only slight modifications to the original procedure (Towbin et al., 1979). The technique is used to identify specific proteins in tissue homogenates or extracts by the use of specific antibodies to the target proteins. In brief, the proteins are denatured and separated by their molecular weight using gel electrophoresis. Subsequently, the proteins are transferred to a membrane, which is then incubated with a primary antibody, either monoclonal antibody or polyclonal antiserum, targeting the specific protein of interest followed by incubation with a labeled secondary antibody recognizing species-specific parts of the primary antibody. Detection of the labeled secondary antibody can then be visualized.

Western blot analysis is a fast, qualitative method combining the high resolution of protein electrophoresis with the specificity and sensitivity of antibody-antigen interactions. Protein purification is not required in the sample preparation and thus proteins can be detected in crude biological tissue samples. Although the signal correlates with the amount of protein, the detection is only semi-quantitative depending on protein transfer efficiency from gel to membrane, and the protein binding capacity of the membrane. Western blotting strongly depends on the specificity and sensitivity of the detection system and particularly the specificity of the antibodies. It is thus important that these are properly validated.

We used the following experimental procedure (Paper II and III): Prior to the gel electrophoresis, the protein concentration of the individual samples was determined to ensure loading equal protein concentrations. Diluted samples were then mixed with loading buffer containing sodium dodecyl sulfate to denature the proteins. Using a wet-transfer blotting system (Criterion™ Blotter, Biorad, Hercules, CA), the proteins were transferred onto methanol-activated PVDF membranes (Biorad). Subsequently, the membranes were washed in Tris-buffered saline with 0.1% Tween 20 (TBS-T), and blocked in TBS containing 5% (w/v) dry milk powder. Incubation with primary antisera was done overnight at 4°C (please refer to Paper II and III for description of the antisera used). The following day, the membranes were washed and incubated for 1 hour with horseradish peroxidase-conjugated secondary antibody at room temperature. The membranes were then covered with enhanced chemiluminescence reagents (Western Lightning® ECL Pro, Perkin Elmer, Waltham, MA) and visualized using a Chemidoc™ XRS system with Quantity One software (Biorad). Densitometric analysis was performed by measuring mean optical densities of bands and subtracting an adjacent background measurement. To determine protein

quantification, the optical density of protein band of interest was divided by the corresponding β-actin and normalized to the respective control group, which was set to 1.

Reverse transcription quantitative PCR

Reverse transcription quantitative polymerase chain reaction (RT-qPCR) is a frequently used sensitive technique to analyze gene expression by measuring mRNA levels in tissue extracts and cell cultures (VanGuilder et al., 2008). The RT-qPCR consists of three steps: 1) the conversion of RNA to cDNA by reverse transcriptase, 2) the amplication of cDNA using PCR, and 3) the real-time detection and quantification of products.

RT-qPCR provides quantification of gene expression with high accuracy and sensitivity, which allows detection of very low amount of the target mRNA. Furthermore, it enables discrimination of almost identical mRNA sequences and has a high throughput. However, the high sensitivity also requires well-designed protocols with proper sample storage, preparation, and high RNA quality as well as efficient primers for the PCR and appropriate data and statistical analyses (Bustin et al., 2009).

Here, the RNA was extracted from the tissue using column-based extraction methods instead of hazardous reagents such as the commonly used TRizol method. RNA was reverse transcribed into cDNA using oligo(dT)15 primers, which binds to the poly-A tail of the mRNA (Nolan et al., 2006). The qPCR reactions were performed by adding the cDNA sample with a SYBR green mixture along with gene-specific primers. SYBR green binds to double-stranded DNA providing a fluorescence signal, which corresponds to the amplified cDNA (Zipper et al., 2004). The PCR products were measured by the cycle threshold (C_T), which is defined as the number of cycles, where the accumulation of fluorescence signal exceeds an arbitrary threshold, where the amplification curve enters the exponential phase. C_T is thereby inversely proportional to the amount of target cDNA.

The RT-qPCR method was validated using serially dilutions of cDNA to establish a standard curve determining the efficiency of the assay, a gel to verify the product, as well as melting curves. Ideally, the efficiency should be 100% corresponding to the PCR product of interest is doubling with each cycle. The efficiencies for the used primer pairs here were all in the range of 90-110%, which is within the range, when using the comparative C_T method (Schmittgen and Livak, 2008). We also used the efficiency correction method, where amplification efficiencies are accounted for in the calculation (Pfaffl, 2001). Several parameters can influence the efficiency such as PCR inhibitors, which include excessive protein sample and preparation reagents, primer design, and the

running conditions of the qPCR. In addition, the PCR products were validated by running the samples on an agarose gel to verify that only a single product of the correct size was produced. Melting curves were also used to verify the amplified products and to distinguish them from formation of primer dimers, since DNA melts at a characteristic temperature. One potential disadvantage of RT-qPCR is the amplification of non-specific products, which can be avoided by treating the samples with DNase to prevent false cDNA and genomic DNA contamination. In addition, lack of specificity of the primers can also result in non-specific products. We designed the gene-specific primers to span across a splice site so they only annealed to cDNA corresponding to spliced mRNA.

Synaptosomal fractionation and affinity purification

Subcellular fractionation is isolation of specific cellular organelles, which allows for identification of which organelle the protein of interest resides, which could indicate the function of the particular protein.

In Paper II, tissue fractionated into nuclear and synaptosomal fractions by differential centrifugation was used to determine the subcellular distribution of the Lynx proteins, Lynx1 and Ly6H. Synaptosomes are *in vitro* preparations of isolated presynaptic nerve terminals, which are used to study neurotransmitter uptake, storage, and release. The identification of synaptosomes has certain morphological criteria such as the presence of mitochondria within a sealed plasma membrane, where size and number of vesicles resemble what is seen in intact nerve terminals and varicosities (Whittaker, 1993). Homogenization of the brain tissue in an isotonic sucrose solution with a mild shear force separates the nerve terminals from their axons followed by a resealing of the presynaptic membrane. Here, differential centrifugation was used in the purification of the synaptosomal fraction, and thus referred to as crude synaptosomal fraction due to contamination of plasma membranes from neurons and glial cells as well as myelin and mitochondria. As an alternative, gradient techniques, such as the Percoll gradient procedure, can be used resulting in a more homogenous synaptosomal fraction (Dunkley et al., 2008). However in our study, crude synaptosomes were adequate to determine the distribution of Lynx proteins.

Preparation of the crude synaptosomes was done according to a previous study (Soliakov et al., 1995). In brief, the dissected brain tissue was homogenized in ice-cold homogenization buffer using a glass Teflon grinder (IKA Labortechnik, Staufen, Germany) followed by centrifugation for 10 minutes at 1,000×*g* at 4°C. The resultant pellet, P1 or nuclear fraction, was lysed and the

supernatant was centrifuged 20 minutes at 20,000×*g* at 4°C. The pellet was resuspended in Krebs-bicarbonate and centrifuged again for 10 minutes at 20,000×*g* at 4°C. The resultant pellet, P2 or crude synaptosomal fraction, was lysed, and both the P1 and P2 lysates were sonicated and processed for western blotting as described above. The synaptosomal preparation was validated by the enrichment of the synaptic protein, syntaxin, in the P2 fraction (See Figure 5 and Figure S2 in Paper II).

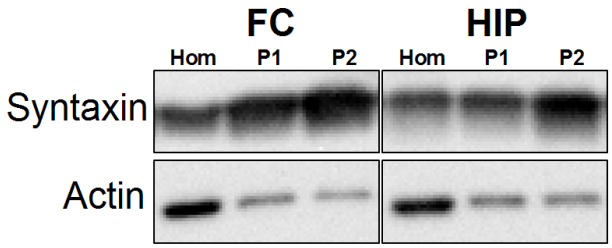

Figure 5. Validation of synaptosome preparation
Representative western blot images of frontal cortical and hippocampal tissue fractionated using differential centrifugation into a pellet 1 (P1, nuclear) and pellet 2 (P2, crude synaptosome) fraction. Enrichment of synaptosomes in P2 is confirmed by enrichment of the synaptic protein Syntaxin (Anti-Syntaxin, MAB336) in the P2 fraction compared to P1 and the total homogenate (Hom).

Co-immunoprecipitation is often used to study protein-protein interaction using specific antibodies to indirectly capture proteins that are bound to the specific target protein. To circumvent the use of antibodies, since selective antibodies against transmembrane and membrane-associated proteins are challenging to generate due to difficulties in recognizing the native proteins, affinity purification with the use of magnetic beads was used instead in Paper III. Magnetic beads have several advantages over the commonly used beaded agarose and porous resins, as they are smaller in size and solid (non-porous), which results in less non-specific binding than porous supports.

Here, magnetic beads capable of binding amine-containing biomolecules was mixed with the target protein, in this case recombinant human GST-tagged PSCA produced in E.coli (purchased from MyBioSource Inc., San Diego, CA). The recombinant protein was coupled to PureProteome™ NHS Flexibind Magnetic Beads (Millipore, Billerica, MA) by formation of stable covalent bonds resulting in permanent immobilization of PSCA to the beads. The residual active groups of the beads were blocked by Quench Buffer (100 mM Tris-HCl, 150 mM NaCl, pH 8.0) prior to the resuspension with tissue lysate. After 18-22 hours incubation of the coupled magnetic beads with the lysed tissue sample, the magnetic beads were collected and separated from the sample using a powerful magnet. Subsequently the beads were washed several times and immediately processed for western blotting, where the addition of loading buffer detached the bound proteins for detection.

Transgenic animal models of Alzheimer's disease

Animal models play a central role when studying diseases of the CNS. The most widely used in AD research are rodent models due to short lifespan, easy breeding, and maintenance, which is economically affordable. The vast majority of AD cases are sporadic with unknown etiology. Hence, the animal models of AD are commonly relying on genetic mutations in APP, presenilin 1 (PS1), or presenilin 2, which are associated with early-onset familial AD cases, a minority of all AD cases. Although the animal models of AD have provided knowledge and understanding of the pathophysiology of AD, which would not have been possible in human subjects, the cellular, biochemical, and behavioral pathology of AD patients are not recapitulated in these models. The transgenic animals are e.g., displaying minimal neurodegeneration and tau pathology, and translation of behavioral phenotypes in the animals is challenging. Hence, discrepancies between preclinical models and human clinical trials have been reported (LaFerla and Green, 2012), and thus the translational aspects of animal models of AD can be questioned.

Here, we used two transgenic AD mouse models: The Tg2576 mice as well as the triple transgenic mice (3×Tg-AD). The protein levels of Lynx proteins were studied in Tg2576 and 3×Tg-AD mice using western blotting in Paper III, while nAChR binding in Tg2576 mice with and without cholinergic degeneration (see below) was investigated by [^{125}I]-α-Bgt and [^{3}H]-epibatidine autoradiography.

The widely used Tg2576 mice overexpress mutant forms of the human APP, the so-called Swedish double mutation K670N/M671L (hAPPSwe), which result in five-fold elevated secretion of both $A\beta_{1-42}$ and the less neurotoxic $A\beta_{1-40}$ (Hsiao et al., 1996). The Tg2576 mice show late onset of β-amyloidosis with diffuse plaques at 12 months of age, whereafter Aβ levels rapidly increase to levels comparable to AD brains (Kawarabayashi et al., 2001). In the other animal model, which was the first to develop both plaque and tangle pathology, the 3×Tg-AD mice are expressing, in addition to the hAPPSwe transgene, a mutation in tau (P301L) as well as the PS1 mutant M146V knock-in construct (Oddo et al., 2003). The 3×Tg-AD mice show early signs of AD pathology with reported plaque onset at 6 months and neurofibrillary tangle formation at 12 months. They are useful when studying the interactions of human Aβ and tau, and the progression of pathology as well as the behavioral phenotype of these mice are similar to those observed in AD patients (Bilkei-Gorzo, 2014). However, the overexpression of APP/PS1 and tau genes is simultaneous in these mice which contrast AD patients, where tau pathology emerges subsequent to Aβ pathology.

Given the hypothesis that cholinergic dysfunction is associated to the cognitive impairments of AD, pharmacology-induced rodent models of cholinergic deficits have been developed. To mimic the degeneration of cholinergic neurons in the basal forebrain, lesion methods with immunotoxins targeting cholinergic neurons are commonly used. Currently, the most selective immunotoxins are the mu p75-saporin (SAP) for mice and its equivalent 192-IgG-SAP in rats resulting in almost total loss of cholinergic neurons when injected (Chang and Gold, 2004). The immunotoxins are conjugated to antibodies against the P75 neurotrophic receptor, which is highly expressed on cholinergic neurons in the basal forebrain. Here, we studied brain tissue from Tg2576 mice and their WT littermates with and without SAP lesions thus combining cognitive and neuropathological characteristics. The male mice were bred on an inbred 129S6 background and obtained from Taconic (Ry, Denmark) by H. Lundbeck A/S (Lundbeck, Valby, Denmark) The mice had at the age of 9 months underwent surgery at Lundbeck performed by Bettina Laursen as described in details elsewhere (Laursen et al., 2013). Briefly described, the mice received intracerebroventricular injections of either 0.6 µg SAP (Advanced Targeting Systems, CA) or PBS, since this was applied to dissolve the immunotoxin. Electrophysiological testing of the animals was then performed in an unrelated set of experiments, and the mice were euthanized at 15 months and the brains dissected. One hemisphere was used for analysis of ChAT activity at Lundbeck described in details elsewhere (Laursen et al., 2013), with the use of a radiochemical micro-assay based on reaction between [^{3}H]-labeled acetyl CoA and unlabeled choline, where the subsequent production of labeled ACh was quantified by scintillation counts. The other hemisphere was snap frozen and kept at -80°C until further procesing. Tissue for western blotting analysis from frontal cortex of PBS-injected WT and Tg2576 mice were collected on a cryostat prior to the sectioning for autoradiography as described above.

Statistical analysis

This section only covers the statistics used for the results presented in the *Results and Discussion* section. For statistics used in Paper I-III please consult the respective papers. Data were analyzed using two-way analysis of variance (ANOVA) with genotype (WT mice *vs.* Tg2576 mice) and treatment (PBS vs. SAP) or genotype (WT mice *vs.* 3×Tg-AD mice) and age (6 months vs. 19-21 months) as the two independent variables. Differences between groups were further analyzed using Holm Sidak post hoc test, when there was an overall statistical difference or unpaired multiple t-tests using the Holm-Sidak method. The statistical calculations were performed using GraphPad

Prism version 6 for Windows. Data are presented as mean ± standard error of the mean (SEM). *P* values were considered significant when $P<0.05$.

Results and Discussion

The α7 nicotinic receptor in human cortical tissue

In Paper I, we studied the human α7 nAChR at the DNA, mRNA, and protein level. Studying α7 nAChR in human tissue at a molecular level is of importance to understand regulation of gene expression and receptor function, however, it has been challenging due to limited sources of human postmortem tissue. Here, we used human temporal cortex obtained from neurosurgical interventions to investigate the human α7 nAChR.

First, we examined the mRNA expression levels of several nAChR subunits including *CHRFAM7A* by RT-qPCR in human temporal cortical tissue obtained from neurosurgical resections in patients with focal epilepsy (see Table 3, Paper I). The highest mRNA expression levels were from *CHRNB2* and *CHRNA4* compared to *CHRNA7*. The *CHRFAM7A* mRNA was detected in all human subjects, and the expression level of *CHRFAM7A* was ~30% with a ratio *CHRNA7:CHRFAM7A* mRNA levels of 3.4. We observed high between-subject variability in the *CHRNA7*:*CHRFAM7A* ratio in temporal cortex with a coefficient of variation of 0.78, defined as standard deviation divided by mean. We found no correlations, when the mRNA levels were compared to age and gender.

The transcript of *CHRFAM7A* has been shown to be more abundant in cortical regions than hippocampus, thalamus, corpus callosum, and cerebellum (Gault et al., 1998; Severance and Yolken, 2008; Villiger et al., 2002). Our data showing 3.4 times higher expression level of *CHRNA7* compared to *CHRFAM7A* are comparable to previous studies in human postmortem cortical tissue (De Luca et al., 2006a; de Lucas-Cerrillo et al., 2011). Similar variation size was also reported from mRNA samples obtained from the prefrontal cortex post-mortem (De Luca et al., 2006a), whereas in the study of de Lucas-Cerillo et al. the expression levels only included cortical tissue sample from one individual (de Lucas-Cerrillo et al., 2011). The relative high expression levels of *CHRFAM7A* compared to *CHRNA7* indicate that the *CHRFAM7A* gene products, dupα7 and dupΔα7, likely could be integrated into α7 nAChR-containing receptors in temporal cortex, and thereby affect the function of these receptors. Interestingly, De Luca et al. reported a lower ratio of *CHRNA7:CHRFAM7A* mRNA in the prefrontal cortex of patients with SCZ and bipolar disorder compared to unaffected controls (De Luca et al., 2006a), suggesting that the dupα7 and dupΔα7 subunits are more abundant in α7 nAChR-containing receptors in affected individuals. Moreover, a positive correlation between *CHRNA7* mRNA and *CHRFAM7A* mRNA levels was observed in

bipolar disorder, which was not seen in unaffected controls and SCZ patients (De Luca et al., 2006a). It should be noted that we did not distinguish, whether the two base pair deletion in *CHRFAM7A* was present or not, when measuring mRNA expression levels.

In general, protein levels cannot be predicted by mRNA expression levels. We observed much higher mRNA expression of *CHRNB2* and *CHRNA4* compared to *CHRNA7* in human temporal cortical extracts, while it has been shown that the α4β2 nAChR binding by [^{3}H]-epibatidine was similar to the α7 nAChR binding by ^{125}I-Bgt in postmortem temporal cortex (Gotti et al., 2006a). This discrepancy may be due to that not all nAChR subunits mature into receptors, but are present as individual subunits, which are not detected by the radioactive labeled ligands. Furthermore, since there are no antibodies or ligands currently available that can differentiate between α7 nAChR and dupα7 and dupΔα7 protein it has not been possible to demonstrate the presence of dupα7 and dupΔα7 *in vitro* or *in vivo* or their ratio to α7 nAChR subunits.

DNA methylation of the *CHRNA7* promoter was further analyzed in the human temporal cortex, since DNA methylation is known to repress transcription. We demonstrated that *CHRNA7* promoter DNA methylation inversely correlated with *CHRNA7* mRNA (r=-0.798, *P*=0.0099) using bisulfite sequencing and qPCR. This finding corresponds well to a recent study reporting tissue-specific correlation between mRNA expression and DNA methylation across human tissues including both brain (cingulate gyrus) and peripheral tissue types (Canastar et al., 2012). In addition, promoter methylation was demonstrated to modulate *CHRNA7* gene transcription in human-derived cell lines, where inhibitors of a DNA methyltransferase were able to significantly increase the *CHRNA7* expression in otherwise transcription-silenced, hypermethylated neuroblastoma SH-EP1 cells (Canastar et al., 2012). Our data show that the expression of human *CHRNA7* is regulated by DNA methylation of the *CHRNA7* promoter, which add a new aspect in regulating the α7 nAChR and thereby the cholinergic function in the human brain.

Currently, there are no reports linking DNA methylation status of the *CHRNA7* promoter region to brain disorders such as AD and SCZ, where the α7 nAChR is suggested to be involved. It has been reported that methylation levels of DNA in many genes are highly correlated between brain and blood, and thus DNA methylation levels may be potential therapeutic biomarkers for brain disorders (Ewald et al., 2014; Tylee et al., 2013). This has been suggested in a recent study for the promoter region of the serotonin transporter gene, where the promoter hypermethylation and the correlated expression observed in drug-naïve patients with SCZ were altered in drug-treated SCZ patients dependent on the antipsychotic treatment (Abdolmaleky et al., 2014). Future studies may

provide knowledge whether the DNA methylation levels of *CHRNA7* promoter region similarly can be used as a therapeutic biomarker in AD and SCZ.

In the human temporal cortex, we further examined the binding of the selective α7 nAChR antagonist [^{125}I]-α-Bgt in the presence of the partial α7 nAChR agonist encenicline (EVP-6124, which is now in phase III trials for cognitive and clinical improvement in AD and SCZ (Preskorn et al., 2014). Encenicline was demonstrated to have a unique profile with co-agonist activity in α7 nAChR-transfected *Xenopus* oocytes (Prickaerts et al., 2012), making this compound interesting to study further in its binding to human α7 nAChRs.

We found that 30 µM encenicline was able to displace [^{125}I]-α-Bgt in human temporal cortex using autoradiography (see Paper I, Figure 2). The displacement was similar to 1 mM nicotine. A high variability in displacing [^{125}I]-α-Bgt at equivalent concentrations of encenicline was observed among the human individuals (Paper I, Figure 3A). Interestingly, we demonstrated that the displacement with encenicline resulted in displacement curves in some of the human subjects, which were best fitted with a two-site competition model, suggesting that encenicline in these individuals is able to bind the α7 nAChR at two different sites, a high affinity binding site in the nanomolar range and low affinity binding site in the micromolar range (6.2 nM and 2.6 µM, respectively), which have the same affinity for [^{125}I]-α-Bgt (see Figure 6). The affinities of the individuals displaying one-site binding were in the low affinity range (~5.8 µM).

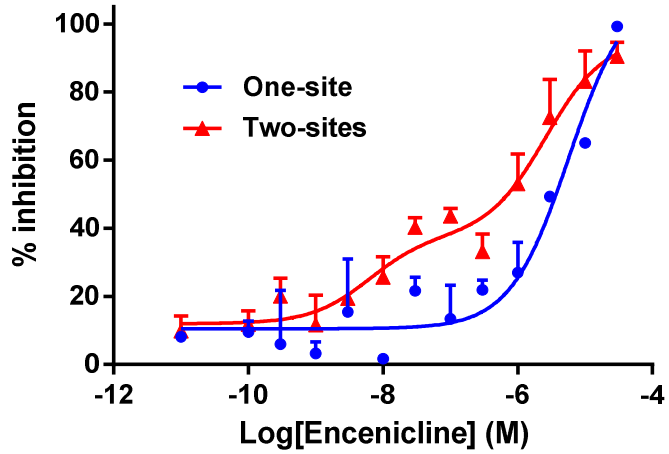

Figure 6. Different [^{125}I]-α-bungarotoxin (α-Bgt) displacement profiles in human cortical tissue. [^{125}I]-α-Bgt was displaced by encenicline in five human subjects. Non-specific binding in the presence of 1 mM nicotine was subtracted and percent inhibition was calculated. Data were separated dependent on whether one-site or two-site model was preferred to determine IC_{50} values in the human individuals, n=2-3.

Encenicline has previously been shown to displace [^{125}I]-α-Bgt in rat brain homogenates with a K_i of 4.3 nM (Prickaerts et al., 2012), which is consistent with the high affinity binding site seen in our data. Given that 1 nM encenicline in transfected *Xenopus* oocytes was shown to enhance acetylcholine-evoked currents without desensitization, whereas concentrations at 3 nM encenicline and above oppositely reduced the currents due to receptor desensitization, a model of co-agonist

activity was proposed (Prickaerts et al., 2012). The model describes how low concentration of a high affinity ligand, such as encenicline, is not sufficient to activate the receptor on its own, but upon brief exposure to another ligand with lower affinity, such as ACh, the receptor will then be activated (Cachelin and Rust, 1994). Our data suggest that, instead of the co-agonist model, the behavior of encenicline may be explained by encenicline binding to two different sites of the α7 nAChR, having a high affinity and a low affinity binding mode, which may result in different effects upon activation. The binding sites might be within the orthosteric site, since α-Bgt has not been reported to have more than one binding site. Interestingly, the displacement profile of memantine, which is an antagonist of both the NMDA receptor and α7 nAChR and in clinical use to treat AD, was also shown to be best fitted to a two-site model when displacing [^{3}H]-MLA (Chipana et al., 2008). Memantine have been demonstrated to interact with two binding sites on the α7 nAChR; one being voltage-sensitive and suggested to be within the channel and the other voltage-insensitive and thus likely situated in the extracellular domain (Aracava et al., 2005). Another explanation than two distinct binding sites could be that the interaction of the α7 nAChR compounds showed cooperativity, which will fit well with the co-agonist model. Speculatively, since we observed the different displacement characteristics in human tissue, the presence of the *CHRFAM7A* gene products, dupα7 and dupΔα7, could also be influencing how encenicline binds to the α7 nAChR. Previously, the presence of dupα7 and dupΔα7 has been demonstrated to differently modulate the sensitivity to α7 nAChR ligands in a heterologous expression system (Wang et al., 2014). Thus, the genotype might affect the efficacy of encenicline, which may lead to personalized treatment in the future. However, further studies are needed to reveal the exact mechanisms of this currently most promising α7 nAChR drug candidate.

Copenhagen University Hospital, Rigshospitalet, is the only place in Denmark performing the temporal lobectomy of patients with temporal lobe epilepsy with hippocampal onset. Thus, the use of resected temporal neocortex from these neurosurgical interventions gave us a unique opportunity to study the α7 nAChR in human tissue, which would be more limited in postmortem tissue. However, it is also a pitfall in our study as the tissue originated from patients with epilepsy, and we did not have control tissue for comparison. Although the cortical tissue appeared micro- and macroscopically normal, projections from the hippocampus, with pronounced pathology, to the temporal neocortex as well as the use of anti-epileptic drugs, and the occurrence of seizures may have an effect on gene and protein expression. Furthermore, DNA methylation of gene promoters

and increased expression of DNA methyltransferases have previously been demonstrated to be altered in patients with temporal lobe epilepsy (Kobow et al., 2009; Zhu et al., 2012).

In summary, our findings in Paper I demonstrated that the α7 nAChR is regulated at both the gene and protein levels in human brain tissue. *CHRFAM7A* mRNA was present in temporal cortex of human individuals, where the ratio *CHRNA7:CHRFAM7A* mRNA levels was found to be 3.4. The DNA methylation status of the *CHRNA7* promoter region was further shown to correlate inversely with expression levels of *CHRNA7* mRNA suggesting the involvement of epigenetic factors in the regulation of *CHRNA7* mRNA expression. When studying the binding of the α7 nAChR, the α7 nAChR agonist encenicline displaced [^{125}I]-α-Bgt with high variability among the human individuals, where encenicline, in some individuals, showed two different binding modes, which may affect the efficacy of the compound in the treatment of cognitive disturbances in AD and SCZ.

Reduced α7 nicotinic receptor binding in Tg2576 mice with cholinergic lesions

Cholinergic degeneration in the basal forebrain and accumulation of Aβ into extracellular plaques are neuropathological characteristics of AD (Auld et al., 2002). However, animal models of AD are usually only presenting one of the two hallmarks. Here, we studied the binding of nAChRs using autoradiography with [^{125}I]-α-Bgt and [^{3}H]-epibatidine in Tg2576 mice and WT controls combined with intracerebroventricular infusion of the selective cholinergic immunotoxin mu p75-saporin (SAP). To our knowledge this study is the first to investigate nAChR binding following cholinergic degeneration of the basal forebrain in a transgenic animal model of AD.

To assess the cholinergic activity in the Tg2576 mice and their WT littermates, the activity of ChAT was measured in frontal cortex and hippocampus following the SAP infusion, which has previously been described to be decreased after infusion with the immunotoxin (Berger-Sweeney et al., 2001). ChAT activity was found to be significantly reduced in frontal cortex and hippocampus (P<0.001) of SAP-treated mice, whereas there was no difference in the levels of cholinergic degeneration with respect to genotype in the two regions. This corresponds to a previous similar experiment with SAP-treated Tg2576 mice and WT controls (Laursen et al., 2014).

We determined the [^{125}I]-α-Bgt binding in frontal cortex, temporal cortex, and hippocampus in 15 month old Tg2576 mice and their WT littermates by autoradiography (see Figure 7A). In frontal cortex using two-way ANOVA with treatment and genotype as variables, there was no interaction of the variables and no significance in main effects. In temporal cortex and hippocampus, there were also no interactions of the variables (P=0.073 and P=0.087, respectively), however in both

regions a significant main effect of the SAP treatment (P=0.024 and P=0.012, respectively) was observed. A few SAP-treated animals, both WT and Tg2576 mice, were excluded in the analysis of hippocampus due to severe hippocampal atrophy. Interestingly, [^{125}I]-α-Bgt binding was significantly reduced in temporal cortex and hippocampus of SAP-treated Tg2576 mice compared to untreated Tg2576 mice revealed by the Holm-Sidak multiple comparisons test (P<0.05). In contrast to the [^{125}I]-α-Bgt binding, we observed no changes in [^{3}H]-epibatidine binding in the three regions using two-way ANOVA (see Figure 7B).

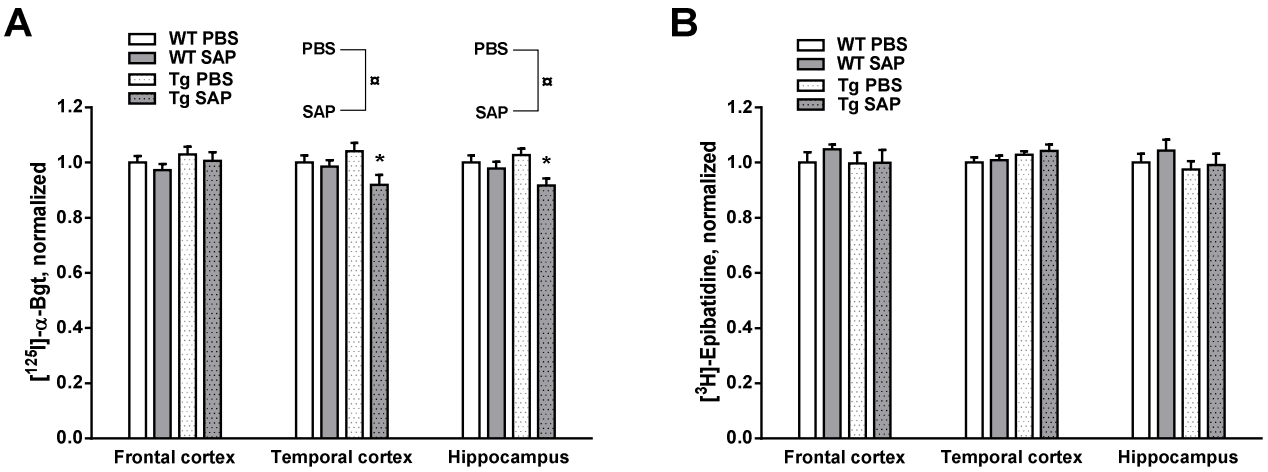

Figure 7. Reduced [^{125}I]-α-bungarotoxin (α-Bgt) binding in temporal cortex and hippocampus of transgenic mice with amyloid pathology and cholinergic degeneration. Using *in vitro* autoradiography, [^{125}I]-α-Bgt **(A)** and [^{3}H]-epibatidine **(B)** binding were measured in Tg2576 mice (Tg) and their wildtype (WT) littermates treated with PBS or the immunotoxin mu 75-saporin (SAP). Data were normalized to the PBS-treated WT group. ¤ indicates P<0.05 main effect of treatment in a two-way ANOVA, and *P<0.05 indicates statistical difference between PBS- and SAP-treated Tg2576 mice by Holm-Sidak multiple comparisons test (n=10-16).

Interestingly, our data showed that combining cholinergic lesion by SAP with overexpression of Aβ resulted in reduced α7 nAChR binding in temporal cortex and hippocampus. We found no changes in [^{125}I]-α-Bgt in untreated Tg2576 mice compared to WT controls in the three brain regions, which corresponds to previous study, where [^{125}I]-α-Bgt binding was unaltered in hippocampus of 6-7 month old Tg2576 mice in comparison to non-transgenic mice (Hedberg et al., 2010). Furthermore, we found no differences in [^{125}I]-α-Bgt binding in SAP-treated WT mice, indicating that SAP treatment alone is not sufficient to affect the α7 nAChR levels. Other lesion studies in rodents showed altered function of α7 nAChR rather than altered α7 nAChR binding. Thus, GABAergic lesions of the rat medial septum/diagonal band of broca, part of the basal forebrain innervating the hippocampus, were demonstrated to alter the function of hippocampal α7 nAChR with no changes in receptor density of α7 nAChR, whereas cholinergic lesions by 192 IgG-SAP had no effects on α7 nAChR function and density (Thinschmidt et al., 2005). In addition, rats demonstrated altered

sensitivity to nicotine with no changes in [^{125}I]-α-Bgt and [^{3}H]-cytisine binding following electrolytic lesions of the medial septum (Frazier et al., 1996) suggesting that the functional changes of the α7 nAChR were caused by structural or biochemical factors such as relocation, altered receptor structure and/or desensitization rates.

When investigating non-α7 nAChRs, we found no changes in [^{3}H]-epibatidine binding in frontal cortex, temporal cortex, and hippocampus of Tg2576 mice compared to WT in both untreated and treated groups. However, reduced [^{3}H]-cytisine binding has previously been demonstrated in cingulate and parietal cortex of 17 month old Tg2576 mice (Apelt et al., 2002). Similar to our findings, SAP-treated rats showed no changes in [^{3}H]-epibatidine binding in frontal cortex, parietal cortex, and hippocampus (Bednar et al., 1998), while in another study SAP treatment was reported to reduce [^{125}I]-A-85380 binding in rat hippocampus with no changes in the cortical regions (Quinlivan et al., 2007). Both radiolabeled epibatidine and cytosine have been widely used in investigating high affinity binding of nAChRs such as the α4β2 nAChR (Paterson and Nordberg, 2000). However, they have different selectivity for the nAChR subtypes e.g., epibatidine also binds with high affinity to the α3 nAChR subtype (Houghtling et al., 1995), and [^{125}I]-A-85380 have been shown to have a greater selectivity in binding α4β2 nAChR than epibatidine (Mukhin et al., 2000). Thus, the observed differences may be due to different selectivity of the radioligands. Given that the EC_{50} of epibatidine for α3-containing nAChRs is much higher than for the α4β2 nAChRs, the low expression of α3 nAChR in cortex and hippocampus (Gotti et al., 2006b; Jensen et al., 2005) and that the vast majority of nAChRs in the forebrain is the α4β2 nAChR subtype (Perry et al., 2002), [^{3}H]-epibatidine should be able to detect changes in α4β2 nAChR in our study.

When comparing the hand-drawn area of the ROIs of the different treatment groups in the autoradiographies, we observed that the area of hippocampus was significantly reduced in SAP-treated mice (P=0.0012) using two-way ANOVA, while there was no difference in area with respect to genotype in the region (See Figure 8). We found that the hippocampal volume loss was evident in both SAP-treated WT and Tg2576 mice (P=0.020 and P=0.027, respectively), when compared to the respective untreated mice using multiple t tests corrected with Holm-Sidak method.

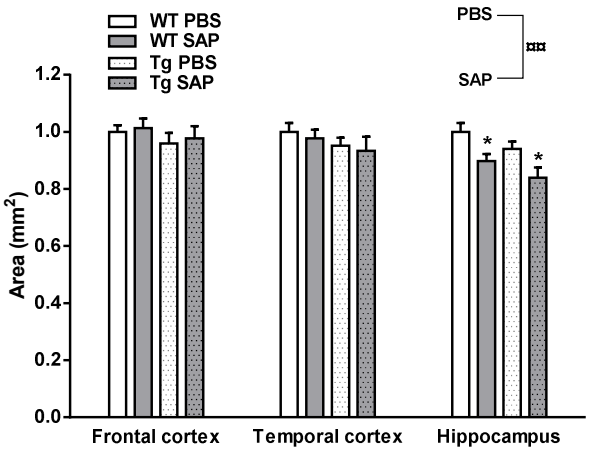

Figure 8. Reduced hippocampal volume in mice with cholinergic lesions by mu p75-saporin (SAP). The measured areas in the autoradiography analysis of Tg2576 mice (Tg) and their wildtype (WT) littermates treated with PBS or the immunotoxin mu 75-saporin (SAP). Data were normalized to the PBS-treated WT group. ¤¤ indicates $P<0.01$ main effect of treatment in a two-way ANOVA, *$P<0.05$ indicates statistical difference between PBS- and SAP-treated mice by multiple t tests corrected with Holm-Sidak method (n=10-16).

Hippocampal atrophy quantified by cresyl-violet staining has previously been demonstrated in 6-8 month old Tg2546 mice in CA1-2 and CA3 regions four weeks after SAP injections, while there were no changes observed in dental gyrus (Gil-Bea et al., 2012). Similar changes were seen with mRNA levels of synaptophysin by *in situ* hybridization in the three hippocampal regions. However, in contrast to our findings the hippocampal atrophy was not observed in SAP-treated WT mice, even though there was a tendency to decreased hippocampal area in the CA3 region in the SAP-treated WT group (Gil-Bea et al., 2012). The short period of only four weeks after the SAP injections in this study might account for the lack of hippocampal atrophy in SAP-treated WT mice. Moreover, SAP was injected in the third ventricle in this study, whereas the lateral ventricle was used as injection site in our study. In line to our data, hippocampal atrophy by acetylcholinesterase histochemical staining was shown in SAP-lesioned C57BL/6 mice, which underwent surgery at 6-7 weeks and were euthanized 55 days later (~15 weeks old), while no changes were observed in the non-treated mice (Moreau et al., 2008).

Recent studies investigating the combination of basal forebrain cholinergic degeneration and overexpression of Aβ in transgenic animals of AD suggest that these models lead to improved models of AD neuropathology and cognitive deficits. Thus, it was demonstrated that SAP-treated Tg2576 mice six months after the lesions had impaired cognitive performance in tests related to spatial working memory and long-term memory, which are correlated to hippocampal dysfunction (Laursen et al., 2014). In addition to deficits in spatial working memory, APPSwe/PS1 mice showed increased levels of both soluble and insoluble $A\beta_{1-42}$ and $A\beta_{1-40}$ only two months after SAP injections (Laursen et al., 2013). Increased non-fibrillar Aβ was also demonstrated in SAP-treated Tg2576 compared to non-treated Tg2576 mice (Gil-Bea et al., 2012), and lesions with SAP in APPSwe/PS1 and 3×Tg-AD transgenic mice with the lateral ventricle as injection site promoted Aβ

deposits as well as tau hyperphosphorylation in cortex and hippocampus (Härtig et al., 2014). It is thus interesting that we only see the reduction in [^{125}I]-α-Bgt binding in temporal cortex and hippocampus in the Tg2576 mice with SAP lesions, which have been demonstrated to have enhanced AD-like pathology and cognitive impairments. However, we did not see altered [^{125}I]-α-Bgt binding in frontal cortex, which is shown to be involved in cognitive functions such as working memory. α7 nAChRs in prefrontal cortex in mice and rats are shown to be localized mainly in postsynaptic dendrites by electron microscopy, and the majority of presynaptic cholinergic neurons were without detectable α7 nAChR (Duffy et al., 2009).

Whether the increased Aβ levels in the combined AD model are affecting the α7 nAChR levels or *vice versa* are not possible to elucidate from our study. However, a study crossing Tg2576 mice with α7 nAChR knock-out mice have shown enhanced Aβ oligomer accumulation, hippocampal volume loss, and more severe learning and memory deficits in these animals compared to Tg2576 mice, and α7 nAChR was therefore suggested to have a neuroprotective role in early AD (Hernandez et al., 2010). It has also been shown that the α-secretase ADAM17 was decreased in hippocampus of SAP-lesioned Tg2576 mice, which might limiting the release of neurotrophic factors causing higher vulnerability of hippocampus to amyloid toxicity (Gil-Bea et al., 2012). Deficiency of brain-derived neurotophic factor (BDNF) in hippocampus of AD patients has been reported (Zuccato and Cattaneo, 2009), and decreased BDNF levels was found in SAP-lesioned rats (Angelucci et al., 2011; Gil-Bea et al., 2011). Since BDNF has previously been demonstrated to increase α7 nAChR levels in cultured hippocampal neurons (Kawai et al., 2002; Massey et al., 2006), the BDNF deficits in AD may alter α7 nAChR levels.

Lesions of a neurotransmitter system, as has been done in our study, will undoubtly be influencing other neurotransmitter systems, which might lead to compensatory mechanisms. Even though the amount of injected SAP in our study was previously shown to have no collateral effects towards other neurotransmission systems (Berger-Sweeney et al., 2001; Hunter et al., 2004), unintended effects on secondary transmitter systems should be considered, when interpreting results in these specific lesion models.

In summary, we demonstrated that α7 nAChR levels measured by [^{125}I]-α-Bgt binding were reduced in temporal cortex and hippocampus in a animal model combining Aβ-overexpressing Tg2576 mice with basal forebrain cholinergic degeneration by the immunotoxin SAP, which could be a new model of AD to investigate the α7 nAChR function and the role of α7 nAChR agonists in cognition and AD pathology. We found no changes in non-α7 nAChRs with [^{3}H]-epibatidine

binding. Furthermore, we observed hippocampal degeneration following the SAP treatment in both WT and Tg2576 mice, while cortical areas were not affected.

Distribution of Lynx proteins and interaction with nicotinic receptors

Although several Lynx proteins have been demonstrated to modulate nAChR function (Miwa et al., 2011; Thomsen and Mikkelsen, 2012a), the studies have primarily been based on heterologous expression systems and transgenic mice, and thus not much is currently known about their distribution and characteristics in native rodent and human tissue.

In Paper II we investigated the subcellular distribution of the Lynx proteins, Lynx1 and Ly6H, in rat frontal cortex and hippocampus. Both proteins were found to be mainly expressed on the cell surface using the cell-impermeable protein cross-linking agent BS^3. Using fractionation of tissue homogenates into nuclear and synaptosmal fractions, Lynx1 was further demonstrated to be localized in the synaptosomes by significant higher levels in frontal cortex and hippocampus compared to the whole-cell homogenate, while Ly6H levels were only significantly increased in the synaptosomal fraction in hippocampus (see Paper II, Figure 2). However, when comparing the levels of Ly6H in the nuclear and synaptosomal fractions, a higher level of Ly6H was observed in the synaptosomal fraction. This was also the case with the β2 nAChR subunit in both brain regions. As a positive control for the fractionation, we used the ionotropic GluR2 receptor, which has previously been shown to be present in the synaptosomal fraction (Srivastava et al., 1998). In addition, Lypd6 was similar predominantly expressed on the cell surface and in synaptosomal fractions (Paper IV).

The presence of Lynx1, Ly6H, and Lypd6 in synaptosomal fractions suggests a synaptic function of these Lynx proteins possibly in terms of modulating synaptic signaling due to their interactions with nAChR. Presynaptic nAChRs, especially the α7 nAChR, have been shown to be involved in neurotransmitter release of dopamine, glutamate, GABA, and noradrenalin (reviewed in (Barik and Wonnacott, 2009; Wonnacott et al., 2006)). Thus, Lynx proteins might influence the release of neurotransmitters directly or indirectly induced by nAChRs.

We further investigated the cellular distribution by fractionating the rat and human cortical tissue into soluble and membrane fractions by ultracentrifugation. Lynx1 and Ly6H were exclusively found to be membrane-bound in rat cortical tissue (Paper II, Figure 3A). This was also found for Lypd6 in rat (Paper IV) as well as in human cortex (Paper III, Figure 1C). These findings correspond to Lynx proteins being tethered to the cell membrane via their GPI-anchor. Remarkably, PSCA was found to be soluble in human cortical tissue (Paper III, Figure 1C). Although PSCA

mRNA has been reported to contain a GPI anchor signaling site (Hruska et al., 2009; Reiter et al., 1998), the PSCA protein was found to be both secreted and cell-associated in PSCA-transfected 293T cells (Reiter et al., 1998). This indicate that PSCA act as a secreted protein and is not involved in chaperoning nAChRs as previously suggested for GPI-anchored Lynx proteins (Lester et al., 2009). The demonstration that Lynx1 is involved in the assembly of α4β2 nAChR within the cell by stabilizing dimerization of α4-α4 subunits (Nichols et al., 2014), indicates that the membrane-bound Lypd6 and Ly6H might also be playing a role in regulating the assembly of heteromeric nAChRs in the ER like Lynx1 perhaps involving other nAChR subtypes.

Lynx1 and Lynx2 have previously been demonstrated to co-immunoprecipitate with α7 and α4β2 nAChRs in transfected HEK293 cells and monkey bronchial epithelial cells (Fu et al., 2012; Ibanez-Tallon et al., 2002; Tekinay et al., 2009). Furthermore, Lynx1 and α4 nAChR subunits co-immunoprecipitated, when the β2 nAChR subunit was not present, whereas no co-immunoprecipitation of Lynx1 and β2 nAChR subunits was detected (Nichols et al., 2014). Here, we demonstrated that PSCA formed stable complex with the α4 but not the α7 nAChR subunit in human cortical tissue using affinity purification (Paper III, Figure 1D). To our knowledge this is the first time that PSCA has been reported to bind to nAChR subunits, and the first time that a Lynx protein is demonstrated to form complexes with nAChR subunits in native tissue, since previous studies have been carried out in heterologous expression systems. In addition, both Lynx1 and Lypd6 were shown to form complexes with several nAChR subunits in the human brain (Paper IV and V).

Interactions between α4 nAChR and PSCA have not previously been reported. However, PSCA has been suggested to act as a negative modulator of α7 nAChRs by reducing nicotine-induced calcium influx in chicken ciliary ganglion neurons (Hruska et al., 2009). The antagonism of α7 nAChRs was demonstrated in chicken embryos infected with PSCA resulting in overexpression of PSCA at an age, where PSCA under normal conditions was almost undetectable. In addition, the nicotine-induced calcium influx response was only blocked by 50% with MLA (Hruska et al., 2009) indicating that other nAChR subunits could be involved in the effect. Alternatively, the lack of binding could be a methodological issue, where the binding between PSCA and the α7 nAChR subunit is not strong enough to be detected in our assay or that binding of PSCA to nAChR subunits differs between species, as has been shown for Lynx1 (Lyukmanova et al., 2011).

Perinatal administration of nicotine was shown to increase Lypd6 protein levels in hippocampus of adult rat offspring, where the increase of Lypd6 expression was observed to be

mostly evident in the nuclear fraction and not in the synaptosomal fraction (Paper IV). To further study the effects of nicotine exposure, we administered nicotine, 0.4 mg/kg nicotine (free base weight) or vehicle (0.9% saline) subcutaneously (s.c.) twice daily for 7 days, to young (postnatal day 8-14) and adult (postnatal day 54-60) rats, which were sacrificed 4 hours after the last administration followed by dissection of frontal cortex and hippocampus. Short-term nicotine exposure did not alter protein levels of Lypd6, Ly6H, or Lynx1 in either the young (see Figure 9) or the adult rats, suggesting that Lypd6 is more sensitive to regulation by nicotine during early development.

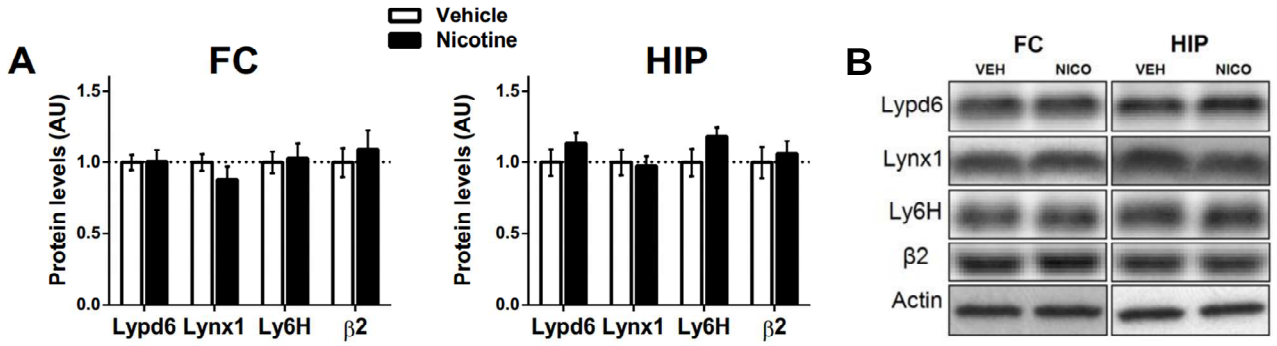

Figure 9. Short-term nicotine exposure does not alter Lypd6, Lynx1 or Ly6H levels in the brain. (A) Lypd6, Lynx1, Ly6H, and β2 nAChR subunit protein levels were analyzed in frontal cortex (FC) and hippocampal (HIP) tissue from rats administered nicotine (NICO; 0.4 mg/kg s.c., b.i.s.) or vehicle (VEH; 0.9% saline) for 7 days from postnatal day 8-14. Data were normalized to Actin and the vehicle group was set to 1. **(B)** Representative images of western blots summarized in **(A)**.

We further demonstrated that administration of PSCA did not alter the expression of β2 nAChR subunit in PC12 cells and neither did silencing of PSCA using PSCA siRNA (Paper III, Figure 2C and 2E). However, in order to investigate whether Lynx proteins had an effect on nAChR function, we found that 10 µM PSCA inhibited nicotine-induced phosphorylation of the MAP kinase ERK in undifferentiated PC12 cells. This was also shown for Lypd6 and Lynx1 at the same concentration (Paper IV and V). Although it is a relative high concentration, it correspond to the concentrations of Lynx1 required to compete with [^{125}I]-α-Bgt binding to ACh binding proteins (IC_{50} ~10 µM). Moreover, 10 µM Lynx1 inhibited ACh-induced currents in *Xenopus* oocytes expressing α7, α4β2, and α3β2 nAChRs, while 1 µM Lynx1 did not (Lyukmanova et al., 2011). It is interesting that the concentration needed to inhibit the nicotine-induced effects is similar for secreted and membrane-bound Lynx proteins. Lypd6 and Lynx1 are supposed to be in close proximity to the nAChRs due to their GPI-anchors, whereas PSCA is required to be secreted in high concentrations to affect nAChR function.

Activation of the intracellular MAPK/ERK signaling pathway by phosphorylation is particular interesting, since it plays a crucial role in the formation of LTP and memory in hippocampus (Adams and Sweatt, 2002). The effect of nicotine on ERK phosphorylation has been shown to be dependent on α3β4-containing nAChRs (Nakayama et al., 2006), but other studies are also suggested involvement of α7 nAChRs in this effect (El Kouhen et al., 2009; Gubbins et al., 2010). Although these findings suggest that PSCA, Lypd6, and Lynx1 are modulating the function of α3β4 and possibly also α7 nAChRs, it does not exclude that these Lynx proteins are able to regulate other nAChR subtypes in the brain.

Previously, Lypd6 was shown to enhance calcium currents through nAChRs (Darvas et al., 2009), whereas in our study Lypd6 was demonstrated to reduce nicotine-induced ERK phosphorylation (Paper IV). This discrepancy might be due to different forms of Lypd6, where Darvas et al. used transgenic mice overexpressing Lypd6, and we used soluble recombinant Lypd6 protein. Lynx1 has previously been shown to affect nAChR function differently, when it was administered in a soluble form (Miwa et al., 1999).

In summary, we found that Lynx1, Ly6H, and Lypd6 were primarily expressed on the cell surface and localized to synaptosomal fractions suggesting a presynaptic function of these Lynx proteins. Furthermore, Lynx1, Ly6H, and Lypd6 were exclusively membrane-bound, whereas PSCA was found to be soluble in human cortical tissue. Short-term nicotine exposure did not alter expression of Lynx1, Ly6H, and Lypd6 in young and adult rats, suggesting that nicotine can only affect Lynx protein levels in early development, since Lypd6 was upregulated in hippocampus of adult rats after perinatal nicotine administration. Finally, PSCA was demonstrated to bind the α4 nAChR subunit and to modulate the effect of nicotine-induced response in PC12 cells similar to the other Lynx proteins, Lynx1 and Lypd6. These findings led us to further investigate Lynx proteins in AD, where nAChRs have been found to by dysregulated.

Lynx proteins levels are altered in Alzheimer's disease

Lypd6 along with Lynx1 and Lynx2 have been suggested to be involved in cognitive function in rodents (Darvas et al., 2009; Miwa et al., 2006; Tekinay et al., 2009), and several studies have proposed a correlation between nAChR levels and cognitive deficits in AD (Okada et al., 2013; Sarter et al., 2009). Since we demonstrated that PSCA and Lypd6 bind to and modulate nAChRs, we therefore studied whether their protein levels were altered in postmortem brains from AD patients and in two transgenic mouse models of AD, 3×Tg-AD and Tg2576 mice, using western blotting.

In Paper III we found that PSCA levels were increased by ~70% in medial frontal gyrus of AD patients, while Lypd6 levels were unaltered (Paper III, Figure 3). Given that PSCA was shown to bind to the α4 nAChR subunit and was reducing nicotine-mediated responses, enhanced protein levels of PSCA might result in negative regulation of nAChR function in AD patients. Thus, if PSCA is able to modulate α4β2 nAChR similar to Lynx1 (Ibanez-Tallon et al., 2002), the reduced function of the receptor might negatively affect the cognitive performance in AD patients, mainly on attentional and executive function, as previously described (Okada et al., 2013; Sarter et al., 2009). Remarkably, PSCA is not the first member of the Lynx protein family, which is associated to AD. The Lynx protein CD59, mainly involved in the innate immune system, has been reported to be decreased in frontal cortex and hippocampus of AD patients and suggested to play a role in neurodegeneration of AD (Yang et al., 2000). Although Lypd6 has been found to modulate nAChR function, we found no alterations in Lypd6 levels in AD brain.

In addition to the changes in PSCA levels, the level of β2 nAChR subunit was shown to be significantly decreased in AD patients, which correspond to previous studies demonstrating regulation of α4β2 expression in frontal cortex of AD patients. Hence, α4β2 binding *in vivo* was demonstrated to be reduced in frontal cortex of patients with mild cognitive impairment and AD (Kendziorra et al., 2011) as well as in patients with early-to-moderate stage AD, which correlated with amyloid deposits determined by high [^{11}C]-PiB uptake (Okada et al., 2013). Furthermore, α4β2 binding *in vitro* was reduced in postmortem frontal cortical tissue of AD patients using [^{3}H]-nicotine autoradiography (Marutle et al., 2013).

To further investigate if the altered PSCA levels were related to AD pathophysiology, we determined the protein levels of PSCA, Lypd6, and the β2 nAChR subunit in 3×Tg-AD and Tg2576 mice. Similar to the findings in AD patients, we found that PSCA and β2 subunit levels were altered in the frontal cortex of 3×Tg-AD mice that display both Aβ and tau pathology, where the alterations were primarily found in the 6 month old 3×Tg-AD mice compared to the 19-21 month old group (see Paper III, Figure 4A). Levels of PSCA and β2 nAChR subunit were not significantly altered in hippocampus of the 3×Tg-AD mice although there were tendencies resembling the finding in frontal cortex. No alterations of Lypd6 were found in both frontal cortex and hippocampus of the 3×Tg-AD mice. When investigating the Tg2576 mice, that display increased Aβ levels by overexpressing APP, we found no changes in the protein levels of PSCA, Lypd6, and the β2 nAChR subunit in the frontal cortex.

Our findings in the two transgenic models of AD suggest that increased expression of Aβ alone is not sufficient to alter the protein levels of PSCA and β2 nAChR subunit. The progression of amyloid plaque depositions is very different in the two animal models. Tg2576 mice display a slower accumulation of Aβ than the 3×Tg-AD mice and is described as a late amyloid plaque model, while the 3×Tg-AD model, which carry both mutations in APP and PS1, is considered to be an early plaque model with accelerated plaque formation from a young age (Lee and Han, 2013). Thus, the lack of effect might be due to lower Aβ load in the Tg2576 mice. However, it should be noted that the mice were represented in different age groups. We assumed that Aβ concentration was more or less equivalent in 6 month old the 3×Tg-AD mice and 15 month old Tg2576 mice due to the slower rate of plaque formation in the latter animal model.

Using immunofluorescence labeling, it was further demonstrated that the 6 month old 3×Tg-AD mice were devoid of amyloid plaques and tau hyperphosphorylation, but displayed low intracellular Aβ immunoreactivity, while 21 month old 3×Tg-AD mice were shown to have pronounced AD-like pathology in frontal cortex and hippocmpus. Thus, these data indicate that the regulation of PSCA levels occurred prior to the formation of amyloid plaques and neurofibrillary tangles in 3×Tg-AD mice, suggesting that PSCA regulation is an early event in the progression of AD pathology in this transgenic model. However, soluble, oligomeric forms of Aβ, which are shown to be more neurotoxic than plaques (Walsh and Selkoe, 2007), might be influencing the PSCA levels at this age. In addition, differences in the plaque composition in AD transgenic have been reported, where the Aβ plaques in Tg2576 mice are composed of Aβ monomers, while the 3×Tg-AD mice generate monomeric, dimeric, and oligomeric Aβ peptides (Kokjohn and Roher, 2009).

It was not possible to validate the hypothesis that PSCA levels may be a precursor to stages of plaque overload in the AD patients, since they were all in later stages of AD. The AD pathology in 3×Tg-AD mice has some similarities to the pathogenesis in AD patients (Bilkei-Gorzo, 2014), where Aβ depositions are first evident in cortical regions and later in hippocampus, while tau pathology begins in the limbic regions and then proceed to cortical regions (Oddo et al., 2003). However, although AD-like pathological conditions are present in the transgenic mice, it is merely a model and only reproduces some of the neuropathological and behavioural features of AD, and Aβ and tau pathology is evident in other neurodegenerative disorders as well as aged non-demented individuals (Kokjohn and Roher, 2009). Furthermore, it is difficult to compare the progression of AD in patients with the appearance of pathology in transgenic mice.

The enhanced PSCA protein levels and the reduced β2 nAChR subunit levels in frontal cortex of AD patients and 3×Tg-AD mice may suggest that altered expression of β2 nAChR is a consequence of the changes in PSCA levels or *vice versa*. However, we did not detect alteration in β2 nAChR expression in PC12 cells at either mRNA nor protein levels in the absence and presence of PSCA, respectively. These assays were cell-based and not involving AD pathology, and therefore does not preclude that PSCA could be modulating expression of β2 nAChR subunit in native tissue and/or under AD pathological conditions.

To test whether other Lynx proteins were affected by AD-like pathology, we investigated Lynx1 protein levels in frontal cortex of the 6 and 19-21 month old 3×Tg-AD mice. We found that the levels of Lynx1 were decreased in 3×Tg-AD mice compared to age-matched WT mice (Figure 10). Remarkably, we also found that the Lynx1 levels were increased with age. Thus, these findings are opposite to our data on PSCA in 3×Tg-AD mice, but correspond to the previous study in AD patients with CD59 (Yang et al., 2000). Unfortunately, we were not able to detect Lynx1 protein in the human tissue with the available assays. The age-dependent increase in Lynx1 levels suggests that the expression of Lynx1 is not stable throughout adulthood. Previously, mRNA and protein levels of Lynx1 were demonstrated to be increased at postnatal day 60 when compared to postnatal day 18 and 28 in visual cortex mice (Morishita et al., 2010). In rat frontal cortex, Lynx1 mRNA and protein levels increased dramatically from birth until postnatal day 26, but then stabilized until postnatal day 60 (Paper II).

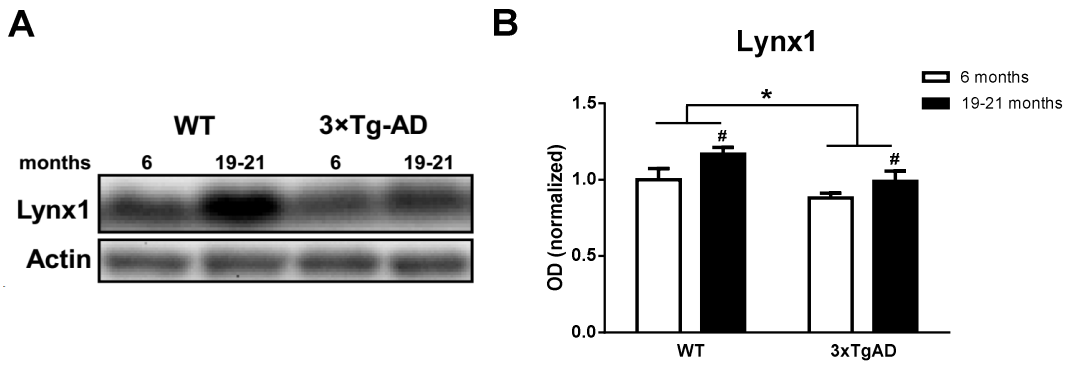

Figure 10. Lynx1 protein levels are decreased in frontal cortex of mice with amyloid and tau pathology. Lynx1 levels were analyzed in frontal cortical extracts from 3×Tg-AD transgenic mice, which display β-amyloidosis and tau hyperphosphorylation and age-mathched wildtype (WT) animals. Mice were sacrificed at 6 or 19-21 months of age. **(A)** Representative images of Lynx1 and Actin western blots. **(B)** Quantification of Lynx1 levels normalized to Actin levels and the 6 month old WT group was set to 1. * and # indicate $P<0.05$ main effects of genotype and age, respectively, in a two-way ANOVA (n=7-8).

Interestingly, oligomeric $A\beta_{1-42}$ was demonstrated to inhibit the interaction between Lynx1 and α3, α4, α5, and α7 nAChR subunits using the affinity purification assay (Paper V). The presence of $A\beta_{1-}$

$_{42}$ did not affect the binding of any of the β-subtype subunits, and the reverse peptide $A\beta_{42-1}$ had no effect on the Lynx1-nAChR binding, indicating that the effect was specific to $A\beta_{1-42}$. These data suggest that Lynx1 and $A\beta_{1-42}$ compete for the same or overlapping binding site of these α-subtype subunits. Given that α7 nAChR was shown to be involved in the internalization of $A\beta_{1-42}$ (Nagele et al., 2002), and that intracellular Aβ is suggested to trigger cognitive deficits in 3×Tg-AD mice (Billings et al., 2005), the dissociation of Aβ-nAChR binding by Lynx1 may improve the cognitive impairments in AD.

In summary, we found that PSCA was increased along with decreased β2 nAChR subunit levels in frontal cortex of AD patients and in 3×Tg-AD mice, while their protein levels were unaltered in the Aβ-overexpressing Tg2576 mice, indicating that the presence of Aβ pathology is not sufficient to regulate PSCA and β2 subunit levels. Lypd6 were unaltered in AD patients as well as in the two transgenic animal models of AD. Furthermore, the alterations of PSCA and β2 nAChR were shown to be prior to the appearance of AD characteristics in relation to Aβ plaque and neurofibrillary tangle formation in 3×Tg-AD mice, suggesting that the regulation of PSCA is an early event in the progression of AD-like pathology in this animal model. Lastly, in frontal cortex of 3×Tg-AD mice a reduction in Lynx1 levels was demonstrated. The alterations of Lynx proteins in AD may be due to a direct interaction between Lynx proteins and Aβ as shown with Lynx1. Thus, with the demonstration that some Lynx proteins are dysregulated in AD, the interactions of these Lynx proteins with nAChRs and/or Aβ may affect cognitive function related to AD.

Conclusion and Perspectives

The results in this thesis provide further knowledge regarding α7 nAChR and Lynx proteins in animals and humans as well as their relation to AD. Especially the novel findings that some Lynx proteins are regulated in AD may promote further investigations of their role in both healthy and diseased states.

In Paper I, we demonstrated the importance of studying the α7 nAChR in human tissue. A partial duplication of the gene encoding the α7 nAChR subunit, *CHRFAM7A*, was found in all human individuals, and the ratio of the α7 nAChR subunit gene, *CHRNA7*, to the *CHRFAM7A* mRNA levels was determined to be 3.4. Displacement of α7 nAChR selective antagonist [^{125}I]-α-Bgt with the partial α7 nAChR agonist encenicline revealed high variability between the human individuals, and indicated that encenicline in some individuals displayed two different binding modes, which suggests that the efficacy of encenicline may be altered in the these individuals. Since mutations in *CHRNA7* and *CHRFAM7A* are associated to SCZ and the gene products of *CHRFAM7A* regulate α7 nAChR function, the *CHRFAM7A* genotype might affect the efficacy of α7 nAChR compounds such as encenicline when used in treatment of cognitive deficits in AD and SCZ, which may underlie the large variation in responses to the α7 nAChR modulators observed in clinical trials. Furthermore, transgenic expression of *CHRFAM7A* in rodent models might prove to be highly relevant to elucidate the role of *CHRFAM7A* gene products *in vivo*, which has not been possible so far.

We further investigated α7 nAChR levels in a combined animal model of AD and demonstrated that [^{125}I]-α-Bgt was decreased in temporal cortex and hippocampus in Tg2576 mice with basal forebrain cholinergic degeneration by the immunotoxin SAP, while there were no alterations in levels of non-α7 nAChRs with [^{3}H]-epibatidine binding in these mice. Despite the inconsistent results that both decreased and unaltered levels of α7 nAChRs have been reported in AD patients, the combination of Aβ pathology with selective cholinergic degeneration could be a new improved animal model to gain further knowledge of the α7 nAChR function in AD, as well as the role of α7 nAChR agonists, e.g. encenicline, or modulators, e.g. Lynx proteins, in cognitive performance and AD pathology.

In Paper II and III, we demonstrated the cellular distribution of Lynx proteins in rats and humans. Ly6H, Lynx1, and Lypd6 were all found to be primarily expressed at the cell surface and in synaptosomal fractions, indicating a synaptic function of these proteins. Neurotransmitter release

assays could be used to test, whether Lynx proteins are involved in regulating nAChR-mediated release of neurotransmitters. PSCA was in contrast to Ly6H, Lynx1, and Lypd6 demonstrated to be exclusively expressed in a soluble form, suggesting that this protein might be able to exert different effects than the other Lynx proteins in regulating the function and/or expression of nAChRs. Furthermore, PSCA was shown to bind the α4 nAChR subunit and modulate nicotine-induced response in PC12 cells similar to Lynx1 and Lypd6, indicating that PSCA might be a new target to modulate the function of nAChRs.

In Paper III, we further investigated Lynx proteins in AD and demonstrated increased PSCA and decreased β2 nAChR subunit protein levels in frontal cortex of AD patients as well as in 3×Tg-AD mice, displaying both Aβ and tau pathology, where the Tg2576 mice with only Aβ pathology showed no alterations in PSCA or β2 subunit levels, suggesting that the presence of Aβ is not driving the regulation of PSCA and β2 nAChR alone. Lypd6 was not regulated in AD, but decreased Lynx1 levels were shown in frontal cortex of 3×Tg-AD mice. In addition, immunofluorescence labeling revealed that the regulation of PSCA and Lynx1 could be an early event in the progression of AD-like pathology in 3×Tg-AD mice. Further studies are needed to validate whether PSCA is driving changes in β2 nAChR expression and/or AD pathology *in vivo*. Crossing PSCA or Lynx1 KO mice with transgenic AD models such as the 3×Tg-AD mice could also elucidate the role of these proteins in AD, and how they might affect cognitive function in relation to AD. These findings open up for further investigation into the function of Lynx proteins in both developmental and adult disorders especially those, where nAChRs are shown to be involved.

References

Abdolmaleky, H.M., Nohesara, S., Ghadirivasfi, M., Lambert, A.W., Ahmadkhaniha, H., Ozturk, S., Wong, C.K., Shafa, R., Mostafavi, A., Thiagalingam, S., 2014. DNA hypermethylation of serotonin transporter gene promoter in drug naive patients with schizophrenia. Schizophr Res 152, 373-380.

Adams, C.E., Stevens, K.E., 2007. Evidence for a role of nicotinic acetylcholine receptors in schizophrenia. Front Biosci 12, 4755-4772.

Adams, J.P., Sweatt, J.D., 2002. Molecular psychology: roles for the ERK MAP kinase cascade in memory. Annu Rev Pharmacol Toxicol 42, 135-163.

Adermann, K., Wattler, F., Wattler, S., Heine, G., Meyer, M., Forssmann, W.G., Nehls, M., 1999. Structural and phylogenetic characterization of human SLURP-1, the first secreted mammalian member of the Ly-6/uPAR protein superfamily. Protein Sci 8, 810-819.

Albuquerque, E.X., Pereira, E.F., Alkondon, M., Rogers, S.W., 2009. Mammalian nicotinic acetylcholine receptors: from structure to function. Physiol Rev 89, 73-120.

Alkondon, M., Pereira, E.F., Cortes, W.S., Maelicke, A., Albuquerque, E.X., 1997. Choline is a selective agonist of alpha7 nicotinic acetylcholine receptors in the rat brain neurons. Eur J Neurosci 9, 2734-2742.

Alzheimer, A., 1907. Uber eine eigenartige Erkrankung der Hirnrinde. Allg Z Psychiatrie Psychisch-Gerichtlich Med 64, 146-148.

Angelucci, F., Croce, N., Spalletta, G., Dinallo, V., Gravina, P., Bossu, P., Federici, G., Caltagirone, C., Bernardini, S., 2011. Paroxetine rapidly modulates the expression of brain-derived neurotrophic factor mRNA and protein in a human glioblastoma-astrocytoma cell line. Pharmacology 87, 5-10.

Apelt, J., Kumar, A., Schliebs, R., 2002. Impairment of cholinergic neurotransmission in adult and aged transgenic Tg2576 mouse brain expressing the Swedish mutation of human beta-amyloid precursor protein. Brain Res 953, 17-30.

Aracava, Y., Pereira, E.F., Maelicke, A., Albuquerque, E.X., 2005. Memantine blocks alpha7* nicotinic acetylcholine receptors more potently than n-methyl-D-aspartate receptors in rat hippocampal neurons. J Pharmacol Exp Ther 312, 1195-1205.

Araud, T., Graw, S., Berger, R., Lee, M., Neveu, E., Bertrand, D., Leonard, S., 2011. The chimeric gene CHRFAM7A, a partial duplication of the CHRNA7 gene, is a dominant negative regulator of alpha7*nAChR function. Biochem Pharmacol 82, 904-914.

Arredondo, J., Chernyavsky, A.I., Jolkovsky, D.L., Webber, R.J., Grando, S.A., 2006. SLURP-2: A novel cholinergic signaling peptide in human mucocutaneous epithelium. J Cell Physiol 208, 238-245.

Arredondo, J., Chernyavsky, A.I., Webber, R.J., Grando, S.A., 2005. Biological effects of SLURP-1 on human keratinocytes. J Invest Dermatol 125, 1236-1241.

Auld, D.S., Kornecook, T.J., Bastianetto, S., Quirion, R., 2002. Alzheimer's disease and the basal forebrain cholinergic system: relations to beta-amyloid peptides, cognition, and treatment strategies. Prog Neurobiol 68, 209-245.

Bamezai, A., 2004. Mouse Ly-6 proteins and their extended family: markers of cell differentiation and regulators of cell signaling. Arch Immunol Ther Exp (Warsz) 52, 255-266.

Barik, J., Wonnacott, S., 2009. Molecular and cellular mechanisms of action of nicotine in the CNS. Handb Exp Pharmacol 173-207.

Bartus, R.T., Dean, R.L., 3rd, Beer, B., Lippa, A.S., 1982. The cholinergic hypothesis of geriatric memory dysfunction. Science 217, 408-414.

Bartus, R.T., Flicker, C., Dean, R.L., Pontecorvo, M., Figueiredo, J.C., Fisher, S.K., 1985. Selective memory loss following nucleus basalis lesions: long term behavioral recovery despite persistent cholinergic deficiencies. Pharmacol Biochem Behav 23, 125-135.

Bednar, I., Zhang, X., Dastranj-Sedghi, R., Nordberg, A., 1998. Differential changes of nicotinic receptors in the rat brain following ibotenic acid and 192-IgG saporin lesions of the nucleus basalis magnocellularis. Int J Dev Neurosci 16, 661-668.

Berger-Sweeney, J., Stearns, N.A., Murg, S.L., Floerke-Nashner, L.R., Lappi, D.A., Baxter, M.G., 2001. Selective immunolesions of cholinergic neurons in mice: effects on neuroanatomy, neurochemistry, and behavior. J Neurosci 21, 8164-8173.

Bierer, L.M., Haroutunian, V., Gabriel, S., Knott, P.J., Carlin, L.S., Purohit, D.P., Perl, D.P., Schmeidler, J., Kanof, P., Davis, K.L., 1995. Neurochemical correlates of dementia severity in Alzheimer's disease: relative importance of the cholinergic deficits. J Neurochem 64, 749-760.

Bilkei-Gorzo, A., 2014. Genetic mouse models of brain ageing and Alzheimer's disease. Pharmacol Ther 142, 244-257.

Billings, L.M., Oddo, S., Green, K.N., McGaugh, J.L., LaFerla, F.M., 2005. Intraneuronal Abeta causes the onset of early Alzheimer's disease-related cognitive deficits in transgenic mice. Neuron 45, 675-688.

Bitner, R.S., Bunnelle, W.H., Anderson, D.J., Briggs, C.A., Buccafusco, J., Curzon, P., Decker, M.W., Frost, J.M., Gronlien, J.H., Gubbins, E., Li, J., Malysz, J., Markosyan, S., Marsh, K., Meyer, M.D., Nikkel, A.L., Radek, R.J., Robb, H.M., Timmermann, D., Sullivan, J.P., Gopalakrishnan, M., 2007. Broad-spectrum efficacy across cognitive domains by alpha7 nicotinic acetylcholine receptor agonism correlates with activation of ERK1/2 and CREB phosphorylation pathways. J Neurosci 27, 10578-10587.

Bloem, B., Poorthuis, R.B., Mansvelder, H.D., 2014. Cholinergic modulation of the medial prefrontal cortex: the role of nicotinic receptors in attention and regulation of neuronal activity. Front Neural Circuits 8, *in press.*

Boess, F.G., De Vry, J., Erb, C., Flessner, T., Hendrix, M., Luithle, J., Methfessel, C., Riedl, B., Schnizler, K., van der Staay, F.J., van Kampen, M., Wiese, W.B., Koenig, G., 2007. The novel alpha7 nicotinic acetylcholine receptor agonist N-[(3R)-1-azabicyclo[2.2.2]oct-3-yl]-7-[2-(methoxy)phenyl]-1-benzofuran-2-carboxa mide improves working and recognition memory in rodents. J Pharmacol Exp Ther 321, 716-725.

Buccafusco, J.J., Terry, A.V., Jr., Decker, M.W., Gopalakrishnan, M., 2007. Profile of nicotinic acetylcholine receptor agonists ABT-594 and A-582941, with differential subtype selectivity, on delayed matching accuracy by young monkeys. Biochem Pharmacol 74, 1202-1211.

Buckingham, S.D., Jones, A.K., Brown, L.A., Sattelle, D.B., 2009. Nicotinic acetylcholine receptor signalling: roles in Alzheimer's disease and amyloid neuroprotection. Pharmacol Rev 61, 39-61.

Bustin, S.A., Benes, V., Garson, J.A., Hellemans, J., Huggett, J., Kubista, M., Mueller, R., Nolan, T., Pfaffl, M.W., Shipley, G.L., Vandesompele, J., Wittwer, C.T., 2009. The MIQE guidelines: minimum information for publication of quantitative real-time PCR experiments. Clin Chem 55, 611-622.

Cachelin, A.B., Rust, G., 1994. Unusual pharmacology of (+)-tubocurarine with rat neuronal nicotinic acetylcholine receptors containing beta 4 subunits. Mol Pharmacol 46, 1168-1174.

Canastar, A., Logel, J., Graw, S., Finlay-Schultz, J., Osborne, C., Palionyte, M., Drebing, C., Plehaty, M., Wilson, L., Eyeson, R., Leonard, S., 2012. Promoter methylation and tissue-specific transcription of the alpha7 nicotinic receptor gene, CHRNA7. J Mol Neurosci 47, 389-400.

Carson, R., Craig, D., Hart, D., Todd, S., McGuinness, B., Johnston, J.A., O'Neill, F.A., Ritchie, C.W., Passmore, A.P., 2008a. Genetic variation in the alpha 7 nicotinic acetylcholine receptor is associated with delusional symptoms in Alzheimer's disease. Neuromolecular Med 10, 377-384.

Carson, R., Craig, D., McGuinness, B., Johnston, J.A., O'Neill, F.A., Passmore, A.P., Ritchie, C.W., 2008b. Alpha7 nicotinic acetylcholine receptor gene and reduced risk of Alzheimer's disease. J Med Genet 45, 244-248.

Castro, N.G., Albuquerque, E.X., 1993. Brief-lifetime, fast-inactivating ion channels account for the alpha-bungarotoxin-sensitive nicotinic response in hippocampal neurons. Neurosci Lett 164, 137-140.

Chang, Q., Gold, P.E., 2004. Impaired and spared cholinergic functions in the hippocampus after lesions of the medial septum/vertical limb of the diagonal band with 192 IgG-saporin. Hippocampus 14, 170-179.

Changeux, J.P., 2010. Nicotine addiction and nicotinic receptors: lessons from genetically modified mice. Nat Rev Neurosci 11, 389-401.

Chimienti, F., Hogg, R.C., Plantard, L., Lehmann, C., Brakch, N., Fischer, J., Huber, M., Bertrand, D., Hohl, D., 2003. Identification of SLURP-1 as an epidermal neuromodulator explains the clinical phenotype of Mal de Meleda. Hum Mol Genet 12, 3017-3024.

Chipana, C., Torres, I., Camarasa, J., Pubill, D., Escubedo, E., 2008. Memantine protects against amphetamine derivatives-induced neurotoxic damage in rodents. Neuropharmacology 54, 1254-1263.

Christensen, D.Z., Mikkelsen, J.D., Hansen, H.H., Thomsen, M.S., 2010. Repeated administration of alpha7 nicotinic acetylcholine receptor (nAChR) agonists, but not positive allosteric modulators, increases alpha7 nAChR levels in the brain. J Neurochem 114, 1205-1216.

Contestabile, A., 2011. The history of the cholinergic hypothesis. Behav Brain Res 221, 334-340.

Cook, L.J., Ho, L.W., Taylor, A.E., Brayne, C., Evans, J.G., Xuereb, J., Cairns, N.J., Pritchard, A., Lemmon, H., Mann, D., St Clair, D., Turic, D., Hollingworth, P., Moore, P.J., Jehu, L., Archer, N., Walter, S., Foy, C., Edmondson, A., Powell, J., Lovestone, S., Owen, M.J., Williams, J., Lendon, C., Rubinsztein, D.C., 2004. Candidate gene association studies of the alpha 4 (CHRNA4) and beta 2 (CHRNB2) neuronal nicotinic acetylcholine receptor subunit genes in Alzheimer's disease. Neurosci Lett 358, 142-146.

Court, J., Martin-Ruiz, C., Piggott, M., Spurden, D., Griffiths, M., Perry, E., 2001. Nicotinic receptor abnormalities in Alzheimer's disease. Biol Psychiatry 49, 175-184.

Criado, M., Valor, L.M., Mulet, J., Gerber, S., Sala, S., Sala, F., 2012. Expression and functional properties of alpha7 acetylcholine nicotinic receptors are modified in the presence of other receptor subunits. J Neurochem 123, 504-514.

Dalley, J.W., Cardinal, R.N., Robbins, T.W., 2004. Prefrontal executive and cognitive functions in rodents: neural and neurochemical substrates. Neurosci Biobehav Rev 28, 771-784.

Dani, J.A., Bertrand, D., 2007. Nicotinic acetylcholine receptors and nicotinic cholinergic mechanisms of the central nervous system. Annu Rev Pharmacol Toxicol 47, 699-729.

Darvas, M., Morsch, M., Racz, I., Ahmadi, S., Swandulla, D., Zimmer, A., 2009. Modulation of the Ca2+ conductance of nicotinic acetylcholine receptors by Lypd6. Eur Neuropsychopharmacol 19, 670-681.

Davies, P., Feisullin, S., 1981. Postmortem stability of alpha-bungarotoxin binding sites in mouse and human brain. Brain Res 216, 449-454.

De Luca, V., Likhodi, O., Van Tol, H.H., Kennedy, J.L., Wong, A.H., 2006a. Regulation of alpha7-nicotinic receptor subunit and alpha7-like gene expression in the prefrontal cortex of patients with bipolar disorder and schizophrenia. Acta Psychiatr Scand 114, 211-215.

De Luca, V., Voineskos, S., Wong, G., Kennedy, J.L., 2006b. Genetic interaction between alpha4 and beta2 subunits of high affinity nicotinic receptor: analysis in schizophrenia. Exp Brain Res 174, 292-296.

de Lucas-Cerrillo, A.M., Maldifassi, M.C., Arnalich, F., Renart, J., Atienza, G., Serantes, R., Cruces, J., Sanchez-Pacheco, A., Andres-Mateos, E., Montiel, C., 2011. Function of partially duplicated human alpha77 nicotinic receptor subunit CHRFAM7A gene: potential implications for the cholinergic anti-inflammatory response. J Biol Chem 286, 594-606.

Dorszewska, J., Florczak, J., Rozycka, A., Jaroszewska-Kolecka, J., Trzeciak, W.H., Kozubski, W., 2005. Polymorphisms of the CHRNA4 gene encoding the alpha4 subunit of nicotinic acetylcholine receptor as related to the oxidative DNA damage and the level of apoptotic proteins in lymphocytes of the patients with Alzheimer's disease. DNA Cell Biol 24, 786-794.

Dougherty, J.J., Wu, J., Nichols, R.A., 2003. Beta-amyloid regulation of presynaptic nicotinic receptors in rat hippocampus and neocortex. J Neurosci 23, 6740-6747.

Drachman, D.A., Leavitt, J., 1974. Human memory and the cholinergic system. A relationship to aging? Arch Neurol 30, 113-121.

Duffy, A.M., Zhou, P., Milner, T.A., Pickel, V.M., 2009. Spatial and intracellular relationships between the alpha7 nicotinic acetylcholine receptor and the vesicular acetylcholine transporter in the prefrontal cortex of rat and mouse. Neuroscience 161, 1091-1103.

Dunkley, P.R., Jarvie, P.E., Robinson, P.J., 2008. A rapid Percoll gradient procedure for preparation of synaptosomes. Nat Protoc 3, 1718-1728.

Dziewczapolski, G., Glogowski, C.M., Masliah, E., Heinemann, S.F., 2009. Deletion of the alpha 7 nicotinic acetylcholine receptor gene improves cognitive deficits and synaptic pathology in a mouse model of Alzheimer's disease. J Neurosci 29, 8805-8815.

El Kouhen, R., Hu, M., Anderson, D.J., Li, J., Gopalakrishnan, M., 2009. Pharmacology of alpha7 nicotinic acetylcholine receptor mediated extracellular signal-regulated kinase signalling in PC12 cells. Br J Pharmacol 156, 638-648.

Ewald, E.R., Wand, G.S., Seifuddin, F., Yang, X., Tamashiro, K.L., Potash, J.B., Zandi, P., Lee, R.S., 2014. Alterations in DNA methylation of Fkbp5 as a determinant of blood-brain correlation of glucocorticoid exposure. Psychoneuroendocrinology 44, 112-122.

Faraone, S.V., Su, J., Taylor, L., Wilcox, M., Van Eerdewegh, P., Tsuang, M.T., 2004. A novel permutation testing method implicates sixteen nicotinic acetylcholine receptor genes as risk factors for smoking in schizophrenia families. Hum Hered 57, 59-68.

Feher, A., Juhasz, A., Rimanoczy, A., Csibri, E., Kalman, J., Janka, Z., 2009. Association between a genetic variant of the alpha-7 nicotinic acetylcholine receptor subunit and four types of dementia. Dement Geriatr Cogn Disord 28, 56-62.

Flomen, R.H., Collier, D.A., Osborne, S., Munro, J., Breen, G., St Clair, D., Makoff, A.J., 2006. Association study of CHRFAM7A copy number and 2 bp deletion polymorphisms with schizophrenia and bipolar affective disorder. Am J Med Genet B Neuropsychiatr Genet 141B, 571-575.

Flomen, R.H., Davies, A.F., Di Forti, M., La Cascia, C., Mackie-Ogilvie, C., Murray, R., Makoff, A.J., 2008. The copy number variant involving part of the alpha7 nicotinic receptor gene contains a polymorphic inversion. Eur J Hum Genet 16, 1364-1371.

Flomen, R.H., Shaikh, M., Walshe, M., Schulze, K., Hall, M.H., Picchioni, M., Rijsdijk, F., Toulopoulou, T., Kravariti, E., Murray, R.M., Asherson, P., Makoff, A.J., Bramon, E., 2013. Association between the 2-bp deletion

polymorphism in the duplicated version of the alpha7 nicotinic receptor gene and P50 sensory gating. Eur J Hum Genet 21, 76-81.

Fox, J.W., 1990. Social class, mental illness, and social mobility: the social selection-drift hypothesis for serious mental illness. J Health Soc Behav 31, 344-353.

Frazier, C.J., Rollins, Y.D., Hall, M.E., Young, D.A., Rose, G.M., 1996. Cholinergic deafferentation enhances rat hippocampal pyramidal neuron responsiveness to locally applied nicotine. Brain Res 727, 217-220.

Freedman, R., Coon, H., Myles-Worsley, M., Orr-Urtreger, A., Olincy, A., Davis, A., Polymeropoulos, M., Holik, J., Hopkins, J., Hoff, M., Rosenthal, J., Waldo, M.C., Reimherr, F., Wender, P., Yaw, J., Young, D.A., Breese, C.R., Adams, C., Patterson, D., Adler, L.E., Kruglyak, L., Leonard, S., Byerley, W., 1997. Linkage of a neurophysiological deficit in schizophrenia to a chromosome 15 locus. Proc Natl Acad Sci U S A 94, 587-592.

Freedman, R., Hall, M., Adler, L.E., Leonard, S., 1995. Evidence in postmortem brain tissue for decreased numbers of hippocampal nicotinic receptors in schizophrenia. Biol Psychiatry 38, 22-33.

Freedman, R., Olincy, A., Buchanan, R.W., Harris, J.G., Gold, J.M., Johnson, L., Allensworth, D., Guzman-Bonilla, A., Clement, B., Ball, M.P., Kutnick, J., Pender, V., Martin, L.F., Stevens, K.E., Wagner, B.D., Zerbe, G.O., Soti, F., Kem, W.R., 2008. Initial phase 2 trial of a nicotinic agonist in schizophrenia. Am J Psychiatry 165, 1040-1047.

Frolich, L., Ashwood, T., Nilsson, J., Eckerwall, G., Sirocco, I., 2011. Effects of AZD3480 on cognition in patients with mild-to-moderate Alzheimer's disease: a phase IIb dose-finding study. J Alzheimers Dis 24, 363-374.

Fu, X.W., Rekow, S.S., Spindel, E.R., 2012. The ly-6 protein, lynx1, is an endogenous inhibitor of nicotinic signaling in airway epithelium. Am J Physiol Lung Cell Mol Physiol 303, 661-668.

Gault, J., Hopkins, J., Berger, R., Drebing, C., Logel, J., Walton, C., Short, M., Vianzon, R., Olincy, A., Ross, R.G., Adler, L.E., Freedman, R., Leonard, S., 2003. Comparison of polymorphisms in the alpha7 nicotinic receptor gene and its partial duplication in schizophrenic and control subjects. Am J Med Genet B Neuropsychiatr Genet 123B, 39-49.

Gault, J., Robinson, M., Berger, R., Drebing, C., Logel, J., Hopkins, J., Moore, T., Jacobs, S., Meriwether, J., Choi, M.J., Kim, E.J., Walton, K., Buiting, K., Davis, A., Breese, C., Freedman, R., Leonard, S., 1998. Genomic organization and partial duplication of the human alpha7 neuronal nicotinic acetylcholine receptor gene (CHRNA7). Genomics 52, 173-185.

Gault, L., Ritchie, C., Robieson, W., Pritchett, Y., Othman, A., Lenz, R., 2013. Efficacy and safety of the alpha7 agonist ABT-126 in mild-to-moderate Alzheimer's dementia. Alzheimer's & Dementia: The Journal of the Alzheimer's Association 9, P138.

Gil-Bea, F.J., Gerenu, G., Aisa, B., Kirazov, L.P., Schliebs, R., Ramirez, M.J., 2012. Cholinergic denervation exacerbates amyloid pathology and induces hippocampal atrophy in Tg2576 mice. Neurobiol Dis 48, 439-446.

Gil-Bea, F.J., Solas, M., Mateos, L., Winblad, B., Ramirez, M.J., Cedazo-Minguez, A., 2011. Cholinergic hypofunction impairs memory acquisition possibly through hippocampal Arc and BDNF downregulation. Hippocampus 21, 999-1009.

Gotti, C., Clementi, F., 2004. Neuronal nicotinic receptors: from structure to pathology. Prog Neurobiol 74, 363-396.

Gotti, C., Moretti, M., Bohr, I., Ziabreva, I., Vailati, S., Longhi, R., Riganti, L., Gaimarri, A., McKeith, I.G., Perry, R.H., Aarsland, D., Larsen, J.P., Sher, E., Beattie, R., Clementi, F., Court, J.A., 2006a. Selective nicotinic acetylcholine receptor subunit deficits identified in Alzheimer's disease, Parkinson's disease and dementia with Lewy bodies by immunoprecipitation. Neurobiol Dis 23, 481-489.

Gotti, C., Zoli, M., Clementi, F., 2006b. Brain nicotinic acetylcholine receptors: native subtypes and their relevance. Trends Pharmacol Sci 27, 482-491.

Gubbins, E.J., Gopalakrishnan, M., Li, J., 2010. Alpha7 nAChR-mediated activation of MAP kinase pathways in PC12 cells. Brain Res 1328, 1-11.

Guillem, K., Bloem, B., Poorthuis, R.B., Loos, M., Smit, A.B., Maskos, U., Spijker, S., Mansvelder, H.D., 2011. Nicotinic acetylcholine receptor beta2 subunits in the medial prefrontal cortex control attention. Science 333, 888-891.

Hardy, J., Selkoe, D.J., 2002. The amyloid hypothesis of Alzheimer's disease: progress and problems on the road to therapeutics. Science 297, 353-356.

Härtig, W., Saul, A., Kacza, J., Grosche, J., Goldhammer, S., Michalski, D., Wirths, O., 2014. Immunolesion-induced loss of cholinergic projection neurones promotes beta-amyloidosis and tau hyperphosphorylation in the hippocampus of triple-transgenic mice. Neuropathol Appl Neurobiol 40, 106-120.

Hauser, T.A., Kucinski, A., Jordan, K.G., Gatto, G.J., Wersinger, S.R., Hesse, R.A., Stachowiak, E.K., Stachowiak, M.K., Papke, R.L., Lippiello, P.M., Bencherif, M., 2009. TC-5619: an alpha7 neuronal nicotinic receptor-selective agonist that demonstrates efficacy in animal models of the positive and negative symptoms and cognitive dysfunction of schizophrenia. Biochem Pharmacol 78, 803-812.

Hedberg, M.M., Clos, M.V., Ratia, M., Gonzalez, D., Lithner, C.U., Camps, P., Munoz-Torrero, D., Badia, A., Gimenez-Llort, L., Nordberg, A., 2010. Effect of huprine X on beta-amyloid, synaptophysin and alpha7 neuronal nicotinic acetylcholine receptors in the brain of 3xTg-AD and APPswe transgenic mice. Neurodegener Dis 7, 379-388.

Hellstrom-Lindahl, E., Mousavi, M., Zhang, X., Ravid, R., Nordberg, A., 1999. Regional distribution of nicotinic receptor subunit mRNAs in human brain: comparison between Alzheimer and normal brain. Brain Res Mol Brain Res 66, 94-103.

Hernandez, C.M., Kayed, R., Zheng, H., Sweatt, J.D., Dineley, K.T., 2010. Loss of alpha7 nicotinic receptors enhances beta-amyloid oligomer accumulation, exacerbating early-stage cognitive decline and septohippocampal pathology in a mouse model of Alzheimer's disease. J Neurosci 30, 2442-2453.

Hill, S.K., Bishop, J.R., Palumbo, D., Sweeney, J.A., 2010. Effect of second-generation antipsychotics on cognition: current issues and future challenges. Expert Rev Neurother 10, 43-57.

Holford, M., Auer, S., Laqua, M., Ibanez-Tallon, I., 2009. Manipulating neuronal circuits with endogenous and recombinant cell-surface tethered modulators. Front Mol Neurosci 2, 21.

Houghtling, R.A., Davila-Garcia, M.I., Kellar, K.J., 1995. Characterization of (+/-)(-)[3H]epibatidine binding to nicotinic cholinergic receptors in rat and human brain. Mol Pharmacol 48, 280-287.

Hruska, M., Keefe, J., Wert, D., Tekinay, A.B., Hulce, J.J., Ibanez-Tallon, I., Nishi, R., 2009. Prostate stem cell antigen is an endogenous lynx1-like prototoxin that antagonizes alpha7-containing nicotinic receptors and prevents programmed cell death of parasympathetic neurons. J Neurosci 29, 14847-14854.

Hsiao, K., Chapman, P., Nilsen, S., Eckman, C., Harigaya, Y., Younkin, S., Yang, F., Cole, G., 1996. Correlative memory deficits, Abeta elevation, and amyloid plaques in transgenic mice. Science 274, 99-102.

Huang, Z.B., Wang, H., Rao, X.R., Zhong, G.F., Hu, W.H., Sheng, G.Q., 2011. Different effects of scopolamine on the retrieval of spatial memory and fear memory. Behav Brain Res 221, 604-609.

Hunter, C.L., Quintero, E.M., Gilstrap, L., Bhat, N.R., Granholm, A.C., 2004. Minocycline protects basal forebrain cholinergic neurons from mu p75-saporin immunotoxic lesioning. Eur J Neurosci 19, 3305-3316.

Ibanez-Tallon, I., Miwa, J.M., Wang, H.L., Adams, N.C., Crabtree, G.W., Sine, S.M., Heintz, N., 2002. Novel modulation of neuronal nicotinic acetylcholine receptors by association with the endogenous prototoxin lynx1. Neuron 33, 893-903.

International Schizophrenia Consortium, 2008. Rare chromosomal deletions and duplications increase risk of schizophrenia. Nature 455, 237-241.

Janas, A.M., Cunningham, S.C., Duffy, K.B., Devan, B.D., Greig, N.H., Holloway, H.W., Yu, Q.S., Markowska, A.L., Ingram, D.K., Spangler, E.L., 2005. The cholinesterase inhibitor, phenserine, improves Morris water maze performance of scopolamine-treated rats. Life Sci 76, 1073-1081.

Jensen, A.A., Frolund, B., Liljefors, T., Krogsgaard-Larsen, P., 2005. Neuronal nicotinic acetylcholine receptors: structural revelations, target identifications, and therapeutic inspirations. J Med Chem 48, 4705-4745.

Kadir, A., Almkvist, O., Wall, A., Langstrom, B., Nordberg, A., 2006. PET imaging of cortical 11C-nicotine binding correlates with the cognitive function of attention in Alzheimer's disease. Psychopharmacology (Berl) 188, 509-520.

Kanekal, S., Sahai, A., Jones, R.E., Brown, D., 1995. Storage-phosphor autoradiography: a rapid and highly sensitive method for spatial imaging and quantitation of radioisotopes. J Pharmacol Toxicol Methods 33, 171-178.

Kawai, H., Zago, W., Berg, D.K., 2002. Nicotinic alpha 7 receptor clusters on hippocampal GABAergic neurons: regulation by synaptic activity and neurotrophins. J Neurosci 22, 7903-7912.

Kawamata, J., Shimohama, S., 2002. Association of novel and established polymorphisms in neuronal nicotinic acetylcholine receptors with sporadic Alzheimer's disease. J Alzheimers Dis 4, 71-76.

Kawarabayashi, T., Younkin, L.H., Saido, T.C., Shoji, M., Ashe, K.H., Younkin, S.G., 2001. Age-dependent changes in brain, CSF, and plasma amyloid (beta) protein in the Tg2576 transgenic mouse model of Alzheimer's disease. J Neurosci 21, 372-381.

Kendziorra, K., Wolf, H., Meyer, P.M., Barthel, H., Hesse, S., Becker, G.A., Luthardt, J., Schildan, A., Patt, M., Sorger, D., Seese, A., Gertz, H.J., Sabri, O., 2011. Decreased cerebral alpha4beta2* nicotinic acetylcholine receptor availability in patients with mild cognitive impairment and Alzheimer's disease assessed with positron emission tomography. Eur J Nucl Med Mol Imaging 38, 515-525.

Khiroug, S.S., Harkness, P.C., Lamb, P.W., Sudweeks, S.N., Khiroug, L., Millar, N.S., Yakel, J.L., 2002. Rat nicotinic ACh receptor alpha7 and beta2 subunits co-assemble to form functional heteromeric nicotinic receptor channels. J Physiol 540, 425-434.

Kim, H.J., Moon, W.J., Han, S.H., 2013. Differential cholinergic pathway involvement in Alzheimer's disease and subcortical ischemic vascular dementia. J Alzheimers Dis 35, 129-136.

Kitagawa, H., Takenouchi, T., Azuma, R., Wesnes, K.A., Kramer, W.G., Clody, D.E., Burnett, A.L., 2003. Safety, pharmacokinetics, and effects on cognitive function of multiple doses of GTS-21 in healthy, male volunteers. Neuropsychopharmacology 28, 542-551.

Kobayashi, A., Parker, R.L., Wright, A.P., Brahem, H., Ku, P., Oliver, K.M., Walz, A., Lester, H.A., Miwa, J.M., 2014. Lynx1 supports neuronal health in the mouse dorsal striatum during aging: an ultrastructural investigation. J Mol Neurosci 53, 525-536.

Kobow, K., Jeske, I., Hildebrandt, M., Hauke, J., Hahnen, E., Buslei, R., Buchfelder, M., Weigel, D., Stefan, H., Kasper, B., Pauli, E., Blumcke, I., 2009. Increased reelin promoter methylation is associated with granule cell dispersion in human temporal lobe epilepsy. J Neuropathol Exp Neurol 68, 356-364.

Kokjohn, T.A., Roher, A.E., 2009. Amyloid precursor protein transgenic mouse models and Alzheimer's disease: understanding the paradigms, limitations, and contributions. Alzheimers Dement 5, 340-347.

Kristensen, S.E., Thomsen, M.S., Hansen, H.H., Timmermann, D.B., Hay-Schmidt, A., Mikkelsen, J.D., 2007. The alpha7 nicotinic receptor agonist SSR180711 increases activity regulated cytoskeleton protein (Arc) gene expression in the prefrontal cortex of the rat. Neurosci Lett 418, 154-158.

Kroker, K.S., Moreth, J., Kussmaul, L., Rast, G., Rosenbrock, H., 2013. Restoring long-term potentiation impaired by amyloid-beta oligomers: comparison of an acetylcholinesterase inhibitior and selective neuronal nicotinic receptor agonists. Brain Res Bull 96, 28-38.

Kumari, V., Postma, P., 2005. Nicotine use in schizophrenia: the self medication hypotheses. Neurosci Biobehav Rev 29, 1021-1034.

LaFerla, F.M., Green, K.N., 2012. Animal models of Alzheimer disease. Cold Spring Harb Perspect Med 2, *in press*.

Lamb, P.W., Melton, M.A., Yakel, J.L., 2005. Inhibition of neuronal nicotinic acetylcholine receptor channels expressed in Xenopus oocytes by beta-amyloid1-42 peptide. J Mol Neurosci 27, 13-21.

Laumet, G., Chouraki, V., Grenier-Boley, B., Legry, V., Heath, S., Zelenika, D., Fievet, N., Hannequin, D., Delepine, M., Pasquier, F., Hanon, O., Brice, A., Epelbaum, J., Berr, C., Dartigues, J.F., Tzourio, C., Campion, D., Lathrop, M., Bertram, L., Amouyel, P., Lambert, J.C., 2010. Systematic analysis of candidate genes for Alzheimer's disease in a French, genome-wide association study. J Alzheimers Dis 20, 1181-1188.

Laursen, B., Mork, A., Plath, N., Kristiansen, U., Bastlund, J.F., 2013. Cholinergic degeneration is associated with increased plaque deposition and cognitive impairment in APPswe/PS1dE9 mice. Behav Brain Res 240, 146-152.

Laursen, B., Mork, A., Plath, N., Kristiansen, U., Bastlund, J.F., 2014. Impaired hippocampal acetylcholine release parallels spatial memory deficits in Tg2576 mice subjected to basal forebrain cholinergic degeneration. Brain Res 1543, 253-262.

Lee, J.E., Han, P.L., 2013. An update of animal models of Alzheimer disease with a reevaluation of plaque depositions. Exp Neurobiol 22, 84-95.

Leonard, S., Gault, J., Hopkins, J., Logel, J., Vianzon, R., Short, M., Drebing, C., Berger, R., Venn, D., Sirota, P., Zerbe, G., Olincy, A., Ross, R.G., Adler, L.E., Freedman, R., 2002. Association of promoter variants in the alpha7 nicotinic acetylcholine receptor subunit gene with an inhibitory deficit found in schizophrenia. Arch Gen Psychiatry 59, 1085-1096.

Lester, H.A., Xiao, C., Srinivasan, R., Son, C.D., Miwa, J., Pantoja, R., Banghart, M.R., Dougherty, D.A., Goate, A.M., Wang, J.C., 2009. Nicotine is a selective pharmacological chaperone of acetylcholine receptor number and stoichiometry. Implications for drug discovery. AAPS J 11, 167-177.

Levin, E.D., 2013. Complex relationships of nicotinic receptor actions and cognitive functions. Biochem Pharmacol 86, 1145-1152.

Levin, E.D., Bradley, A., Addy, N., Sigurani, N., 2002. Hippocampal alpha 7 and alpha 4 beta 2 nicotinic receptors and working memory. Neuroscience 109, 757-765.

Levin, E.D., McClernon, F.J., Rezvani, A.H., 2006. Nicotinic effects on cognitive function: behavioral characterization, pharmacological specification, and anatomic localization. Psychopharmacology (Berl) 184, 523-539.

Lieberman, J.A., Dunbar, G., Segreti, A.C., Girgis, R.R., Seoane, F., Beaver, J.S., Duan, N., Hosford, D.A., 2013. A randomized exploratory trial of an alpha-7 nicotinic receptor agonist (TC-5619) for cognitive enhancement in schizophrenia. Neuropsychopharmacology 38, 968-975.

Liu, Q., Huang, Y., Shen, J., Steffensen, S., Wu, J., 2012. Functional alpha7beta2 nicotinic acetylcholine receptors expressed in hippocampal interneurons exhibit high sensitivity to pathological level of amyloid beta peptides. BMC Neurosci 13, 155, *in press*.

Liu, Q., Huang, Y., Xue, F., Simard, A., DeChon, J., Li, G., Zhang, J., Lucero, L., Wang, M., Sierks, M., Hu, G., Chang, Y., Lukas, R.J., Wu, J., 2009. A novel nicotinic acetylcholine receptor subtype in basal forebrain cholinergic neurons with high sensitivity to amyloid peptides. J Neurosci 29, 918-929.

Locke, D.P., Archidiacono, N., Misceo, D., Cardone, M.F., Deschamps, S., Roe, B., Rocchi, M., Eichler, E.E., 2003. Refinement of a chimpanzee pericentric inversion breakpoint to a segmental duplication cluster. Genome Biol 4, R50.

Lombardo, S., Maskos, U., 2014. Role of the nicotinic acetylcholine receptor in Alzheimer's disease pathology and treatment. Neuropharmacology, *in press*.

Lyukmanova, E.N., Shenkarev, Z.O., Shulepko, M.A., Mineev, K.S., D'Hoedt, D., Kasheverov, I.E., Filkin, S.Y., Krivolapova, A.P., Janickova, H., Dolezal, V., Dolgikh, D.A., Arseniev, A.S., Bertrand, D., Tsetlin, V.I., Kirpichnikov, M.P., 2011. NMR structure and action on nicotinic acetylcholine receptors of water-soluble domain of human LYNX1. J Biol Chem 286, 10618-10627.

Lyukmanova, E.N., Shulepko, M.A., Buldakova, S.L., Kasheverov, I.E., Shenkarev, Z.O., Reshetnikov, R.V., Filkin, S.Y., Kudryavtsev, D.S., Ojomoko, L.O., Kryukova, E.V., Dolgikh, D.A., Kirpichnikov, M.P., Bregestovski, P.D., Tsetlin, V.I., 2013. Water-soluble LYNX1 residues important for interaction with muscle-type and/or neuronal nicotinic receptors. J Biol Chem 288, 15888-15899.

Malhotra, A.K., Pinals, D.A., Adler, C.M., Elman, I., Clifton, A., Pickar, D., Breier, A., 1997. Ketamine-induced exacerbation of psychotic symptoms and cognitive impairment in neuroleptic-free schizophrenics. Neuropsychopharmacology 17, 141-150.

Malhotra, A.K., Pinals, D.A., Weingartner, H., Sirocco, K., Missar, C.D., Pickar, D., Breier, A., 1996. NMDA receptor function and human cognition: the effects of ketamine in healthy volunteers. Neuropsychopharmacology 14, 301-307.

Marutle, A., Gillberg, P.G., Bergfors, A., Yu, W., Ni, R., Nennesmo, I., Voytenko, L., Nordberg, A., 2013. (3)H-deprenyl and (3)H-PIB autoradiography show different laminar distributions of astroglia and fibrillar beta-amyloid in Alzheimer brain. J Neuroinflammation 10, *in press*.

Marutle, A., Zhang, X., Court, J., Piggott, M., Johnson, M., Perry, R., Perry, E., Nordberg, A., 2001. Laminar distribution of nicotinic receptor subtypes in cortical regions in schizophrenia. J Chem Neuroanat 22, 115-126.

Massey, K.A., Zago, W.M., Berg, D.K., 2006. BDNF up-regulates alpha7 nicotinic acetylcholine receptor levels on subpopulations of hippocampal interneurons. Mol Cell Neurosci 33, 381-388.

Medeiros, R., Castello, N.A., Cheng, D., Kitazawa, M., Baglietto-Vargas, D., Green, K.N., Esbenshade, T.A., Bitner, R.S., Decker, M.W., LaFerla, F.M., 2014. alpha7 Nicotinic receptor agonist enhances cognition in aged 3xTg-AD mice with robust plaques and tangles. Am J Pathol 184, 520-529.

Miwa, J.M., Freedman, R., Lester, H.A., 2011. Neural systems governed by nicotinic acetylcholine receptors: emerging hypotheses. Neuron 70, 20-33.

Miwa, J.M., Ibanez-Tallon, I., Crabtree, G.W., Sanchez, R., Sali, A., Role, L.W., Heintz, N., 1999. lynx1, an endogenous toxin-like modulator of nicotinic acetylcholine receptors in the mammalian CNS. Neuron 23, 105-114.

Miwa, J.M., Lester, H.A., Walz, A., 2012. Optimizing cholinergic tone through lynx modulators of nicotinic receptors: implications for plasticity and nicotine addiction. Physiology (Bethesda) 27, 187-199.

Miwa, J.M., Stevens, T.R., King, S.L., Caldarone, B.J., Ibanez-Tallon, I., Xiao, C., Fitzsimonds, R.M., Pavlides, C., Lester, H.A., Picciotto, M.R., Heintz, N., 2006. The prototoxin lynx1 acts on nicotinic acetylcholine receptors to balance neuronal activity and survival in vivo. Neuron 51, 587-600.

Miwa, J.M., Walz, A., 2012. Enhancement in motor learning through genetic manipulation of the Lynx1 gene. PLoS One 7, *in press*.

Moreau, P.H., Cosquer, B., Jeltsch, H., Cassel, J.C., Mathis, C., 2008. Neuroanatomical and behavioral effects of a novel version of the cholinergic immunotoxin mu p75-saporin in mice. Hippocampus 18, 610-622.

Moretti, M., Zoli, M., George, A.A., Lukas, R.J., Pistillo, F., Maskos, U., Whiteaker, P., Gotti, C., 2014. The Novel alpha7beta2-Nicotinic Acetylcholine Receptor Subtype Is Expressed in Mouse and Human Basal Forebrain: Biochemical and Pharmacological Characterization. Mol Pharmacol 86, 306-317.

Morishita, H., Miwa, J.M., Heintz, N., Hensch, T.K., 2010. Lynx1, a cholinergic brake, limits plasticity in adult visual cortex. Science 330, 1238-1240.

Mouri, A., Noda, Y., Enomoto, T., Nabeshima, T., 2007. Phencyclidine animal models of schizophrenia: approaches from abnormality of glutamatergic neurotransmission and neurodevelopment. Neurochem Int 51, 173-184.

Mueser, K.T., McGurk, S.R., 2004. Schizophrenia. Lancet 363, 2063-2072.

Mukhin, A.G., Gundisch, D., Horti, A.G., Koren, A.O., Tamagnan, G., Kimes, A.S., Chambers, J., Vaupel, D.B., King, S.L., Picciotto, M.R., Innis, R.B., London, E.D., 2000. 5-Iodo-A-85380, an alpha4beta2 subtype-selective ligand for nicotinic acetylcholine receptors. Mol Pharmacol 57, 642-649.

Murray, T.A., Bertrand, D., Papke, R.L., George, A.A., Pantoja, R., Srinivasan, R., Liu, Q., Wu, J., Whiteaker, P., Lester, H.A., Lukas, R.J., 2012. alpha7beta2 nicotinic acetylcholine receptors assemble, function, and are activated primarily via their alpha7-alpha7 interfaces. Mol Pharmacol 81, 175-188.

Nagele, R.G., D'Andrea, M.R., Anderson, W.J., Wang, H.Y., 2002. Intracellular accumulation of beta-amyloid(1-42) in neurons is facilitated by the alpha 7 nicotinic acetylcholine receptor in Alzheimer's disease. Neuroscience 110, 199-211.

Nakayama, H., Shimoke, K., Isosaki, M., Satoh, H., Yoshizumi, M., Ikeuchi, T., 2006. Subtypes of neuronal nicotinic acetylcholine receptors involved in nicotine-induced phosphorylation of extracellular signal-regulated protein kinase in PC12h cells. Neurosci Lett 392, 101-104.

Newhouse, P.A., Potter, A., Singh, A., 2004. Effects of nicotinic stimulation on cognitive performance. Curr Opin Pharmacol 4, 36-46.

Nichols, W.A., Henderson, B.J., Yu, C., Parker, R.L., Richards, C.I., Lester, H.A., Miwa, J.M., 2014. Lynx1 Shifts alpha4beta2 Nicotinic Receptor Subunit Stoichiometry by Affecting Assembly in the Endoplasmic Reticulum. J Biol Chem 289, 31423-31432.

Nolan, T., Hands, R.E., Bustin, S.A., 2006. Quantification of mRNA using real-time RT-PCR. Nat Protoc 1, 1559-1582.

Oddo, S., Caccamo, A., Shepherd, J.D., Murphy, M.P., Golde, T.E., Kayed, R., Metherate, R., Mattson, M.P., Akbari, Y., LaFerla, F.M., 2003. Triple-transgenic model of Alzheimer's disease with plaques and tangles: intracellular Abeta and synaptic dysfunction. Neuron 39, 409-421.

Okada, H., Ouchi, Y., Ogawa, M., Futatsubashi, M., Saito, Y., Yoshikawa, E., Terada, T., Oboshi, Y., Tsukada, H., Ueki, T., Watanabe, M., Yamashita, T., Magata, Y., 2013. Alterations in alpha4beta2 nicotinic receptors in cognitive decline in Alzheimer's aetiopathology. Brain 136, 3004-3017.

Olincy, A., Harris, J.G., Johnson, L.L., Pender, V., Kongs, S., Allensworth, D., Ellis, J., Zerbe, G.O., Leonard, S., Stevens, K.E., Stevens, J.O., Martin, L., Adler, L.E., Soti, F., Kem, W.R., Freedman, R., 2006. Proof-of-concept trial of an alpha7 nicotinic agonist in schizophrenia. Arch Gen Psychiatry 63, 630-638.

Olincy, A., Stevens, K.E., 2007. Treating schizophrenia symptoms with an alpha7 nicotinic agonist, from mice to men. Biochem Pharmacol 74, 1192-1201.

Ozhan, G., Sezgin, E., Wehner, D., Pfister, A.S., Kuhl, S.J., Kagermeier-Schenk, B., Kuhl, M., Schwille, P., Weidinger, G., 2013. Lypd6 enhances Wnt/beta-catenin signaling by promoting Lrp6 phosphorylation in raft plasma membrane domains. Dev Cell 26, 331-345.

Palma, E., Maggi, L., Barabino, B., Eusebi, F., Ballivet, M., 1999. Nicotinic acetylcholine receptors assembled from the alpha7 and beta3 subunits. J Biol Chem 274, 18335-18340.

Parihar, M.S., Brewer, G.J., 2010. Amyloid-beta as a modulator of synaptic plasticity. J Alzheimers Dis 22, 741-763.

Parikh, V., Ji, J., Decker, M.W., Sarter, M., 2010. Prefrontal beta2 subunit-containing and alpha7 nicotinic acetylcholine receptors differentially control glutamatergic and cholinergic signaling. J Neurosci 30, 3518-3530.

Parri, R.H., Dineley, T.K., 2010. Nicotinic acetylcholine receptor interaction with beta-amyloid: molecular, cellular, and physiological consequences. Curr Alzheimer Res 7, 27-39.

Paterson, D., Nordberg, A., 2000. Neuronal nicotinic receptors in the human brain. Prog Neurobiol 61, 75-111.

Paxinos, G., Franklin, K. 2001. The Mouse Brain in Stereotaxic Coordinates. Academic Press.

Perry, D.C., Xiao, Y., Nguyen, H.N., Musachio, J.L., Davila-Garcia, M.I., Kellar, K.J., 2002. Measuring nicotinic receptors with characteristics of alpha4beta2, alpha3beta2 and alpha3beta4 subtypes in rat tissues by autoradiography. J Neurochem 82, 468-481.

Pettit, D.L., Shao, Z., Yakel, J.L., 2001. beta-Amyloid(1-42) peptide directly modulates nicotinic receptors in the rat hippocampal slice. J Neurosci 21, RC120.

Pfaffl, M.W., 2001. A new mathematical model for relative quantification in real-time RT-PCR. Nucleic Acids Res 29, e45.

Pichat, P., Bergis, O.E., Terranova, J.P., Urani, A., Duarte, C., Santucci, V., Gueudet, C., Voltz, C., Steinberg, R., Stemmelin, J., Oury-Donat, F., Avenet, P., Griebel, G., Scatton, B., 2007. SSR180711, a novel selective alpha7 nicotinic receptor partial agonist: (II) efficacy in experimental models predictive of activity against cognitive symptoms of schizophrenia. Neuropsychopharmacology 32, 17-34.

Preskorn, S.H., 2014. The role of proof of concept (POC) studies in drug development using the EVP-6124 POC study as an example. J Psychiatr Pract 20, 59-60.

Preskorn, S.H., Gawryl, M., Dgetluck, N., Palfreyman, M., Bauer, L.O., Hilt, D.C., 2014. Normalizing effects of EVP-6124, an alpha-7 nicotinic partial agonist, on event-related potentials and cognition: a proof of concept, randomized trial in patients with schizophrenia. J Psychiatr Pract 20, 12-24.

Prickaerts, J., van Goethem, N.P., Chesworth, R., Shapiro, G., Boess, F.G., Methfessel, C., Reneerkens, O.A., Flood, D.G., Hilt, D., Gawryl, M., Bertrand, S., Bertrand, D., Konig, G., 2012. EVP-6124, a novel and selective alpha7 nicotinic acetylcholine receptor partial agonist, improves memory performance by potentiating the acetylcholine response of alpha7 nicotinic acetylcholine receptors. Neuropharmacology 62, 1099-1110.

Querfurth, H.W., LaFerla, F.M., 2010. Alzheimer's disease. N Engl J Med 362, 329-344.

Quinlivan, M., Chalon, S., Vergote, J., Henderson, J., Katsifis, A., Kassiou, M., Guilloteau, D., 2007. Decreased vesicular acetylcholine transporter and alpha(4)beta(2) nicotinic receptor density in the rat brain following 192 IgG-saporin immunolesioning. Neurosci Lett 415, 97-101.

Reiter, R.E., Gu, Z., Watabe, T., Thomas, G., Szigeti, K., Davis, E., Wahl, M., Nisitani, S., Yamashiro, J., Le Beau, M.M., Loda, M., Witte, O.N., 1998. Prostate stem cell antigen: a cell surface marker overexpressed in prostate cancer. Proc Natl Acad Sci U S A 95, 1735-1740.

Riley, B., Williamson, M., Collier, D., Wilkie, H., Makoff, A., 2002. A 3-Mb map of a large Segmental duplication overlapping the alpha7-nicotinic acetylcholine receptor gene (CHRNA7) at human 15q13-q14. Genomics 79, 197-209.

Ripoll, N., Bronnec, M., Bourin, M., 2004. Nicotinic receptors and schizophrenia. Curr Med Res Opin 20, 1057-1074.

Sacco, K.A., Bannon, K.L., George, T.P., 2004. Nicotinic receptor mechanisms and cognition in normal states and neuropsychiatric disorders. J Psychopharmacol 18, 457-474.

Sarter, M., Bruno, J.P., 1997. Cognitive functions of cortical acetylcholine: toward a unifying hypothesis. Brain Res Brain Res Rev 23, 28-46.

Sarter, M., Parikh, V., Howe, W.M., 2009. nAChR agonist-induced cognition enhancement: integration of cognitive and neuronal mechanisms. Biochem Pharmacol 78, 658-667.

Schmittgen, T.D., Livak, K.J., 2008. Analyzing real-time PCR data by the comparative C(T) method. Nat Protoc 3, 1101-1108.

Science, 2005. So much more to know. Science 309, 78-102.

Severance, E.G., Yolken, R.H., 2008. Novel alpha7 nicotinic receptor isoforms and deficient cholinergic transcription in schizophrenia. Genes Brain Behav 7, 37-45.

Shankar, G.M., Li, S., Mehta, T.H., Garcia-Munoz, A., Shepardson, N.E., Smith, I., Brett, F.M., Farrell, M.A., Rowan, M.J., Lemere, C.A., Regan, C.M., Walsh, D.M., Sabatini, B.L., Selkoe, D.J., 2008. Amyloid-beta protein dimers isolated directly from Alzheimer's brains impair synaptic plasticity and memory. Nat Med 14, 837-842.

Sinkus, M.L., Lee, M.J., Gault, J., Logel, J., Short, M., Freedman, R., Christian, S.L., Lyon, J., Leonard, S., 2009. A 2-base pair deletion polymorphism in the partial duplication of the alpha7 nicotinic acetylcholine gene (CHRFAM7A) on chromosome 15q14 is associated with schizophrenia. Brain Res 1291, 1-11.

Soliakov, L., Gallagher, T., Wonnacott, S., 1995. Anatoxin-a-evoked [3H]dopamine release from rat striatal synaptosomes. Neuropharmacology 34, 1535-1541.

Srivastava, S., Osten, P., Vilim, F.S., Khatri, L., Inman, G., States, B., Daly, C., DeSouza, S., Abagyan, R., Valtschanoff, J.G., Weinberg, R.J., Ziff, E.B., 1998. Novel anchorage of GluR2/3 to the postsynaptic density by the AMPA receptor-binding protein ABP. Neuron 21, 581-591.

Stefansson, H., Rujescu, D., Cichon, S., Pietilainen, O.P., Ingason, A., Steinberg, S., Fossdal, R., Sigurdsson, E., Sigmundsson, T., Buizer-Voskamp, J.E., Hansen, T., Jakobsen, K.D., Muglia, P., Francks, C., Matthews, P.M., Gylfason, A., Halldorsson, B.V., Gudbjartsson, D., Thorgeirsson, T.E., Sigurdsson, A., Jonasdottir, A., Jonasdottir, A., Bjornsson, A., Mattiasdottir, S., Blondal, T., Haraldsson, M., Magnusdottir, B.B., Giegling, I., Moller, H.J., Hartmann, A., Shianna, K.V., Ge, D., Need, A.C., Crombie, C., Fraser, G., Walker, N., Lonnqvist, J., Suvisaari, J., Tuulio-Henriksson, A., Paunio, T., Toulopoulou, T., Bramon, E., Di Forti, M., Murray, R., Ruggeri, M., Vassos, E., Tosato, S., Walshe, M., Li, T., Vasilescu, C., Muhleisen, T.W., Wang, A.G., Ullum, H., Djurovic, S., Melle, I., Olesen, J., Kiemeney, L.A., Franke, B., Group, Sabatti, C., Freimer, N.B., Gulcher, J.R., Thorsteinsdottir, U., Kong, A., Andreassen, O.A., Ophoff, R.A., Georgi, A., Rietschel, M., Werge, T., Petursson, H., Goldstein, D.B., Nothen, M.M., Peltonen, L., Collier, D.A., St Clair, D., Stefansson, K., 2008. Large recurrent microdeletions associated with schizophrenia. Nature 455, 232-236.

Stephens, S.H., Logel, J., Barton, A., Franks, A., Schultz, J., Short, M., Dickenson, J., James, B., Fingerlin, T.E., Wagner, B., Hodgkinson, C., Graw, S., Ross, R.G., Freedman, R., Leonard, S., 2009. Association of the 5'-

upstream regulatory region of the alpha7 nicotinic acetylcholine receptor subunit gene (CHRNA7) with schizophrenia. Schizophr Res 109, 102-112.

Sweatt, J.D., 2004. Hippocampal function in cognition. Psychopharmacology (Berl) 174, 99-110.

Tekinay, A.B., Nong, Y., Miwa, J.M., Lieberam, I., Ibanez-Tallon, I., Greengard, P., Heintz, N., 2009. A role for LYNX2 in anxiety-related behavior. Proc Natl Acad Sci U S A 106, 4477-4482.

Thinschmidt, J.S., Frazier, C.J., King, M.A., Meyer, E.M., Papke, R.L., 2005. Septal innervation regulates the function of alpha7 nicotinic receptors in CA1 hippocampal interneurons. Exp Neurol 195, 342-352.

Thomsen, M.S., Christensen, D.Z., Hansen, H.H., Redrobe, J.P., Mikkelsen, J.D., 2009. alpha(7) Nicotinic acetylcholine receptor activation prevents behavioral and molecular changes induced by repeated phencyclidine treatment. Neuropharmacology 56, 1001-1009.

Thomsen, M.S., El-Sayed, M., Mikkelsen, J.D., 2011a. Differential immediate and sustained memory enhancing effects of alpha7 nicotinic receptor agonists and allosteric modulators in rats. PLoS One 6, *in press*.

Thomsen, M.S., Hansen, H.H., Mikkelsen, J.D., 2010a. alpha7 nicotinic receptor agonism mitigates phencyclidine-induced changes in synaptophysin and Arc gene expression in the mouse prefrontal cortex. Neurochem Int 57, 756-761.

Thomsen, M.S., Hansen, H.H., Timmerman, D.B., Mikkelsen, J.D., 2010b. Cognitive improvement by activation of alpha7 nicotinic acetylcholine receptors: from animal models to human pathophysiology. Curr Pharm Des 16, 323-343.

Thomsen, M.S., Hay-Schmidt, A., Hansen, H.H., Mikkelsen, J.D., 2010c. Distinct neural pathways mediate alpha7 nicotinic acetylcholine receptor-dependent activation of the forebrain. Cereb Cortex 20, 2092-2102.

Thomsen, M.S., Mikkelsen, J.D., 2012a. The alpha7 nicotinic acetylcholine receptor complex: one, two or multiple drug targets? Curr Drug Targets 13, 707-720.

Thomsen, M.S., Mikkelsen, J.D., 2012b. Type I and II positive allosteric modulators differentially modulate agonist-induced up-regulation of alpha7 nicotinic acetylcholine receptors. J Neurochem 123, 73-83.

Thomsen, M.S., Mikkelsen, J.D., Timmermann, D.B., Peters, D., Hay-Schmidt, A., Martens, H., Hansen, H.H., 2008. The selective alpha7 nicotinic acetylcholine receptor agonist A-582941 activates immediate early genes in limbic regions of the forebrain: Differential effects in the juvenile and adult rat. Neuroscience 154, 741-753.

Thomsen, M.S., Weyn, A., Mikkelsen, J.D., 2011b. Hippocampal alpha7 nicotinic acetylcholine receptor levels in patients with schizophrenia, bipolar disorder, or major depressive disorder. Bipolar Disord 13, 701-707.

Towbin, H., Staehelin, T., Gordon, J., 1979. Electrophoretic transfer of proteins from polyacrylamide gels to nitrocellulose sheets: procedure and some applications. Proc Natl Acad Sci U S A 76, 4350-4354.

Tregellas, J.R., Tanabe, J., Rojas, D.C., Shatti, S., Olincy, A., Johnson, L., Martin, L.F., Soti, F., Kem, W.R., Leonard, S., Freedman, R., 2011. Effects of an alpha 7-nicotinic agonist on default network activity in schizophrenia. Biol Psychiatry 69, 7-11.

Tribollet, E., Bertrand, D., Marguerat, A., Raggenbass, M., 2004. Comparative distribution of nicotinic receptor subtypes during development, adulthood and aging: an autoradiographic study in the rat brain. Neuroscience 124, 405-420.

Tsetlin, V., 1999. Snake venom alpha-neurotoxins and other 'three-finger' proteins. Eur J Biochem 264, 281-286.

Tylee, D.S., Kawaguchi, D.M., Glatt, S.J., 2013. On the outside, looking in: a review and evaluation of the comparability of blood and brain "-omes". Am J Med Genet B Neuropsychiatr Genet 162B, 595-603.

Valles, A.S., Borroni, M.V., Barrantes, F.J., 2014. Targeting brain alpha7 nicotinic acetylcholine receptors in Alzheimer's disease: rationale and current status. CNS Drugs 28, 975-987.

VanGuilder, H.D., Vrana, K.E., Freeman, W.M., 2008. Twenty-five years of quantitative PCR for gene expression analysis. Biotechniques 44, 619-626.

Villiger, Y., Szanto, I., Jaconi, S., Blanchet, C., Buisson, B., Krause, K.H., Bertrand, D., Romand, J.A., 2002. Expression of an alpha7 duplicate nicotinic acetylcholine receptor-related protein in human leukocytes. J Neuroimmunol 126, 86-98.

Wallace, T.L., Bertrand, D., 2013. Importance of the nicotinic acetylcholine receptor system in the prefrontal cortex. Biochem Pharmacol 85, 1713-1720.

Wallace, T.L., Porter, R.H., 2011. Targeting the nicotinic alpha7 acetylcholine receptor to enhance cognition in disease. Biochem Pharmacol 82, 891-903.

Walsh, D.M., Selkoe, D.J., 2007. A beta oligomers - a decade of discovery. J Neurochem 101, 1172-1184.

Wang, H.Y., Bakshi, K., Shen, C., Frankfurt, M., Trocme-Thibierge, C., Morain, P., 2010. S 24795 limits beta-amyloid-alpha7 nicotinic receptor interaction and reduces Alzheimer's disease-like pathologies. Biol Psychiatry 67, 522-530.

Wang, H.Y., Lee, D.H., Davis, C.B., Shank, R.P., 2000. Amyloid peptide Abeta(1-42) binds selectively and with picomolar affinity to alpha7 nicotinic acetylcholine receptors. J Neurochem 75, 1155-1161.

Wang, Y., Xiao, C., Indersmitten, T., Freedman, R., Leonard, S., Lester, H.A., 2014. The duplicated alpha7 subunits assemble and form functional nicotinic receptors with the full-length alpha7. J Biol Chem 289, 26451-63.

Wevers, A., Monteggia, L., Nowacki, S., Bloch, W., Schutz, U., Lindstrom, J., Pereira, E.F., Eisenberg, H., Giacobini, E., de Vos, R.A., Steur, E.N., Maelicke, A., Albuquerque, E.X., Schroder, H., 1999. Expression of nicotinic acetylcholine receptor subunits in the cerebral cortex in Alzheimer's disease: histotopographical correlation with amyloid plaques and hyperphosphorylated-tau protein. Eur J Neurosci 11, 2551-2565.

Whittaker, V.P., 1993. Thirty years of synaptosome research. J Neurocytol 22, 735-742.

Wonnacott, S., Barik, J., Dickinson, J., Jones, I.W., 2006. Nicotinic receptors modulate transmitter cross talk in the CNS: nicotinic modulation of transmitters. J Mol Neurosci 30, 137-140.

Woodward, N.D., Purdon, S.E., Meltzer, H.Y., Zald, D.H., 2005. A meta-analysis of neuropsychological change to clozapine, olanzapine, quetiapine, and risperidone in schizophrenia. Int J Neuropsychopharmacol 8, 457-472.

Woolf, N.J., 1998. A structural basis for memory storage in mammals. Prog Neurobiol 55, 59-77.

Wu, J., Kuo, Y.P., George, A.A., Xu, L., Hu, J., Lukas, R.J., 2004. beta-Amyloid directly inhibits human alpha4beta2-nicotinic acetylcholine receptors heterologously expressed in human SH-EP1 cells. J Biol Chem 279, 37842-37851.

Yang, L.B., Li, R., Meri, S., Rogers, J., Shen, Y., 2000. Deficiency of complement defense protein CD59 may contribute to neurodegeneration in Alzheimer's disease. J Neurosci 20, 7505-7509.

Zhu, Q., Wang, L., Zhang, Y., Zhao, F.H., Luo, J., Xiao, Z., Chen, G.J., Wang, X.F., 2012. Increased expression of DNA methyltransferase 1 and 3a in human temporal lobe epilepsy. J Mol Neurosci 46, 420-426.

Zipper, H., Brunner, H., Bernhagen, J., Vitzthum, F., 2004. Investigations on DNA intercalation and surface binding by SYBR Green I, its structure determination and methodological implications. Nucleic Acids Res 32, e103.

Zuccato, C., Cattaneo, E., 2009. Brain-derived neurotrophic factor in neurodegenerative diseases. Nat Rev Neurol 5, 311-322.

Zwart, R., Strotton, M., Ching, J., Astles, P.C., Sher, E., 2014. Unique pharmacology of heteromeric alpha7beta2 nicotinic acetylcholine receptors expressed in Xenopus laevis oocytes. Eur J Pharmacol 726, 77-86.

Appendices

Paper I-III

I. **Jensen MM**, Dyrvig M, Bertelsen B, Tümer Z, Christiansen SH, Pinborg LH, Thomsen MS, Lichota J, Mikkelsen JD. Expression and binding profiles of the α7 nicotinic acetylcholine receptor in human cortical tissue. *Manuscript in preparation for Mol. Pharmacol.*

II. Thomsen MS, Cinar B, **Jensen MM**, Lyukmanova EN, Shulepko MA, Tsetlin V, Klein AB, Mikkelsen JD (2014). Expression of the Ly-6 family proteins Lynx1 and Ly6H in the rat brain is compartmentalized, cell-type specific, and developmentally regulated. *Brain Struct Funct, 219(6):1923-34.*

III. **Jensen MM**, Mikkelsen JD, Arvaniti M, Michalski D, Härtig W, Thomsen MS (2015). Prostate stem cell antigen interacts with nicotinic acetylcholine receptors and is affected in Alzheimer's disease. *Neurobiol Aging, in press.*

Paper I

Jensen MM, Dyrvig M, Bertelsen B, Tümer Z, Christiansen SH, Pinborg LH, Thomsen MS, Lichota J, Mikkelsen JD.

Expression and binding profiles of the α7 nicotinic acetylcholine receptor in human cortical tissue.

Manuscript.

Expression and binding profiles of the α7 nicotinic acetylcholine receptor in human cortical tissue

Majbrit M. Jensen[1], Mads Dyrvig[2], Birgitte Bertelsen[3], Zeynep Tümer[3], Søren H. Christiansen[4], Lars H. Pinborg[1,5], Morten S. Thomsen[1], Jacek Lichota[2], Jens D. Mikkelsen[1,*]

[1]Neurobiology Research Unit, Copenhagen University Hospital, Rigshospitalet, Copenhagen, Denmark

[2]Laboratory of Neurobiology, Department of Health Science and Technology, Aalborg University, Aalborg, Denmark

[3]Applied Human Molecular Genetics, Kennedy Center, Copenhagen University Hospital, Rigshospitalet, Glostrup, Denmark

[4]Laboratory of Neural Plasticity, Department of Neuroscience and Pharmacology, University of Copenhagen, Copenhagen, Denmark

[5]Epilepsy Clinic, University Hospital Copenhagen, Rigshospitalet, Copenhagen, Denmark

*** Corresponding Author:**

Jens D. Mikkelsen

Neurobiology Research Unit

Copenhagen University Hospital, Rigshospitalet, section 6931

Juliane Maries Vej 28

DK-2100 Copenhagen, Denmark

E-mail: jens_mikkelsen@dadlnet.dk, jdm@nru.dk

Abbreviations: α-bungarotoxin, α-Bgt; nicotinic acetylcholine receptor, nAChR; reverse-transcription quantitative polymerase chain reaction, RT-qPCR; specific binding, SB

Abstract

Compounds targeting the α7 nicotinic acetylcholine receptor (nAChR) are currently in development for the treatment of Alzheimer's disease and schizophrenia. Even though clinical trials have shown promising effects, high interindividual variability has been observed. Variability is also seen in the promoter region of the α7 nAChR gene, *CHRNA7*, and in the partial duplication of the *CHRNA7* gene (*CHRFAM7A*), and these genetic variabilities have been linked with schizophrenia. In this study, the expression of *CHRNA7* and *CHRFAM7A* as well as DNA methylation of the *CHRNA7* promoter were examined in human temporal cortical tissue obtained from neurosurgical resections in patients with focal epilepsy. We found that the mRNA levels of *CHRNA7* are 3.4 times higher than *CHRFAM7A*. Interestingly, an inverse correlation between promoter DNA methylation and *CHRNA7* mRNA levels (r=-0.798, *P*=0.0099) was observed, suggesting that not only promoter variations, but also the level of methylation is critical for expression of the gene. Displacement of the selective α7 nAChR antagonist [^{125}I]-α-bungarotoxin (α-Bgt) by the partial α7 nAChR agonist encenicline (EVP-6124) was also studied in the human cortical tissue. The displacement curve with encenicline was best fitted to a two-site model in some human individuals giving IC_{50} values of 6.2 nM and 2.6 μM, whereas only the lower-affinity component was identified in other individuals (IC_{50} ~5.8 μM). The findings emphasize the large variations in methylation status, gene expression, and binding properties of the α7 nAChR in native human brain tissue. These interindividual differences may underlie the large individual differences in responses to α7 nAChR modulators.

Introduction

Cognitive impairments are common features in several psychiatric and neurological diseases such as schizophrenia and Alzheimer's disease, and current medication has only limited effects. The α7 nicotinic acetylcholine receptor (nAChR) is considered an important drug target for improvement of the cognitive impairments in these diseases (reviewed in (Thomsen et al., 2010; Wallace and Porter, 2011)). The α7 nAChR partial agonist, encenicline (EVP-6124, FORUM Pharmaceuticals) was reported to produce effects in domains of the CogState Schizophrenia Battery such as memory and executive function at very low doses in patients with schizophrenia in a recent randomized clinical trial (Preskorn et al., 2014). The improvement in higher cognitive functions was similar to earlier proof of concept studies with another less selective partial α7 nAChR agonist, GTS-21, both in healthy volunteers (Kitagawa et al., 2003) and in patients with schizophrenia (Freedman et al., 2008; Olincy et al., 2006). In addition, a recent study demonstrated effects with the α7 nAChR partial agonist TC-5619 in executive function and Scale for Assessment of Negative Symptoms in patients with schizophrenia as well as positive effects in working memory in smokers (Lieberman et al., 2013).

The α7 nAChR is a pentameric ligand-gated ion channel, which is widely distributed in the brain (Albuquerque et al., 2009; Dani and Bertrand, 2007). The human gene encoding α7 nAChR, *CHRNA7*, is located at chromosome 15q13.3, and variations in the gene have been linked to schizophrenia (Leonard and Freedman, 2006). Thus, polymorphisms in the proximal promoter region and in regulatory regions upstream of *CHRNA7* are more frequent in patients with schizophrenia (Leonard et al., 2002; Stephens et al., 2009) and are associated to the endophenotype, the P50 sensory gating deficit. Interestingly, many of the polymorphisms in the promoter region show reduced transcription when investigated in an *in vitro* reporter gene assay (Leonard et al., 2002). In addition, an inverse correlation between the methylation of the promoter and *CHRNA7* mRNA levels has been found across several human tissue types as well as human-derived cell lines (Canastar et al., 2012).

In humans, the *CHRNA7* gene is partially duplicated (Gault et al., 1998). Exons 5-10 of *CHRNA7* along with additional DNA (~200 Kbp) are duplicated upstream of the *CHRNA7* and interrupting a second partial duplication of the *ULK4* gene. Remarkably, the duplication is a recent evolutionary event and unique to humans, since it is not found in other mammalian species including closely related primates (Locke et al., 2003). The partially duplicated, chimeric gene, *CHRFAM7A*, maps centromeric to the full-length *CHRNA7* by 1.6 Mb (Gault et al., 1998; Riley et al., 2002). Most

people (>95%) have one or two copies of *CHRFAM7A* (Sinkus et al., 2009). Furthermore, a two base pair deletion in exon 6 of *CHRFAM7A* has been identified, and this deletion was found to be significantly associated with schizophrenia and the P50 sensory gating deficit (Flomen et al., 2013; Gault et al., 2003; Sinkus et al., 2009). Co-expression of *CHRNA7* and *CHRFAM7A* gene products in *Xenopus* oocytes reduced the amplitude of acetylcholine-evoked currents suggesting that the duplicated gene products act as negative modulators of α7 nAChR function (Araud et al., 2011; de Lucas-Cerrillo et al., 2011).

Poor translability of the effects of α7 nAChR agonists observed in preclinical animal models to the effect in randomized clinical trials in patients is evident (reviewed by (Thomsen et al., 2010)). In clinical trials for pro-cognitive drugs, large variabilities in positive effects are observed and often the variabilities are compromising these effects (Husain and Mehta, 2011). It is not clear what differences that account for the variability, but genotypic differences is likely part of the explanation (Costa e Silva, 2013; Lesko and Woodcock, 2004) that could lead to differences in mRNA expression and DNA methylation. However, it is also possible that proteins binding to the α7 nAChR subunit may account for the variability in the response to drugs. For example variations in the expression of *CHRFAM7A* may account for different receptor efficacies in humans compared to animals, which are lacking the duplicated gene. Furthermore, heterogeneity of α7 nAChR receptors could be important, given that α7 nAChR form complexes with the β2 nAChR subunit in human basal forebrain (Moretti et al., 2014) and members of the Ly-6/neurotoxin protein family (Miwa et al., 2011; Thomsen and Mikkelsen, 2012), which have been demonstrated to alter the function of the α7 nAChR. More studies in human native tissues on the transcriptional regulation, the composition, and structure of the human α7 nAChR receptor target are important to understand and correlate the effect of α7 nAChR modulators in clinical trials.

Studying gene expression in the human brain has been challenging due to RNA degradation by RNAases as well as pre- and postmortem variables affecting the RNA quality (Durrenberger et al., 2010). In this study, we have used freshly frozen human temporal cortical tissue obtained from neurosurgical interventions to investigate the mRNA expression of *CHRNA7* and *CHRFAM7A*, DNA methylation of the *CHRNA7* promoter, and characteristics in receptor binding properties by displacing [^{125}I]-α-bungarotoxin (α-Bgt) binding by encenicline.

Materials and Methods

Human brain tissue

Temporal cortical tissue was obtained from anterior temporal lobectomies in a total of 13 patients with medically intractable temporal lobe epilepsy with hippocampal onset listed in Table 1. Performing anterior temporal lobectomy, the lateral temporal neocortex was resected in addition to the mesial temporal structures expected to contain the epileptogenic zone. In all cases lateral temporal neocortex appeared normal on both MRI and at neuropathological examination. Written informed consent was obtained from all patients before surgery. The study was approved by the Ethical Committee in the Capital Region of Denmark (H-2-2011-104) and performed in accordance with the Declaration of Helsinki. The tissue was resected during the neurosurgical procedure, immediately frozen on dry ice, and stored at -80°C until use.

Reverse-transcription quantitative PCR

Levels of mRNA were determined by reverse-transcription quantitative polymerase chain reaction (RT-qPCR). Total RNA from human cortical extracts (subjects HB01-12 in Table 1) was extracted with RNeasy Mini Kit (Qiagen, Hilden, Germany) according to the manufacturer's protocol. The samples were dissolved in RNase-free water and RNA content was quantified on a Nanodrop ND-2000 spectrophotometer (Thermo Fisher Scientific, Wilmington, DE). Extracted RNA was reverse transcribed into single-stranded cDNA with the ImPromII™ Reverse Transcription System (Promega, Madison, WI) according to the manufacturer's protocol using oligo$(dT)_{15}$ primers, 6 mM $MgCl_2$, and 20 units of RNase inhibitor. RT-qPCR reactions were performed in a total volume of 20 µl, containing 5 µl sample cDNA, 10 µl 2×Brilliant II SYBR® Green qPCR Master Mix (Agilent Technologies, Santa Clara, CA), 15 pmol each of the forward and reverse primer (DNA Technology, Aarhus, Denmark), and combined with distilled water to the final volume. The primers used in these experiments are described in Table 2. RT-qPCR was performed on a Light Cycler 480 (Roche, Indianapolis, IN) and initiated with a 10 minute preincubation at 94°C followed by 45 cycles of 30 seconds at 94°C, 45 seconds at 60°C, and 1.5 minutes at 72°C. After finished amplification, a melting curve program was run. All samples were run in triplex and all primers were validated by using serially diluted cDNA to establish a standard curve to generate efficiencies for each primer pair, which were all in the range of 90-110%, and by confirming the size of each product on a 2% agarose gel (data not shown). Quantification of mRNA expression was calculated

as E^{-C_T}, where C_T defines the threshold cycle and E the efficiency of the primer pair, according to the efficiency corrected Pfaffl method (Pfaffl, 2001).

DNA methylation analysis and qPCR

Genomic DNA and total RNA were extracted from human cortical extracts (subjects HB01-09 in Table 1) with an AllPrep DNA/RNA Mini Kit (Qiagen, Germany). The tissue was disrupted and homogenized for 30 seconds with a T10 basic ULTRA TURRAX Homogenizer (IKA, Germany) and processed according to manufacturer's protocol for simultaneous purification of genomic DNA and total RNA from Animal Tissues. DNA and RNA were stored at -80°C until further use. Purity and concentration of RNA and DNA were assessed with a NanoPhotometer™ (IMPLEN, Germany).

Synthesis of cDNA and RT-qPCR reactions were run as above with slight modifications. RNA was reverse transcribed with a RevertAid™ Premium First Strand cDNA Synthesis Kit (Thermo Scientific, Germany), PCR reactions were run in an Mx3000P Real-Time PCR System (Stratagene, USA), and reaction mixtures consisted of 1×Maxima SYBR Green qPCR Master Mix (2×), ROX solution provided (Thermo Scientific, Germany).

The stability of several reference genes has previously been tested in human neocortex from epilepsy patients (Wierschke et al., 2010). Using Normfinder software (Andersen et al., 2004), it was found that the geometric mean of TATA-box binding protein (*TBP*) and neuron-specific enolase (*NSE*) were the best suited combination of reference genes for normalization. We included these housekeeping genes as well as β-actin (*ACTB*) and since no difference in using the geometric mean of *TBP/NSE* or *TBP/ACTB* was found, the latter was used for normalization. Gene expression was calculated using the efficiency corrected Pfaffl method (Pfaffl, 2001).

All DNA samples were bisulfite converted with an EpiTect® Bisulfite kit (Qiagen, Germany), according to the manufacturer's protocol for sodium bisulfite conversion of unmethylated cytosines. The human *CHRNA7* promoter was amplified with HotStarTaq DNA Polymerase (Qiagen, Germany) with the primers listed in Table 2. To prevent amplification bias, the primers were tested at several annealing temperatures, and the highest temperature providing sufficient product was selected (Shen et al., 2007). As the *CHRNA7* promoter has a very high CpG density, primer placement is difficult. Therefore, the primers were designed to target the antisense strand to ensure optimal placement. 20 µL reaction were prepared according to protocol with 30 ng bisulfite converted DNA, 0.5 µM of each primer, and 3 mM $MgCl_2$. The cycling conditions were: 95°C for 15 minutes, 40 cycles (94°C for 30 seconds, 60°C for 2 minutes, 72°C for 1 minute), and 72°C for

10 minutes. PCR products were gel electrophorized on a 2% agarose gel stained with ethidium bromide. Subsequently, the PCR products were cut from the gel and isolated with a QIAquick Gel Extraction Kit (Qiagen, Germany), and concentrations were assessed with a NanoPhotometer™ (IMPLEN, Germany). PCR products were cloned using the InsTAclone™ PCR Cloning Kit (Fermentas, Lithuania). Selected plasmid DNA were extracted with a GeneJET Plasmid Miniprep Kit (Fermentas, Lithuania) and 1.5 µg of each preparation was freeze-dried and sent to Beckman Coulter Genomics (United Kingdom) for sequencing.

In vitro receptor autoradiography and analysis

Human temporal cortical tissue was cut in 12 µm sections on a cryostat, thaw-mounted onto Super Frost Plus slides, and stored at -80°C until further processing. 15 slides from each subject (subjects HB04, HB06, HB10, HB12, and HB14 in Table 1) were thawed at room temperature for 30 minutes, followed by 30 minutes hydration in 50 mM Tris buffer with 0.1% BSA, pH 7.3 (binding buffer). To assess total binding, one set of slides was incubated for 2 hours at room temperature in binding buffer containing [^{125}I]Tyr-54-mono-iodo-α-bungarotoxin ([^{125}I]-α-Bgt; 2,200 Ci/mmol; Perkin Elmer, Skovlunde, Denmark) mixed 1:10 with non-radioactive α-Bgt yielding a total of 5 nM. Serial dilutions of encenicline (kindly provided by Dr. Dan Peters, Neurosearch, Ballerup; concentrations 0.01 nM - 30 µM) were included in the incubation for the subsequent 13 slides, and finally 1 mM (-)-nicotine (Sigma Aldrich, Brøndby, Denmark) was added to the last set of slides for analysis of non-specific binding. Slides were then briefly rinsed in binding buffer, followed by 2×30 minutes washes in ice-cold binding buffer, and briefly rinsed in ice-cold distilled water. Subsequently, slides were dried under an air stream and fixated overnight at 4°C in a sealed chamber containing paraformaldehyde vapour. Finally, slides were dried for 2-3 hours in an excicator, exposed to a BASMS2040 phosphor imaging plate (Science Imaging Scandinavia AB, Nacka, Sweden) for ~17 hours, and scanned with a BAS-2500 imaging plate scanner (Fujifilm Europe GmbH, Düsseldorf, Germany).

Mean optical densities from autoradiographies were quantified using a computer image analysis system (Quantity One®, Bio-Rad,CA,USA). Only the outer cortical layers were measured (see Figure 2D). The individual value for each slide was calculated as the average measurement from 2-3 individual sections. The average value from a corresponding slice with non-specific binding (presence of 1 mM nicotine) was subtracted to yield specific binding (SB), and the percent inhibition by which encenicline displaced [^{125}I]-α-Bgt was calculated as:

$$\% \text{ inhibition} = \frac{(SB_{total} - SB_{encenicline})}{SB_{total}} \cdot 100\%,$$

where SB_{total} and $SB_{encenicline}$ is the specific binding of [^{125}I]-α-Bgt in the absence and presence of encenicline, respectively.

Statistical analysis

The correlation between *CHRNA7* expression and promoter DNA methylation was examined using Pearson correlation. IC_{50} values were determined from plots of binding activity versus log encenicline concentration using non-linear regression analysis where one-site and two-sites models were compared by extra sum-of-squares F test. The simpler one-site model was chosen unless the *P* value of the extra sum-of-squares F test was significant. All analyses were conducted using GraphPad Prism 6.03 (GraphPad software, San Diego, CA, USA). *P* values <0.05 were considered to be statistically significant.

Results

CHRFAM7A mRNA expression in human temporal cortex

Expression levels of *CHRNA7*, *CHRFAM7A*, *CHRNA4*, and *CHRNB2* mRNA were measured in human temporal cortical extracts by RT-qPCR (see Table 3). The level of *CHRNB2* mRNA expression was highest, and both *CHRNB2* and *CHRNA4* were more expressed than *CHRNA7*. Interestingly, the *CHRFAM7A* mRNA was detected though at lower levels than *CHRNA7* mRNA in all subjects and accounted for ~30% compared to *CHRNA7* mRNA in the individuals with a ratio *CHRNA7:CHRFAM7A* mRNA levels of 3.4 and a coefficient of variation of 0.78. No correlations between mRNA levels and age or gender were observed.

DNA methylation of the human CHRNA7 promoter correlates with mRNA expression

The human *CHRNA7* gene has a CpG island in its promoter. We focused on the core promoter and also included parts of the first exon, as DNA methylation of the first exon is tightly linked to transcriptional silencing (Brenet et al., 2011). We examined 53 CpGs from position -114 to +243 in the human *CHRNA7* promoter. Nine to ten clones from each subject were included and the sum of methylated cytosines was divided by the total amount of CpG sites examined. Both *CHRNA7* expression and promoter DNA methylation displayed large variation in the subjects. In general, the promoter was methylated to a low degree but even few methylation sites have previously been

found to correlate with transcriptional repression (Zhang et al., 2010). Because of the large differences in both methylation and expression between samples, we analyzed the correlation between *CHRNA7* gene expression and DNA methylation (Figure 1). The inverse relationship between *CHRNA7* mRNA quantity and promoter methylation was significantly correlated (r=-0.798, *P*=0.0099).

Encenicline displaces [^{125}I]-α-bungarotoxin in human cortical tissue

Using autoradiography, 30 µM encenicline was found to displace [^{125}I]-α-Bgt in human temporal cortical slices similar to 1 mM nicotine (see Figure 2). Dose-response curves with encenicline revealed a high variability among the human individuals in displacing [^{125}I]-α-Bgt at equivalent concentrations of encenicline (Figure 3A). When determining the IC_{50} values of encenicline in the five human individuals the best fit of the data was analyzed and validated, where the displacement profiles were tested for the presence of a two-site model. Data from a two-site model were accepted only if the residual sum of squares was significantly lower in a two-site model compared to a one-site model (F-test, $P<0.05$). A one-site competition model was preferred in two of the human subjects (HB10 and HB12; $P>0.4$), whereas in three of the individuals a two-site competition model was accepted (HB04, HB06, HB14; *P* values 0.037, 0.034, 0.012, respectively).

The calculated IC_{50} and log IC_{50} values of all five individuals are presented in Table 4. One of the individuals having two-site characteristics showed a high affinity IC_{50} value at subnanomolar concentration, whereas the high affinity IC_{50} values of the two others were ~10 nM. Low affinity IC_{50} values in all three subjects were in the micromolar range and comparable to IC_{50} values determined by the one-site model (5.89 µM and 5.54 µM, respectively). Data from the human subjects were pooled dependent on the preferred model (Figure 3B) and IC_{50} values of the pooled data were determined (Table 4). The high affinity and low affinity IC_{50} values for the two-site competition model were 6.22 nM and 2.63 µM, respectively, while the IC_{50} value for the one-site competition model was 5.75 µM.

Discussion

Gene expression, synthesis, and function of the α7 nAChR are regulated by a number of mechanisms and further complicated by the involvement of other gene products integrated in the receptor. Transcriptional regulation is complex with epigenetic regulation playing an important role, and the function of the α7 nAChR might be affected by the presence of the partially duplicated

chimeric gene *CHRFAM7A*, and possible formation of α7-containing heteromeric receptors that are pharmacologically different from the homomeric receptor (Khiroug et al., 2002; Liu et al., 2009; Murray et al., 2012; Palma et al., 1999; Zwart et al., 2014). In the present study using human temporal cortical extracts, it was shown that the transcription of *CHRNA7* is 3.4 times higher than *CHRFAM7A* and that the levels of *CHRNA7* was inversely related to DNA methylation of the promoter. Finally, the α7 nAChR agonist encenicline was demonstrated to displace [^{125}I]-α-Bgt differently in human cortex, however the displacement profiles were highly different between the human individuals.

The demonstration that the expression of *CHRNA7* mRNA is 3.4 times higher than *CHRFAM7A* in human temporal cortex is consistent with previous studies (De Luca et al., 2006; de Lucas-Cerrillo et al., 2011). We observed high between-subject variability in the *CHRNA7*:*CHRFAM7A* ratio with a coefficient of variation of 0.78, which was also seen in prefrontal cortex of patients with schizophrenia or bipolar disorder as well as in unaffected controls with the coefficient of variation ~0.6 (De Luca et al., 2006). However, we did not distinguish, whether the two base pair deletion in *CHRFAM7A* is present or not. The transcript of *CHRFAM7A* is suggested to be more abundant in cortical regions including temporal cortex than other regions, where it has been identified, such as hippocampus, thalamus, corpus callosum, and cerebellum (Gault et al., 1998; Severance and Yolken, 2008; Villiger et al., 2002). Interestingly, in peripheral cells the *CHRNA7*:*CHRFAM7A* ratio seems to be opposite than in the brain, where high levels of *CHRFAM7A* mRNA have been observed in macrophages and monocytes (Benfante et al., 2011; de Lucas-Cerrillo et al., 2011).

DNA methylation is known to repress transcription. In accordance, modulation of the *CHRNA7* gene transcription by promoter methylation has recently been demonstrated in human-derived cell lines, where inhibitors of a DNA methyltransferase significantly increased the *CHRNA7* expression in transcription-silenced, hypermethylated neuroblastoma SH-EP1 cells (Canastar et al., 2012). Moreover, a tissue-specific correlation between mRNA expression and DNA methylation was shown for a selection of human tissues (Canastar et al., 2012). The demonstration that the degree of promoter DNA methylation significantly correlates with *CHRNA7* expression in individual human cortical extracts supports the concept from the studies in cell lines and human tissue that methylation is important for gene expression. Our data revealed that ~1% of the examined CpG sites were methylated, which contrast previous finding in human brain, where ~22% methylation was found in human cingulate gyrus (Canastar et al., 2012). This could indicate methylation variability across brain regions, but may also be partially explained by differences in the applied

methods, as the human cingulate gyrus was examined by methylation-sensitive restriction enzyme analysis.

Generally, CpG-island methylation levels are highly correlated between brain and blood suggesting that DNA methylation levels could be potential biomarkers for brain disorders (Ewald et al., 2014; Tylee et al., 2013). Transcription of *CHRNA7* in human primary lymphocytes is demonstrated to be silenced by a high promoter methylation level (Canastar et al., 2012). Thus, it is pertinent to study the mechanisms behind epigenetic modifications of the *CHRNA7* gene and whether they are related to disease.

Though, the cortical tissue used in the present experiments appeared micro- and macroscopically normal, the tissue was resected from patients with medically refractory epilepsy and frequent epileptic seizures. These patients have usually experienced convulsions and are under treatment with a number of anti-epileptic drugs, and both affect DNA methylation and gene expression patterns. Alterations in DNA methylation of gene promoters and increased expression of DNA methyltransferases have previously been demonstrated in patients with temporal lobe epilepsy (Kobow et al., 2009; Zhu et al., 2012). Nevertheless, the direct correlation between methylation and mRNA levels suggests that epigenetic factors are important for expression of the α7 nAChR.

We have previously studied [^{125}I]-α-Bgt binding in human postmortem tissue and observed high levels of specific binding in temporal cortex (Thomsen et al., 2011). Here, we further demonstrate that the α7 nAChR partial agonist encenicline displaces [^{125}I]-α-Bgt binding in human temporal cortex. Encenicline shows two-site displacement profile of α-Bgt in some human subjects, which indicate that there are two classes of sites with identical affinity for [^{125}I]-α-Bgt, but different affinities for encenicline, with high affinity in the nanomolar range and low affinity in the micromolar range. Subjects displaying one-site displacement profile have affinities in the low affinity range. Previously, encenicline has been shown to displace [^{125}I]-α-Bgt in rat brain homogenates with a K_i of 4.3 nM (pIC_{50}=8.07) (Prickaerts et al., 2012), which is consistent with the high affinity site in our data. Interestingly, encenicline was suggested to act through a co-agonist mechanism given that concentrations below 1 nM encenicline enhanced acetylcholine-evoked currents without desensitization in transfected *Xenopus* oocytes, while concentrations at 3 nM encenicline and above reduced the currents due to receptor desensitization. In addition, estimated low doses of encenicline restored memory function in an object recognition task in scopolamine-treated rats (Prickaerts et al., 2012). Our data suggest that the observations instead of the proposed co-agonist model could be explained by encenicline having two different binding modes, a high

affinity and a low affinity binding mode, which may influence the function of the α7 nAChR in different ways.

Given that the two-site model is not observed in rat cortical tissue, the presence of the truncated α7 nAChR subunits unique to humans could change the binding characteristics of encenicline, which could also be dependent on whether the individuals carry the two base pair deletion in *CHRFAM7A* or not. The gene product of *CHRFAM7A*, dupα7, is lacking a large part of the N terminal of the α7 nAChR containing the ligand binding domain (Gault et al., 1998), whereas the two base pair deletion causes a frame shift resulting in an even smaller gene product, dupΔα7, which is lacking nearly the entire ligand binding domain (Araud et al., 2011). α-Bgt binds to the extracellular N terminal region encoded by exons 1-5 of *CHRNA7* (McLane et al., 1990), and co-expression of dupα7 or dupΔα7 with α7 nAChR in *Xenopus* oocytes displayed a reduced binding of [^{125}I]-α-Bgt compared to expression of α7 nAChR alone (Araud et al., 2011). A lower [^{125}I]-α-Bgt binding in human hippocampus than in rat and monkey has previously been demonstrated (Breese et al., 1997), which could be due to the presence of dupα7 in the human tissue. It has further been hypothesized that the presence of dupα7 or dupΔα7 could result in inactivated receptors or altered binding sites, since at an equivalent current evoked by acetylcholine, a higher binding of α-Bgt was observed in oocytes, when dupα7 was present (Araud et al., 2011). Furthermore, co-expression of α7 with dupα7 or dupΔα7 showed altered sensitivity to choline and varenicline, where α7/dupΔα7 heteromeric receptors displayed lower sensitivity to choline than α7/dupα7 receptors, while it was opposite with varenicline (Wang et al., 2014). Thus, the presence of dupα7 and dupΔα7 could modulate the efficacy of α7 nAChR ligands, which should be taken into account when characterizing new compounds targeting the α7 nAChR for the treatment of cognitive deficits in schizophrenia and Alzheimer's disease. Another factor that could influence the efficacy is the formation of heteromeric receptor assemblies involving α7 and β-subunits. Moreover, several members of Ly-6/neurotoxins protein superfamily have been shown to bind to and modulate the function of nAChRs (reviewed in (Miwa et al., 2011; Thomsen and Mikkelsen, 2012)) and thus could also be affecting drug efficacy.

Temporal neocortex from neurosurgical interventions, as has been used in this study, may be a beneficial tool to investigate binding characteristics of various α7 nAChR compounds in human tissue, and how it might be affected by the genotype of the individual, which could give insight into personalized treatment in the future.

Acknowledgements

This work was supported by the Danish Strategic Research Council (COGNITO) and the Lundbeck Foundation.

References

Albuquerque, E.X., Pereira, E.F., Alkondon, M., Rogers, S.W., 2009. Mammalian nicotinic acetylcholine receptors: from structure to function. Physiol Rev 89, 73-120.

Andersen, C.L., Jensen, J.L., Orntoft, T.F., 2004. Normalization of real-time quantitative reverse transcription-PCR data: a model-based variance estimation approach to identify genes suited for normalization, applied to bladder and colon cancer data sets. Cancer Res 64, 5245-5250.

Araud, T., Graw, S., Berger, R., Lee, M., Neveu, E., Bertrand, D., Leonard, S., 2011. The chimeric gene CHRFAM7A, a partial duplication of the CHRNA7 gene, is a dominant negative regulator of alpha7*nAChR function. Biochem Pharmacol 82, 904-914.

Benfante, R., Antonini, R.A., De Pizzol, M., Gotti, C., Clementi, F., Locati, M., Fornasari, D., 2011. Expression of the alpha7 nAChR subunit duplicate form (CHRFAM7A) is down-regulated in the monocytic cell line THP-1 on treatment with LPS. J Neuroimmunol 230, 74-84.

Breese, C.R., Adams, C., Logel, J., Drebing, C., Rollins, Y., Barnhart, M., Sullivan, B., Demasters, B.K., Freedman, R., Leonard, S., 1997. Comparison of the regional expression of nicotinic acetylcholine receptor alpha7 mRNA and [125I]-alpha-bungarotoxin binding in human postmortem brain. J Comp Neurol 387, 385-398.

Brenet, F., Moh, M., Funk, P., Feierstein, E., Viale, A.J., Socci, N.D., Scandura, J.M., 2011. DNA methylation of the first exon is tightly linked to transcriptional silencing. PLoS One 6, *in press.*

Canastar, A., Logel, J., Graw, S., Finlay-Schultz, J., Osborne, C., Palionyte, M., Drebing, C., Plehaty, M., Wilson, L., Eyeson, R., Leonard, S., 2012. Promoter methylation and tissue-specific transcription of the alpha7 nicotinic receptor gene, CHRNA7. J Mol Neurosci 47, 389-400.

Costa e Silva, J.A., 2013. Personalized medicine in psychiatry: new technologies and approaches. Metabolism 62 Suppl 1, S40-44.

Dani, J.A., Bertrand, D., 2007. Nicotinic acetylcholine receptors and nicotinic cholinergic mechanisms of the central nervous system. Annu Rev Pharmacol Toxicol 47, 699-729.

De Luca, V., Likhodi, O., Van Tol, H.H., Kennedy, J.L., Wong, A.H., 2006. Regulation of alpha7-nicotinic receptor subunit and alpha7-like gene expression in the prefrontal cortex of patients with bipolar disorder and schizophrenia. Acta Psychiatr Scand 114, 211-215.

de Lucas-Cerrillo, A.M., Maldifassi, M.C., Arnalich, F., Renart, J., Atienza, G., Serantes, R., Cruces, J., Sanchez-Pacheco, A., Andres-Mateos, E., Montiel, C., 2011. Function of partially duplicated human alpha77 nicotinic receptor subunit CHRFAM7A gene: potential implications for the cholinergic anti-inflammatory response. J Biol Chem 286, 594-606.

Durrenberger, P.F., Fernando, S., Kashefi, S.N., Ferrer, I., Hauw, J.J., Seilhean, D., Smith, C., Walker, R., Al-Sarraj, S., Troakes, C., Palkovits, M., Kasztner, M., Huitinga, I., Arzberger, T., Dexter, D.T., Kretzschmar, H., Reynolds, R., 2010. Effects of antemortem and postmortem variables on human brain mRNA quality: a BrainNet Europe study. J Neuropathol Exp Neurol 69, 70-81.

Ewald, E.R., Wand, G.S., Seifuddin, F., Yang, X., Tamashiro, K.L., Potash, J.B., Zandi, P., Lee, R.S., 2014. Alterations in DNA methylation of Fkbp5 as a determinant of blood-brain correlation of glucocorticoid exposure. Psychoneuroendocrinology 44, 112-122.

Flomen, R.H., Shaikh, M., Walshe, M., Schulze, K., Hall, M.H., Picchioni, M., Rijsdijk, F., Toulopoulou, T., Kravariti, E., Murray, R.M., Asherson, P., Makoff, A.J., Bramon, E., 2013. Association between the 2-bp deletion polymorphism in the duplicated version of the alpha7 nicotinic receptor gene and P50 sensory gating. Eur J Hum Genet 21, 76-81.

Freedman, R., Olincy, A., Buchanan, R.W., Harris, J.G., Gold, J.M., Johnson, L., Allensworth, D., Guzman-Bonilla, A., Clement, B., Ball, M.P., Kutnick, J., Pender, V., Martin, L.F., Stevens, K.E., Wagner, B.D., Zerbe, G.O., Soti, F., Kem, W.R., 2008. Initial phase 2 trial of a nicotinic agonist in schizophrenia. Am J Psychiatry 165, 1040-1047.

Gault, J., Hopkins, J., Berger, R., Drebing, C., Logel, J., Walton, C., Short, M., Vianzon, R., Olincy, A., Ross, R.G., Adler, L.E., Freedman, R., Leonard, S., 2003. Comparison of polymorphisms in the alpha7 nicotinic receptor gene and its partial duplication in schizophrenic and control subjects. Am J Med Genet B Neuropsychiatr Genet 123B, 39-49.

Gault, J., Robinson, M., Berger, R., Drebing, C., Logel, J., Hopkins, J., Moore, T., Jacobs, S., Meriwether, J., Choi, M.J., Kim, E.J., Walton, K., Buiting, K., Davis, A., Breese, C., Freedman, R., Leonard, S., 1998. Genomic organization and partial duplication of the human alpha7 neuronal nicotinic acetylcholine receptor gene (CHRNA7). Genomics 52, 173-185.

Husain, M., Mehta, M.A., 2011. Cognitive enhancement by drugs in health and disease. Trends Cogn Sci 15, 28-36.

Khiroug, S.S., Harkness, P.C., Lamb, P.W., Sudweeks, S.N., Khiroug, L., Millar, N.S., Yakel, J.L., 2002. Rat nicotinic ACh receptor alpha7 and beta2 subunits co-assemble to form functional heteromeric nicotinic receptor channels. J Physiol 540, 425-434.

Kitagawa, H., Takenouchi, T., Azuma, R., Wesnes, K.A., Kramer, W.G., Clody, D.E., Burnett, A.L., 2003. Safety, pharmacokinetics, and effects on cognitive function of multiple doses of GTS-21 in healthy, male volunteers. Neuropsychopharmacology 28, 542-551.

Kobow, K., Jeske, I., Hildebrandt, M., Hauke, J., Hahnen, E., Buslei, R., Buchfelder, M., Weigel, D., Stefan, H., Kasper, B., Pauli, E., Blumcke, I., 2009. Increased reelin promoter methylation is associated with granule cell dispersion in human temporal lobe epilepsy. J Neuropathol Exp Neurol 68, 356-364.

Leonard, S., Freedman, R., 2006. Genetics of chromosome 15q13-q14 in schizophrenia. Biol Psychiatry 60, 115-122.

Leonard, S., Gault, J., Hopkins, J., Logel, J., Vianzon, R., Short, M., Drebing, C., Berger, R., Venn, D., Sirota, P., Zerbe, G., Olincy, A., Ross, R.G., Adler, L.E., Freedman, R., 2002. Association of promoter variants in the alpha7 nicotinic acetylcholine receptor subunit gene with an inhibitory deficit found in schizophrenia. Arch Gen Psychiatry 59, 1085-1096.

Lesko, L.J., Woodcock, J., 2004. Translation of pharmacogenomics and pharmacogenetics: a regulatory perspective. Nat Rev Drug Discov 3, 763-769.

Lieberman, J.A., Dunbar, G., Segreti, A.C., Girgis, R.R., Seoane, F., Beaver, J.S., Duan, N., Hosford, D.A., 2013. A randomized exploratory trial of an alpha-7 nicotinic receptor agonist (TC-5619) for cognitive enhancement in schizophrenia. Neuropsychopharmacology 38, 968-975.

Liu, Q., Huang, Y., Xue, F., Simard, A., DeChon, J., Li, G., Zhang, J., Lucero, L., Wang, M., Sierks, M., Hu, G., Chang, Y., Lukas, R.J., Wu, J., 2009. A novel nicotinic acetylcholine receptor subtype in basal forebrain cholinergic neurons with high sensitivity to amyloid peptides. J Neurosci 29, 918-929.

Locke, D.P., Archidiacono, N., Misceo, D., Cardone, M.F., Deschamps, S., Roe, B., Rocchi, M., Eichler, E.E., 2003. Refinement of a chimpanzee pericentric inversion breakpoint to a segmental duplication cluster. Genome Biol 4, R50.

McLane, K.E., Wu, X.D., Conti-Tronconi, B.M., 1990. Identification of a brain acetylcholine receptor alpha subunit able to bind alpha-bungarotoxin. J Biol Chem 265, 9816-9824.

Miwa, J.M., Freedman, R., Lester, H.A., 2011. Neural systems governed by nicotinic acetylcholine receptors: emerging hypotheses. Neuron 70, 20-33.

Moretti, M., Zoli, M., George, A.A., Lukas, R.J., Pistillo, F., Maskos, U., Whiteaker, P., Gotti, C., 2014. The Novel alpha7beta2-Nicotinic Acetylcholine Receptor Subtype Is Expressed in Mouse and Human Basal Forebrain: Biochemical and Pharmacological Characterization. Mol Pharmacol 86, 306-317.

Murray, T.A., Bertrand, D., Papke, R.L., George, A.A., Pantoja, R., Srinivasan, R., Liu, Q., Wu, J., Whiteaker, P., Lester, H.A., Lukas, R.J., 2012. alpha7beta2 nicotinic acetylcholine receptors assemble, function, and are activated primarily via their alpha7-alpha7 interfaces. Mol Pharmacol 81, 175-188.

Olincy, A., Harris, J.G., Johnson, L.L., Pender, V., Kongs, S., Allensworth, D., Ellis, J., Zerbe, G.O., Leonard, S., Stevens, K.E., Stevens, J.O., Martin, L., Adler, L.E., Soti, F., Kem, W.R., Freedman, R., 2006. Proof-of-concept trial of an alpha7 nicotinic agonist in schizophrenia. Arch Gen Psychiatry 63, 630-638.

Palma, E., Maggi, L., Barabino, B., Eusebi, F., Ballivet, M., 1999. Nicotinic acetylcholine receptors assembled from the alpha7 and beta3 subunits. J Biol Chem 274, 18335-18340.

Pfaffl, M.W., 2001. A new mathematical model for relative quantification in real-time RT-PCR. Nucleic Acids Res 29, e45.

Preskorn, S.H., Gawryl, M., Dgetluck, N., Palfreyman, M., Bauer, L.O., Hilt, D.C., 2014. Normalizing effects of EVP-6124, an alpha-7 nicotinic partial agonist, on event-related potentials and cognition: a proof of concept, randomized trial in patients with schizophrenia. J Psychiatr Pract 20, 12-24.

Prickaerts, J., van Goethem, N.P., Chesworth, R., Shapiro, G., Boess, F.G., Methfessel, C., Reneerkens, O.A., Flood, D.G., Hilt, D., Gawryl, M., Bertrand, S., Bertrand, D., Konig, G., 2012. EVP-6124, a novel and selective alpha7 nicotinic acetylcholine receptor partial agonist, improves memory performance by potentiating the acetylcholine response of alpha7 nicotinic acetylcholine receptors. Neuropharmacology 62, 1099-1110.

Riley, B., Williamson, M., Collier, D., Wilkie, H., Makoff, A., 2002. A 3-Mb map of a large Segmental duplication overlapping the alpha7-nicotinic acetylcholine receptor gene (CHRNA7) at human 15q13-q14. Genomics 79, 197-209.

Severance, E.G., Yolken, R.H., 2008. Novel alpha7 nicotinic receptor isoforms and deficient cholinergic transcription in schizophrenia. Genes Brain Behav 7, 37-45.

Shen, L., Guo, Y., Chen, X., Ahmed, S., Issa, J.P., 2007. Optimizing annealing temperature overcomes bias in bisulfite PCR methylation analysis. Biotechniques 42, 48, 50, 52 passim.

Sinkus, M.L., Lee, M.J., Gault, J., Logel, J., Short, M., Freedman, R., Christian, S.L., Lyon, J., Leonard, S., 2009. A 2-base pair deletion polymorphism in the partial duplication of the alpha7 nicotinic acetylcholine gene (CHRFAM7A) on chromosome 15q14 is associated with schizophrenia. Brain Res 1291, 1-11.

Stephens, S.H., Logel, J., Barton, A., Franks, A., Schultz, J., Short, M., Dickenson, J., James, B., Fingerlin, T.E., Wagner, B., Hodgkinson, C., Graw, S., Ross, R.G., Freedman, R., Leonard, S., 2009. Association of the 5'-upstream regulatory region of the alpha7 nicotinic acetylcholine receptor subunit gene (CHRNA7) with schizophrenia. Schizophr Res 109, 102-112.

Thomsen, M.S., Hansen, H.H., Timmerman, D.B., Mikkelsen, J.D., 2010. Cognitive improvement by activation of alpha7 nicotinic acetylcholine receptors: from animal models to human pathophysiology. Curr Pharm Des 16, 323-343.

Thomsen, M.S., Mikkelsen, J.D., 2012. The alpha7 nicotinic acetylcholine receptor complex: one, two or multiple drug targets? Curr Drug Targets 13, 707-720.

Thomsen, M.S., Weyn, A., Mikkelsen, J.D., 2011. Hippocampal alpha7 nicotinic acetylcholine receptor levels in patients with schizophrenia, bipolar disorder, or major depressive disorder. Bipolar Disord 13, 701-707.

Tylee, D.S., Kawaguchi, D.M., Glatt, S.J., 2013. On the outside, looking in: a review and evaluation of the comparability of blood and brain "-omes". Am J Med Genet B Neuropsychiatr Genet 162B, 595-603.

Villiger, Y., Szanto, I., Jaconi, S., Blanchet, C., Buisson, B., Krause, K.H., Bertrand, D., Romand, J.A., 2002. Expression of an alpha7 duplicate nicotinic acetylcholine receptor-related protein in human leukocytes. J Neuroimmunol 126, 86-98.

Wallace, T.L., Porter, R.H., 2011. Targeting the nicotinic alpha7 acetylcholine receptor to enhance cognition in disease. Biochem Pharmacol 82, 891-903.

Wang, Y., Xiao, C., Indersmitten, T., Freedman, R., Leonard, S., Lester, H.A., 2014. The duplicated alpha7 subunits assemble and form functional nicotinic receptors with the full-length alpha7. J Biol Chem 89, 26451-63

Wierschke, S., Gigout, S., Horn, P., Lehmann, T.N., Dehnicke, C., Brauer, A.U., Deisz, R.A., 2010. Evaluating reference genes to normalize gene expression in human epileptogenic brain tissues. Biochem Biophys Res Commun 403, 385-390.

Zhang, T.Y., Hellstrom, I.C., Bagot, R.C., Wen, X., Diorio, J., Meaney, M.J., 2010. Maternal care and DNA methylation of a glutamic acid decarboxylase 1 promoter in rat hippocampus. J Neurosci 30, 13130-13137.

Zhu, Q., Wang, L., Zhang, Y., Zhao, F.H., Luo, J., Xiao, Z., Chen, G.J., Wang, X.F., 2012. Increased expression of DNA methyltransferase 1 and 3a in human temporal lobe epilepsy. J Mol Neurosci 46, 420-426.

Zwart, R., Strotton, M., Ching, J., Astles, P.C., Sher, E., 2014. Unique pharmacology of heteromeric alpha7beta2 nicotinic acetylcholine receptors expressed in Xenopus laevis oocytes. Eur J Pharmacol 726, 77-86.

Figures and figure legends

Table 1:

Table 1. Human subjects

Subjects	Gender	Age (years)
HB01	F	44
HB02	M	50
HB03	F	19
HB04	F	58
HB05	F	30
HB06	M	47
HB07	F	52
HB08	F	42
HB09	F	41
HB10	M	57
HB11	M	33
HB12	F	56
HB14	F	33
Average	9F, 4M	43.2 ± 3.3

F, female; M, male

Table 2:

Table 2. Primer sequences used for expression analysis and bisulfite sequencing

Gene	Forward primer 5'-3'	Reverse primer 5'-3'	Size	Accesion no./ ref.
Real-time qPCR primers				
CHRNA7	CGTCTACTTCTCCCTGAGCC	CTGTCCAAGACATTTGCAGC	95	NM_000746.5/ NM_001190455.2
CHRFAM7A	CAATTGCTAATCCAGCATTTGT	CCCAGAAGAATTCACCAACACG	102	Lucas-Cerillo et al., 2011 (NM_13932.1)
CHRNA4	GAGAATGTCACCTCCATCCG	GCCTTGGTCAGGTGGGT	107	NM_000744.6
CHRNB2	AGCGAGGACGATGACCAG	GGTGCCAAAGACACAGACAA	105	NM_000748.2
TBP	CGTGCCCGAAACGCCGAATA	AATCAGTGCCGTGGTTCGTG	84	NM_003194.4/ NM_001172085.1
ACTB	CCGCCGCCAGCTCACCAT	GCCCCACGATGGAGGGGAAG	125	NM_001101.3
NSE	ACAGGCCAGATCAAGACTGGTG	TCACAGCACACTGGGATTACGGA	138	NM_001975.2
Bisulfite sequencing primers				
CHRNA7	GGAGATTTTAAATTTGGTTTAGG	AACTACAATTCCCTAAATAACC	402	NC_000015.9

Table 3:

Table 3. mRNA expression levels of nAChR subunits and *CHRFAM7A*

Gene	mRNA ($E^{\wedge-C_T}$; 10^{-9})
CHRNA7	1.46 ± 0.25
CHRFAM7A	0.54 ± 0.08
CHRNA4	22.2 ± 3.4
CHRNB2	28.1 ± 4.9
Ratio	
CHRNA7/CHRFAM7A	3.42 ± 0.80
CHRNA4/CHRNA7	18.6 ± 3.8
CHRNB2/CHRNA7	21.4 ± 2.9

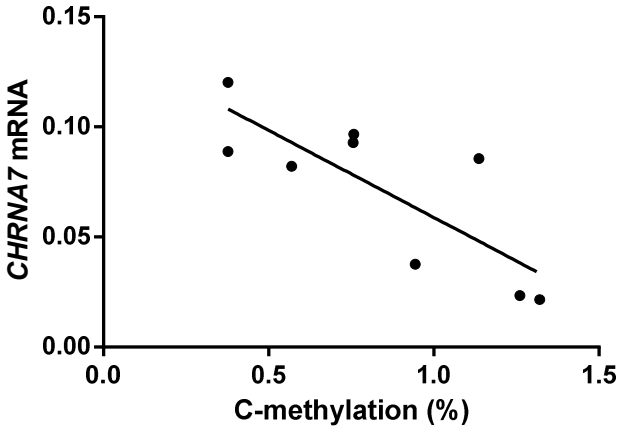

Figure 1. Association between *CHRNA7* expression and promoter DNA methylation in human cortical tissue. *CHRNA7* mRNA was detected by qPCR in human cortical extracts and normalized to the geometric mean of β-actin and TATA-box binding protein. 53 CpGs from position -114 to +243 in the *CHRNA7* promoter were cloned and sequenced. DNA methylation was calculated as the sum of methylated cytosine (C) divided by the total amount of CpG sites examined. Nine to ten clones per human subject. The expression of *CHRNA7* shows a strong inverse correlation with increasing DNA methylation (r=-0.798, *P*=0.0099) using Pearson correlation.

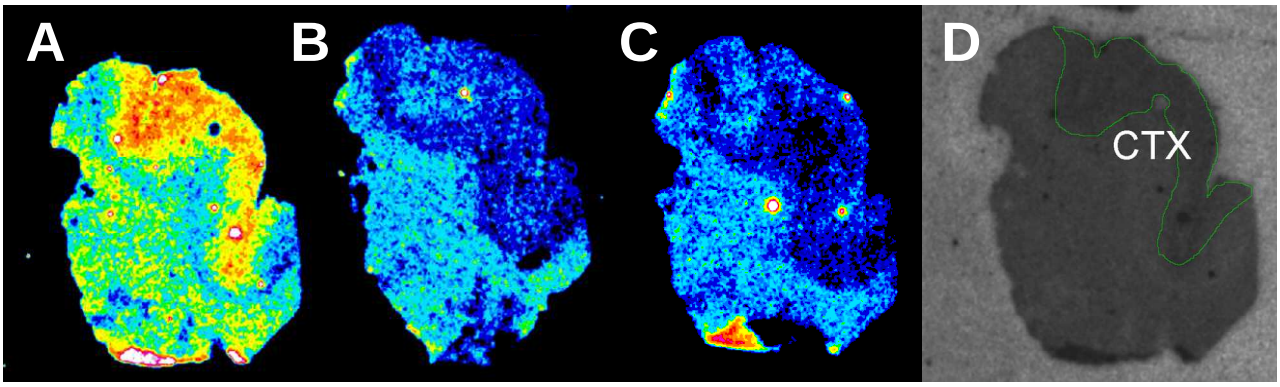

Figure 2. Encenicline displaces [^{125}I]-α-bungarotoxin binding in human cortical tissue. Representative autoradiographs of sections from human subject (HB12) showing total [^{125}I]-α-bungarotoxin binding **(A)** in the presence of 30 µM encenicline **(B)**, and 1 mM nicotine **(C)**, respectively. Total signal intensity **(A)** was corrected for nonspecific background signal by subtracting the signal in the presence of 1 mM nicotine **(C)**. The relative intensity is red > yellow > green > blue. **(D)** Graphical representation of the measured cortical region of interest (CTX).

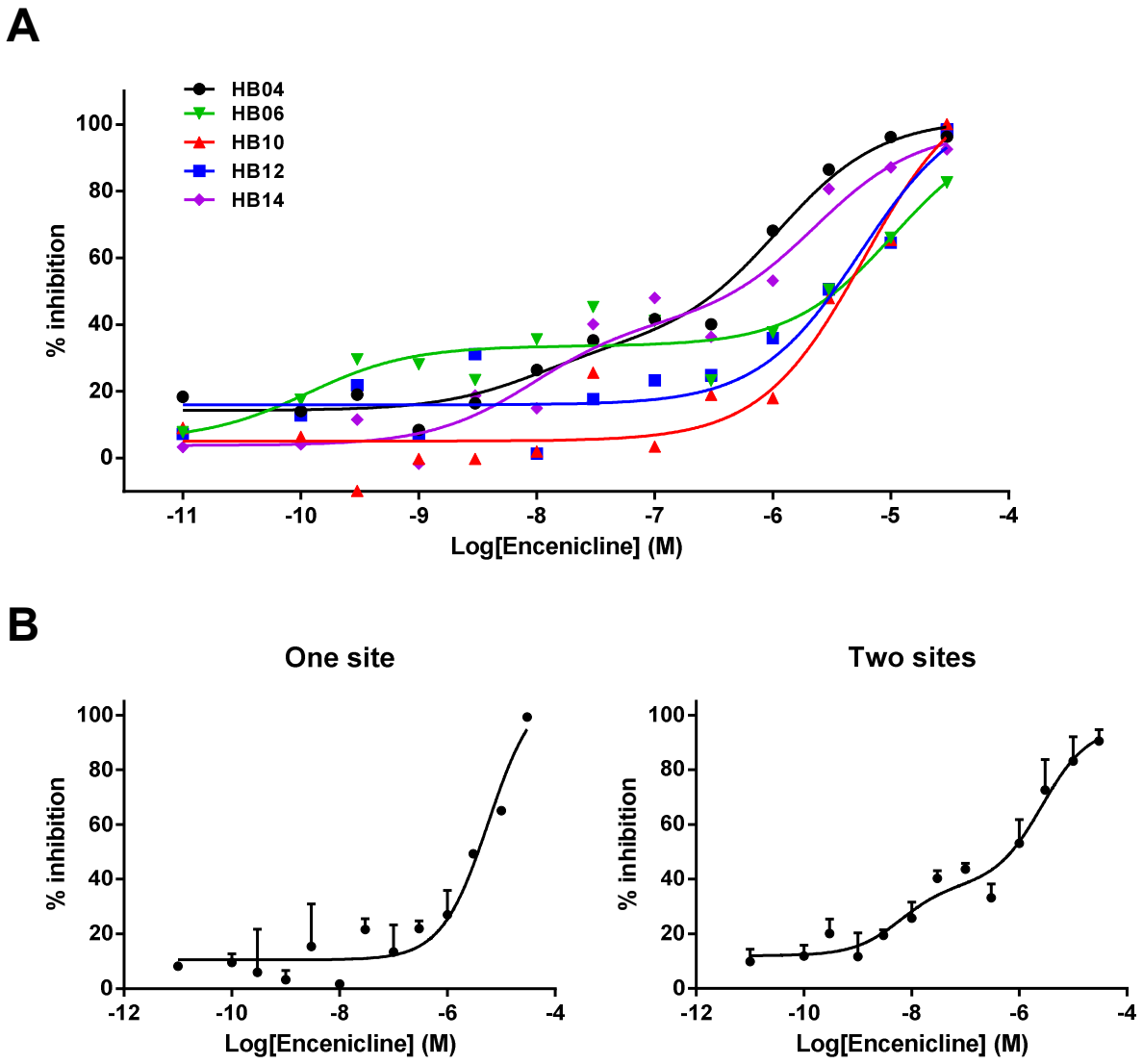

Figure 3. Different [^{125}I]-α-bungarotoxin (α-Bgt) displacement profiles of encenicline in human cortical tissue. **(A)** Displacement of [^{125}I]-α-Bgt by encenicline in five human subjects. Non-specific binding in the presence of 1 mM nicotine was subtracted and percent inhibition was calculated. **(B)** Data were separated and pooled dependent on whether a one-site or two-site model was preferred to determine IC_{50} values in the human individuals (n=2-3).

Table 4:

Table 4. IC_{50} values of encenicline against [^{125}I]-α-bungarotoxin binding in human cortical tissue.

Subjects	Non-linear regression	IC_{50} High	IC_{50} Low	$logIC_{50}$ (± SE) High	$logIC_{50}$ (± SE) Low
HB04	Two site	10.1 nM	1.12 µM	-7.96 (± 0.57)	-5.95 (± 0.20)
HB06	Two sites	0.11 nM	10.6 µM	-9.94 (± 0.63)	-4.98 (± 0.43)
HB14	Two sites	9.25 nM	2.31 µM	-8.03 (± 0.43)	-5.64 (± 0.35)
HB10	One site		5.89 µM		-5.23 (± 0.21)
HB12	One site		5.54 µM		-5.26 (± 0.25)
Pooled	Two sites	6.22 nM	2.63 µM	-8.21 (± 0.46)	-5.58 (± 0.26)
Pooled	One site		5.75 µM		-5.24 (± 0.17)

Paper II

Thomsen MS, Cinar B, **Jensen MM**, Lyukmanova EN, Shulepko MA, Tsetlin V, Klein AB, Mikkelsen JD.

Expression of the Ly-6 family proteins Lynx1 and Ly6H in the rat brain is compartmentalized, cell-type specific, and developmentally regulated.

Brain Struct Funct, 219(6):1923-34 (2014).

Brain Struct Funct (2014) 219:1923–1934
DOI 10.1007/s00429-013-0611-x

ORIGINAL ARTICLE

Expression of the Ly-6 family proteins Lynx1 and Ly6H in the rat brain is compartmentalized, cell-type specific, and developmentally regulated

Morten Skøtt Thomsen · Betül Cinar · Majbrit Myrup Jensen · Ekaterina N. Lyukmanova · Mikhail A. Shulepko · Victor Tsetlin · Anders Bue Klein · Jens D. Mikkelsen

Received: 21 February 2013 / Accepted: 8 July 2013 / Published online: 17 July 2013

Abstract The Ly-6 superfamily of proteins, which affects diverse processes in the immune system, has attracted renewed attention due to the ability of some Ly-6 proteins to bind to and modulate the function of neuronal nicotinic acetylcholine receptors (nAChRs). However, there is a scarcity of knowledge regarding the distribution and developmental regulation of these proteins in the brain. We use protein cross-linking and synaptosomal fractions to demonstrate that the Ly-6 proteins Lynx1 and Ly6H are membrane-bound proteins in the brain, which are present on the cell surface and localize to synaptic compartments. We further estimate the amount of Lynx1 in the rat cortex using known amounts of a heterologously expressed soluble Lynx1 variant (ws-Lynx1) to be approximately 8.6 ng/μg total protein, which is in line with the concentrations of ws-Lynx1 required to affect nAChR function. In addition, we demonstrate that Lynx1 and Ly6H are expressed in cultured neurons, but not cultured micro- or astroglial cultures. In addition, Lynx1, but not Ly6H was detected in the CSF. Finally, we show that the Ly-6 proteins Lynx1, Lynx2, Ly6H, and PSCA, display distinct expression patterns during postnatal development in the rat frontal cortex and hippocampus at the mRNA and protein level, and that this is paralleled to some degree by the expression of the nAChR subunits α2, α4, α7 and β2. Our results demonstrate a developmental pattern, localization, and concentration of Ly-6 proteins in the brain, which support a role for these proteins in the modulation of signaling at synaptic membranes.

Keywords Nicotinic acetylcholine receptor · Allosteric modulator · Frontal cortex · Hippocampus · Synaptosomes · Lynx1 · Lynx2 · Ly6H · PSCA

Abbreviations

aCSF	Artificial cerebrospinal fluid
BS^3	Bis(sulfosuccinimidyl) suberate
CSF	Cerebrospinal fluid
DIV	Day in vitro
FC	Frontal cortex
HIP	Hippocampus
NAChR	Nicotinic acetylcholine receptor
ws-Lynx1	Water-soluble variant of human Lynx1

Introduction

The Ly-6 superfamily comprises proteins with structural similarity to snake venom toxins and is characterized by a three-dimensional consensus motif, termed the three-finger fold that is involved in protein–protein binding (Tsetlin 1999; Bamezai 2004). These proteins exist primarily as GPI-anchored membrane proteins, but some are also expressed as soluble proteins (Adermann et al. 1999).

Electronic supplementary material The online version of this article (doi:10.1007/s00429-013-0611-x) contains supplementary material, which is available to authorized users.

M. S. Thomsen (✉) · B. Cinar · M. M. Jensen · A. B. Klein · J. D. Mikkelsen
Neurobiology Research Unit, Copenhagen University Hospital, Rigshospitalet, Juliane Maries Vej 24, Copenhagen 2100, Denmark
e-mail: morten.s.thomsen@nru.dk

E. N. Lyukmanova · M. A. Shulepko · V. Tsetlin
Shemyakin-Ovchinnikov Institute of Bioorganic Chemistry, Russian Academy of Sciences, Moscow, Russia

M. A. Shulepko
Lomonosov Moscow State University, Moscow, Russia

Originally used as differentiation markers for lymphocytes, studies during the last decade have demonstrated the presence of these proteins in a range of cell types and implicated them in several diseases including the skin disorders Mal de Meleda and psoriasis vulgaris (Chimienti et al. 2003; Tsuji et al. 2003). Notably, the presence of several members of the Ly-6 superfamily namely Lynx1, Lynx2, Ly6H, Lypd6, Lypd6B, PATE-M, and PSCA, has been demonstrated in the brain (reviewed in (Miwa et al. 2012)).

Several Ly-6 proteins have been shown to modulate nicotinic acetylcholine receptor (nAChR) function in the brain (reviewed in (Miwa et al. 2011; Thomsen and Mikkelsen 2012a)). Thus, Lynx1 and Lynx2 have been shown to form stable complexes with and negatively modulate the response of α7 and α4β2 nAChRs using co-immunoprecipitation and electrophysiology, respectively (Miwa et al. 2006; Tekinay et al. 2009; Fu et al. 2012). In addition, retroviral expression of PSCA reduces nicotine-induced activation of the α7 nAChR in dissociated ciliary ganglion neurons (Hruska et al. 2009). Contrarily, transgenic overexpression of Lypd6 increases nicotine-induced currents in dissociated trigeminal ganglion neurons (Darvas et al. 2009). Lypd6 is thus the only Ly-6 protein demonstrated to positively modulate nAChR function in the CNS. However, other Ly-6 superfamily members, which positively modulate nAChRs, have been identified in keratinocytes and in insects (Chimienti et al. 2003; Choo et al. 2008; Liu et al. 2009).

Nicotinic receptors are important for several forms of cognition, such as attention and memory function, as well as synaptic plasticity (reviewed in (Sarter et al. 2009; Thomsen et al. 2010)). Since the function of several subtypes of nAChRs is regulated by Ly-6 proteins in vitro, it is pertinent to study the effect of Ly-6 proteins on cognitive function. This has been the focus of a few seminal works. Thus, Lynx1 knock-out mice exhibit improved associative learning in a fear-conditioning paradigm (Miwa et al. 2006), and it was recently shown that Lynx1, acting through nAChRs, is critical for the loss of synaptic plasticity in the visual cortex that occurs in adulthood (Morishita et al. 2010). In addition, Lynx2 knock-out mice have been shown to display increased anxiety-like behavior (Tekinay et al. 2009), and overexpression of Lypd6 enhances pre-pulse inhibition of the acoustic startle response, a measure of pre-attentional processing (Darvas et al. 2009).

The above studies demonstrate the importance of Ly-6 proteins for cognitive function. However, the current knowledge is based primarily on heterologous expression systems and transgenic animals, and very little is therefore known about the distribution and developmental regulation of Ly-6 proteins in the brain. Since nAChR expression is high during early development and is important for the development of synapses (Lozada et al. 2012a, b), it is particularly pertinent to investigate the potential interaction between nAChRs and Ly-6 proteins during development. It has been shown that α7 nAChR and PSCA mRNA levels correlate, and that exposure to the α7 nAChR antagonist α-bungarotoxin decreases PSCA expression in the developing ciliary ganglion (Hruska et al. 2009) suggesting an association between expression and activation of nAChRs and Ly-6 protein levels.

Here we characterize the distribution of the Ly-6 proteins Lynx1 and Ly6H at the organ, cellular, and sub-cellular level, since the localization of these proteins is an important basis for determining their potential function in terms of neuronal signaling. In addition, we examine the developmental expression of the Ly-6 proteins Lynx1, Lynx2, Ly6H, and PSCA at the mRNA and protein level and relate this to the expression of the nAChR subunits α2, α4, α7, and β2.

Experimental procedures

Animals and materials

Sprague–Dawley rats were obtained from Charles River Laboratories (Germany). Males were housed two per cage, and pregnant rats were housed individually. Pups were weaned at postnatal day 21. Only male pups were used in this study. Animals were kept on a 12/12 h light/dark cycle provided with standard rodent diet and water ad libitum. The animals were acclimatized for a minimum of 7 days after arrival before experiments began.

A recombinant water-soluble variant of human Lynx1 (ws-Lynx1) was expressed in *E. coli* and purified as previously described (Lyukmanova et al. 2011).

Cross-linking of surface proteins

Adult male rats (200–250 g, $n = 11$) were decapitated and the frontal cortex (FC) and hippocampus (HIP) from the left hemisphere were dissected and chopped into 350 µm slices using a McIlwain tissue chopper (Brinkman Instruments, Westbury, NY). The slices were then divided equally into tubes containing artificial cerebrospinal fluid (aCSF, Tocris, Bristol, UK) with or without 1 mg/ml of the cell-impermeable cross-linking agent bis(sulfosuccinimidyl) suberate (BS^3, Pierce Biotechnology) and incubated for 1 h on ice while shaking. To quench the reaction, Tris buffer (pH 7.5) was added to a final concentration of 50 mM and incubated another 5 min. The slices were then washed 2 × 5 min in aCSF containing 50 mM Tris, centrifuged briefly, and the supernatant replaced with 100 µl

lysis buffer (100 mM NaCl, 25 mM EDTA, 10 mM Tris, 1 % (v/v) Triton X-100, 1 % (v/v) NP-40, 1 µl/ml protease inhibitor cocktail (Sigma-Aldrich, Brøndby, Denmark) pH 7.4). Finally, the lysates were sonicated for 5 s on ice and centrifuged 10 min at 1,000×*g* at 4 °C and the pellet discarded.

Preparation of synaptosomal fractions

Crude synaptosomes were prepared according to Soliakov et al. (1995). Briefly, the FC and HIP were dissected from the right hemisphere of adult male rats (200–250 g, $n = 5$) and homogenized in 1.5 ml of ice-cold homogenization buffer (0.32 M sucrose, 5 mM HEPES, pH 7.4) using a glass-Teflon grinder (IKA Labortechnik, Staufen, Germany) with 12 strokes at 900 rpm for 1 min. The homogenate was then centrifuged 10 min at 1,000×*g* at 4 °C. The resulting pellet, P1, was resuspended in lysis buffer. The supernatant was centrifuged 20 min at 20,000×*g* at 4 °C, and the pellet was resuspended in Krebs-bicarbonate buffer and centrifuged once more for 10 min at 20,000×*g* at 4 °C. Lysis buffer was added to the resulting pellet, P2, and both P1 and P2 lysates were sonicated 5 s on ice. The P2 pellet is enriched in synaptosomes (see Figure S2).

Cortical neuronal cultures

Rat embryos (E18) were decapitated, and their brains dissected under aseptical conditions. The neocortex was dissected while carefully avoiding the meninges or blood vessels. The dissected tissue was briefly minced using tweezers and transferred to ice-cold dissection medium (minimal essential medium (MEM)) containing 0.1 mg/ml gentamycin (GIBCO, Invitrogen, Carlsbad, CA). After centrifugating for 2 min at 200×*g* at 20–22 °C the medium was removed and the cortices incubated with 0.05 % Trypsin–EDTA (Invitrogen) containing 0.0015 KU DNase I (Sigma-Aldrich) for 15 min at 37 °C while shaking. Culture medium (dissection medium + 10 % fetal bovine serum) was added and the tissue was gently dissociated by aspirating it through a 10 ml pipette and centrifuged for 5 min at 200×*g* at 20–22 °C. The supernatant was discarded and culture medium was added to the pellet, which was dissociated by aspirating it five times through a flame-polished Pasteur pipette. The number of viable cells was counted using a hemocytometer and trypan blue, and cells were seeded at 0.5×10^6 cells/ml in 24-well poly-L-lysine (Sigma-Aldrich) coated plates, and maintained in a humidified incubator at 37 °C with 5 % CO_2. On the 3rd day in vitro (DIV3), 6 µM 1-β-D-arabinofuranosylcytosine (GIBCO, Invitrogen, CA) was added to inhibit glial and fibroblast proliferation. At DIV7 half the media was changed, if the cultures were continued past this day. Cells were lysed in 50 µl lysis buffer as described above. This procedure yields neuron-enriched cultures (see Figure S3).

Glia cultures

Mixed glia cultures were prepared from 1- to 5-day-old rat pups as described above, except that the dissection medium was 2 mM glutamine, 1 mM sodium pyruvate, 100 units/ml penicillin and 100 ug/ml streptomycin in high glucose Dulbecco's MEM, and that cells were triturated several times through a 10 ml pipette, and then through a 10 ml pipette fitted with a 200 µl pipette tip after trypsinization. Cells were seeded at $0.5–1 \times 10^5$ cells/ml in poly-L-lysine coated culture flasks. The culture medium was changed every 3–4 days. The mixed glia cultures were confluent after 12–14 days. Microglia-enriched cultures were prepared by shaking confluent mixed glia cultures on a shaking table at 180 rpm for 3–5 h at 37 °C. The microglia-containing medium was then removed, centrifuged 8 min at 200×*g* at 20–22 °C, and resuspended in a smaller volume of culture medium. Cells were seeded at $0.5–1 \times 10^5$ cells/well in poly-L-lysine coated 96-well plates. This procedure yields microglia cultures with <1 % astroglia (Thomsen and Mikkelsen 2012b). Astroglia-enriched cultures were prepared by treating the remaining cells after shaking with 20 µM 1-β-D-arabinofuranosylcytosine for 2–3 days. Cells were lysed in 50 µl lysis buffer as described for tissue above. This procedure yields astroglia cultures with <1 % neurons or microglia, based on MAP-2 and OX-42 immunostaining (see Figure S4).

Tissue fractionation

To fraction tissue into membrane and soluble fractions, cortical tissue from adult male rats (200–250 g, $n = 4$) was homogenized 2×30 s in Buffer1 (0.5 M NaCl, 50 mM Tris–HCl, 10 mM $MgCl_2$, 2 mM EDTA, 10 µl/ml protease inhibitor cocktail, pH 7.3) using a PT1200C polytron blender (Kinematica, Luzern, Switzerland), centrifuged 30 min at 126,000×*g* at 20–22 °C using an air-driven ultracentrifuge (Airfuge®, Copenhagen, Denmark). The supernatant containing the soluble fraction was transferred to a new tube while taking care not to disturb the pellet. The pellet containing the membrane fraction was washed twice in Buffer1, resuspended by blending 2×30 s in Buffer2 (4 M urea, 50 mM Tris–HCl, 1 % SDS, 10 µl/ml protease inhibitor cocktail, pH 7.3), and sonicated 3×5 s on ice.

Cerebrospinal fluid sampling

The procedure for cerebrospinal fluid (CSF) sampling was adapted from Nirogi et al. (2009), and was performed on

adult male rats (200–250 g, $n = 4$). Briefly, the rat was anesthetized using isoflurane, the fur on the back of the neck was shaved off, and the rat was placed in a stereotactical frame with the head at an angle of ~45° from the rest of the body. A hole was drilled above the cisterna magna (in the midline ~3 mm above the end of the skull), and a 23-gauge needle attached to PE-50 tubing and a syringe was inserted ~5 mm into the cisterna magna. 100–150 µl CSF was drawn into the syringe by aspiration, transferred to a microcentrifuge tube, centrifuged 10 min at 10,000×*g* at 4 °C to remove potential blood contamination, and the supernatant was transferred to a new tube. The CSF samples were concentrated using Amicon Ultra-2 Filters (Millipore, Hellerup, Denmark).

Developmental study

Male rats (34 in total) from 5 litters were assigned to each experimental group in a pseudo-random fashion and decapitated at postnatal day (P) 1, 7, 14, 26, 42, or 60. Their brains were rapidly dissected and the FC and HIP were dissected from each hemisphere and frozen in microfuge tubes in dry ice. Samples were kept at −80 °C until use. Tissue from the left hemisphere was used to extract mRNA and perform RT-qPCR as described below. Tissue from the right hemisphere was lysed in 300 µl lysis buffer. The lysates were sonicated for 5 s on ice and centrifuged 10 min at 1,000×*g* at 4 °C. The pellet was discarded, and the supernatant used for western blotting as described below.

Western blotting

Total protein content was measured using a DC Protein Assay Kit (Biorad, Hercules, CA). Equal amounts of lysates were then diluted in loading buffer (120 mM Tris, 20 % (v/v) glycerol, 10 % (v/v) mercaptoethanol, 4 % (w/v) SDS, 0.05 % (w/v) bromophenol blue, pH 6.8), incubated for 5 min at 95 °C and submitted to gel electrophoresis using AnykD™ gels (Biorad), and blotted onto PVDF membranes (BioRad). Membranes were washed in TBS-T and blocked in TBS containing 5 % (w/v) dry milk powder, which was also used for antibody incubations. Incubation in primary antibody against Lynx1 (1:1,000, #sc-23060, Santa Cruz Biotechnology, Heidelberg, Germany), Ly6H (1:1,000, #H00004062-M01, Novus Biologicals, Cambridge, UK), β2 (1:1,000, #834 a gift from Dr. Cecilia Gotti), Actin (1:10,000, #A5060, Sigma-Aldrich), GluR2 (1:200, #MABN71, Millipore), PSD-95 (1:2,000, #ab9708, Millipore) or Erk1 (1:4,000, #610031, BD Transduction Laboratories, Franklin Lakes, NJ) was done overnight at 4 °C on parafilm in a humidified container, followed by 3 × 10 min washes in TBS-T and 1 h incubation at 20–22 °C in horseradish peroxidase-coupled secondary antibody (1:2,000, Dako, Glostrup, Denmark). After thorough washing in TBS-T, enhanced chemiluminescence Western blotting detection reagents (Western Lightning® ECL Pro, Perkin Elmer, Waltham, MA) were used for signal detection and protein bands were visualized using an automated film developer (Colenta Labortechnik, Wiener Neustadt, Austria). Mean optical densities of bands were measured and their corresponding background measurement subtracted. Validation of the Lynx1, Ly6H, and β2 antibodies is shown in Figure S1.

For determination of the absolute amount of Lynx1 in rat cortex, samples were loaded together with samples with a known amount of ws-Lynx1 (3, 10, 29, 87, or 260 ng), and a standard curve was created based on the ws-Lynx1 samples. This curve was used to determine the amount of Lynx1 in the cortical samples.

mRNA extraction and qPCR

Total RNA was isolated using Trizol Reagent (Sigma-Aldrich) according to the manufacturer's instructions. RNA samples were dissolved in RNase-free water and RNA content was quantified using a Nanodrop ND-1000 Spectrophotometer (Nanodrop Technologies, Wilmington, DE). Samples were diluted with RNase-free water to equal RNA concentrations and reverse transcribed into single-stranded cDNA with the ImProm-II™ Reverse Transcription System (Promega, Madison, WI) according to the manufacturer's directions using 0.5 g/reaction oligo$(dT)_{15}$ primers, 6 mM $MgCl_2$, and 20 units of RNase inhibitor. Real-time qPCR reactions were performed in a total volume of 20 µl, containing 1 µl sample cDNA, 1× Brilliant® II SYBR® Green qPCR Master Mix (Stratagene, La Jolla, CA), and 15 pmol each of the forward and reverse primers (Table 1, DNA technology, Aarhus, Denmark). PCR was performed on a Light Cycler® 480 Real-Time PCR System (Roche, Indianapolis, IN) with a 10 min preincubation at 94 °C followed by 40 cycles of 30 s at 94 °C, 45 s at 60 °C and 90 s at 72 °C. Primer pairs were validated using serially diluted cDNA to establish a standard curve and by confirming the existence of a single product on a gel at the correct molecular weight. Quantification of mRNA expression was performed according to the comparative C_T method as described by Schmittgen and Livak (2008). For each sample, the amount of target mRNA was normalized to the mean of the P60 group.

Statistical analysis

Data were analyzed using Bonferroni-corrected ratio paired *t* tests. The statistical calculations were performed using GraphPad Prism version 6 for Windows (GraphPad

Table 1 Primers used for real-time qPCR

Gene	Forward primer 5′–3′	Reverse primer 5′–3′	Product size (bp)
Lynx1	ACCACTCGAACTTACTTCACC	ATCGTACACGGTCTCAAAGC	81
Lynx2	GTTCTGGCTTCCAGGGCTGG	GGCTGCTGACGATGCACACG	191
Ly6H	CTACTGGCCTTGCTTCTCTG	AATGATCCTTCCTGCTGCTG	163
PSCA	GCCCTACCAGTTCTGATCAG	TCACACCCACCTAGCTTCAT	154
α2	TGCCCAGGTGGCTGATGATGAACC	GCTTTCTGTATTTGAGGTGACAGC	300
α4	GTCAAAGACAACTGCCGGAGACTT	TGATGAGCATTGGAGCCCCACTGC	300
α7	AACTGGTGTGCATGGTTTCTGCGC	AGATCTTGGCCAGGTCGGGGTCCC	300
β2	ACGGTGTTCCTGCTGCTCATC	CACACTCTGGTCATCATCCTC	507

Software, San Diego, USA). All data are presented as mean ± standard error of the mean, and a P value of less than 0.05 was considered statistically significant.

Results

Subcellular distribution of Lynx1 and Ly6H

To determine the extent of surface expression of the Ly-6 proteins Lynx1 and Ly6H tissue extracts from the FC or HIP of adult rats were cross-linked using the cell-impermeable protein cross-linking agent BS^3 (Fig. 1). The ionotropic GluR2 receptor was used as a positive control as it is known to be located predominantly on the cell surface (Grosshans et al. 2002; Mielke and Mealing 2009; Carino et al. 2012). Cross-linking reduced the intensity of the GluR2 signal by 62 and 48 %, respectively, in the FC and HIP ($P < 0.01$ and $P < 0.001$, respectively). In the FC, the Lynx1 signal was reduced by 60 % ($P < 0.01$), corresponding to 98 % of the signal reduction seen with GluR2, indicating that Lynx1 is primarily present on the cell surface in the FC. Contrarily, in the HIP the Lynx1 signal was reduced by only 20 % and was not significantly different from vehicle controls. In the FC and HIP, the Ly6H signal was reduced by 23 and 34 %, respectively ($P < 0.05$ and $P < 0.01$, respectively), corresponding to 37 and 70 % of the signal reduction seen with GluR2. In the FC, the signal intensity of the β2 nAChR subunit was not significantly different from vehicle controls in the FC or HIP.

In a further attempt to demonstrate the localization of Ly-6 proteins, tissue homogenates from the FC and HIP were fractionated into nuclear and synaptosomal fractions (Fig. 2). GluR2 was used as a positive control as it is known to be located in the synaptosomal fraction (Srivastava et al. 1998). There was a significantly higher level

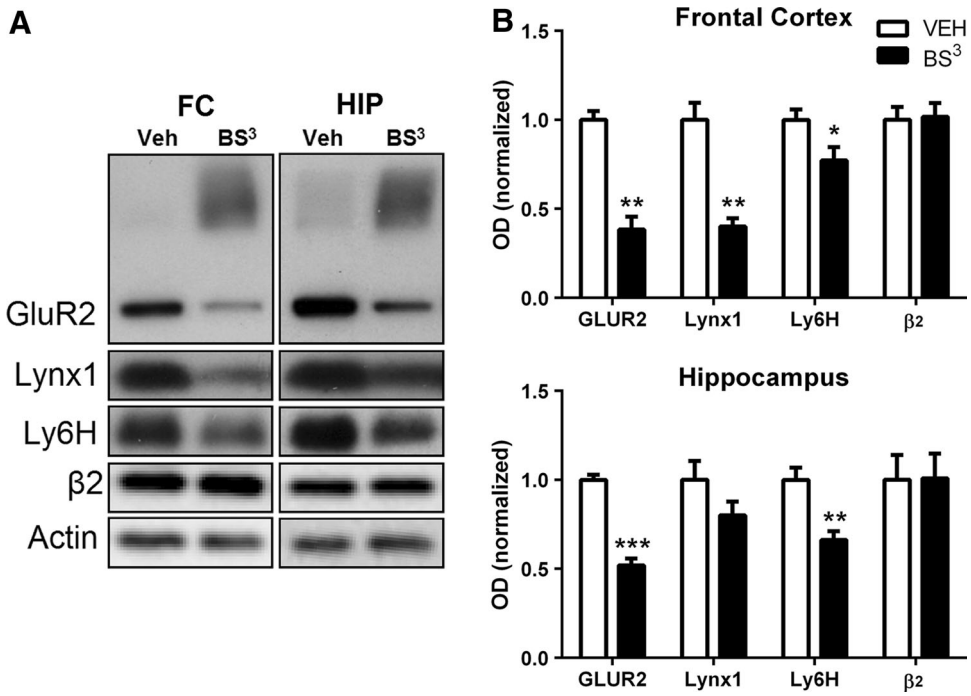

Fig. 1 Expression of Lynx1 and Ly6H proteins on the cell surface. **a** Representative western blot images of minced tissue extracts from the frontal cortex or hippocampus of adult rats cross-linked with bis(sulfosuccinimidyl) suberate (BS^3) or vehicle (*Veh*). The staining for GluR2 shows that cross-linking with BS^3 reduces the intensity of the GluR2 band at 95 kDa, and produces a smear of high-molecular weight cross-linked proteins. **b** Quantification of protein levels in vehicle- and BS^3-treated tissue. Data are normalized to Actin levels and the vehicle group was set to 1. $^{*}P < 0.05$, $^{**}P < 0.01$, $^{***}P < 0.001$ indicates statistical difference between vehicle- and BS^3-treated samples in a Bonferroni-corrected ratio paired t test. $n = 9$–11

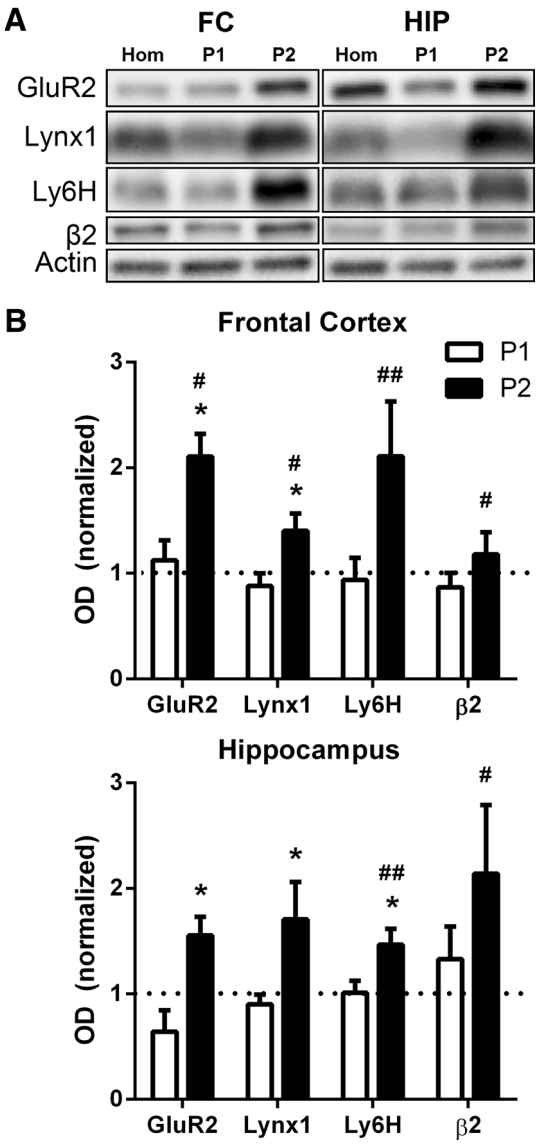

Fig. 2 Expression of Lynx1 and Ly6H proteins in synaptosomal fractions. **a** Representative western blot images of frontal cortical and hippocampal tissue fractionated using differential centrifugation into a pellet 1 (*P1*, nuclear) and pellet 2 (*P2*, crude synaptosome) fractions. **b** Quantification of protein levels in P1 and P2 fractions. Data are normalized to Actin levels and the level of the non-fractionated homogenate (*Hom*) was set to 1 (*dashed line*). $^{*}P < 0.05$, $^{**}P < 0.01$ indicates statistical difference between non-fractionated homogenate and the P2 fraction, $^{\#}P < 0.05$, $^{\#\#}P < 0.01$ indicates statistical difference from the P1 fraction in a Bonferroni-corrected ratio paired *t* test. $n = 5$

of Lynx1 in the synaptosomal fraction compared to the whole-cell homogenate in both the FC and HIP (both $P < 0.05$) and of Ly6H in the HIP ($P < 0.05$). In addition, comparing the synaptosomal and nuclear fractions revealed a significantly higher level of Ly6H in synaptosomes in the FC ($P < 0.01$), and of β2 in both the FC and HIP (both $P < 0.05$).

Lynx1 and Ly6H are exclusively membrane-bound proteins in the brain

Cortical rat tissue was fractionated into soluble and membrane fractions by ultracentrifugation and the resulting fractions submitted to western blotting (Fig. 3a). Lynx1 and Ly6H were detectable only in the membrane fractions, and not in the soluble fractions, demonstrating that in the rat cortex, Lynx1 and Ly6H are exclusively membrane bound. To validate the method, we demonstrated that the integral membrane proteins PSD-95 and GluR2 were only present in the membrane fraction, whereas the soluble protein Erk1 was only present in the soluble fraction.

Cell- and tissue-type specific expression of Lynx1 and Ly6H

We analyzed the expression of Lynx1 and Ly6H protein in adult rat cortical tissue compared to rat cortical primary neurons cultured to DIV7 or 14, rat primary microglia cultured to DIV15, and rat primary astroglia cultured to DIV18 (Fig. 3b). Lynx1 was detected in adult cortical tissue and neurons at DIV14, but was not detectable in neurons at DIV7, microglia, or astroglia. Ly6H protein was detected in neurons at DIV7, but much more prominently at DIV14, although to a lesser extent than in adult cortical tissue. Ly6H protein was not detectable in micro- or astroglia culture.

At the organ level, Lynx1 was detected in high amounts in cortex and cerebellum and in low amounts in lung tissue (Fig. 3c). Lynx1 was not detected in heart, liver, kidney, or prostate. Ly6H was only detected in the cortex with no expression in the cerebellum or other organs.

Concentration of Lynx1 in cortical rat brain tissue and CSF

Lynx1 protein levels were measured using Western blotting with cortical tissue and CSF samples by comparing with ws-Lynx1 samples with known concentration (Fig. 4). Based on a standard curve for ws-Lynx1, cortical tissue was estimated to contain 8.6 ng Lynx1/μg total protein. With a molecular weight of ws-Lynx1 of 8,399.6 g/mol this corresponds to 1.0 pmol/μg total protein. Similarly, the concentration in the CSF was estimated at 1.1 ng Lynx1/μg total protein, corresponding to 0.13 pmol/μg. Relating this to the volume of CSF loaded onto the gel gives a concentration of 0.5 μM of Lynx1 in the rat CSF.

Developmental expression of Ly-6 proteins and nAChRs in the brain

We analyzed the mRNA levels of the Ly-6 genes Lynx1, Lynx2, Ly6H, and PSCA and the nAChR subunits α2, α4,

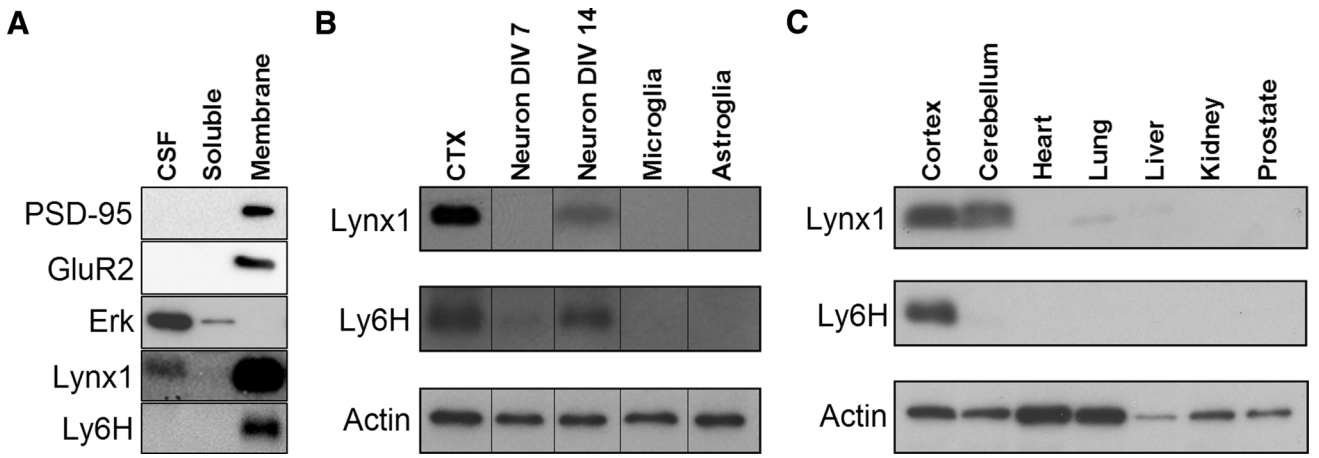

Fig. 3 Cellular and organ distribution of Lynx1 and Ly6H proteins. The cellular and organ distribution of Lynx1 and Ly6H protein in rats were analyzed using western blotting. **a** Protein levels in cerebrospinal fluid (*CSF*) and soluble and membrane fractions of cortical tissue showing that Lynx1 and Ly6H are exclusively membrane bound. However, Lynx1 protein is also present in the CSF. The membrane-bound proteins PSD-95 and GluR2 and the soluble protein extracellular-signal-regulated kinase 1 (*Erk*) are used as controls for effective fractionation ($n = 4$). **b** Protein levels in cortical tissue from an adult male rat (*CTX*), in rat cortical primary neurons cultured for 7 or 14 days in vitro (*Neuron DIV7* and *14*, respectively), in rat primary microglia cultured for 15 days in vitro, and in rat primary astroglia cultured for 18 days in vitro ($n = 3$). Lynx1 and Ly6H are both present in neuronal cultures, but not in micro- or astroglial cultures **c** Protein levels in different organs from adult male rat ($n = 2$)

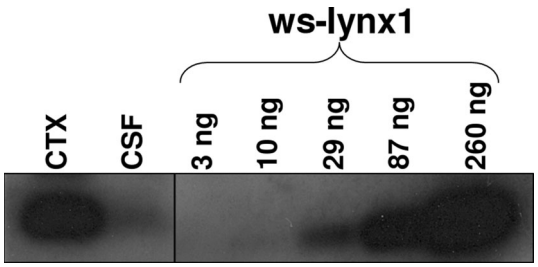

Fig. 4 Concentration of Lynx1 in cortical tissue and CSF. The levels of Lynx1 protein were detected by Western blotting in membrane fractions of cortical tissue (*CTX*) and cerebrospinal fluid (*CSF*) samples (20 μg each) from an adult male rat together with a titration of a recombinant water-soluble variant of human Lynx1 (ws-Lynx1) $n = 2$

α7, and β2 and the protein levels of Lynx1 and Ly6H as well as the β2 nAChR subunit in the FC and HIP of rats at P1, 7, 14, 26, 42, and 60 (Fig. 5). We were not able to identify house-keeping genes that were expressed at constant levels throughout postnatal development. Therefore, we have not normalized protein or mRNA data from this experiment to a reference gene. To ensure the validity of the data, we have performed three independent analyses of the samples.

Lynx1 mRNA was not detectable at birth in the FC or HIP, but increased from P7 to P14, reaching adult levels in the FC, and higher than adult levels in the HIP, which gradually declined to adult levels. This pattern of expression was paralleled by Lynx1 protein levels. Ly6H mRNA levels increased almost twofold during the first postnatal week and were elevated compared to adult levels until P26. Ly6H protein was present in very low amounts at birth in the FC and HIP, but increased dramatically from P1 to P14 when it reached adult levels. Lynx2 mRNA was detectable at birth in the FC and HIP. In the FC, Lynx2 mRNA increased more than twofold during the first two postnatal weeks after which it declined gradually until P60. In the HIP, Lynx2 mRNA increased threefold during the first postnatal week followed by a decline to adult levels between P14 and P26. PSCA mRNA in the FC was present at near-adult levels at birth and increased gradually throughout the postnatal period. In the HIP, PSCA mRNA was present at birth, but increased fourfold during the first two postnatal weeks after which it declined gradually to adult levels.

Among the nAChR subunits β2 displayed a marked postnatal peak in mRNA levels at P7, most prominently in the FC, which almost completely declined before P14. β2 protein levels in the FC were stable from birth until P14 and increased gradually from P14 until P60. In the HIP, β2 protein levels were constant throughout postnatal development. α2 mRNA in the FC displayed a marked postnatal peak at P7, which declined to near-adult levels before P14. In the HIP, there was no detectable α2 mRNA at birth, but the expression gradually increased during the first two postnatal weeks to adult levels. α4 mRNA levels remained constant throughout postnatal development in the FC, whereas there was a postnatal peak in the HIP that did not reach adult levels before P42. α7 mRNA displayed a marked postnatal peak at P7 in the FC, which almost completely declined before P14. In the HIP, α7 mRNA increased during the first postnatal week, where it stabilized at near-adult levels.

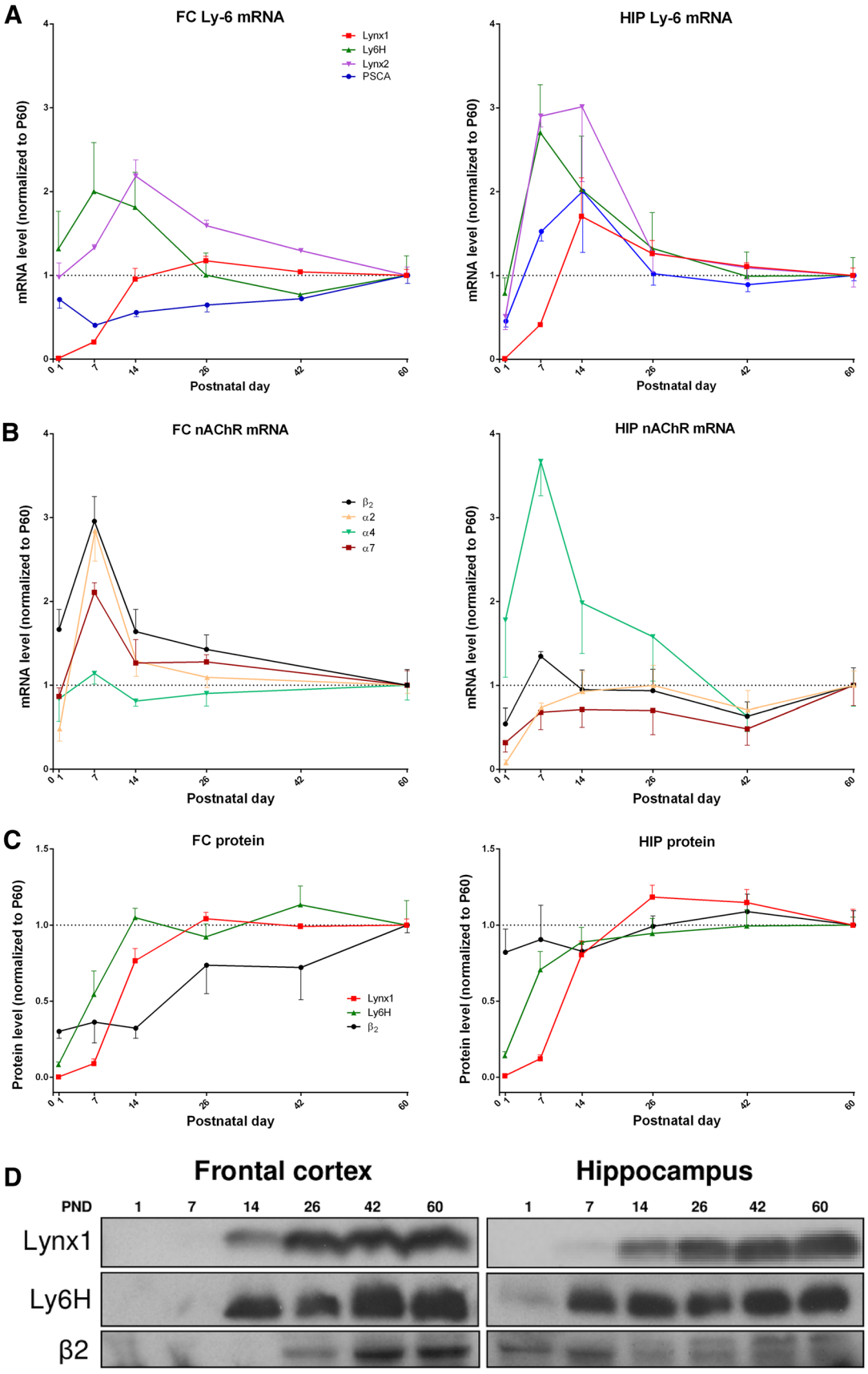
A
FC Ly-6 mRNA
HIP Ly-6 mRNA
Lynx1
Ly6H
Lynx2
PSCA
mRNA level (normalized to P60)
Postnatal day
B
FC nAChR mRNA
HIP nAChR mRNA
β2
α2
α4
α7
C
FC protein
HIP protein
Protein level (normalized to P60)
D
Frontal cortex
Hippocampus
PND
1
7
14
26
42
60
Lynx1
Ly6H
β2

◀ **Fig. 5** Developmental expression of Ly-6 proteins. Male rats were decapitated at postnatal day 1, 7, 14, 26, 42, or 60 and the frontal cortex (*FC*) and hippocampus (*HIP*) dissected and analyzed. **a** mRNA levels in the FC and HIP of Lynx1, Lynx2, Ly6H and PSCA as analyzed by qPCR. **b** mRNA levels in the FC and HIP of the nAChR subunits β2, α2, α4, and α7 as analyzed by qPCR. **c** Protein levels of Lynx1, Ly6H, and the β2 subunit as analyzed by western blotting. **d** Representative western blotting images. $n = 5$–6 in each group

Discussion

Here we show that the Ly-6 proteins Lynx1 and Ly6H are localized to the cell surface and synaptosomal fractions, and that their expression is cell-type specific and developmentally regulated.

Lynx1

Lynx1 binds to and modulates the function of nAChRs in vitro (Miwa et al. 1999, 2006; Ibañez-Tallon et al. 2002; Lyukmanova et al. 2011; Fu et al. 2012) and Lynx1-dependent modulation of cholinergic signaling is critical for visual synaptic plasticity (Morishita et al. 2010). Here we demonstrate that Lynx1 is present on the cell surface, particularly in the FC, where Lynx1 has a ratio of surface to intracellular receptors similar to that of GluR2, indicating that it is predominantly localized to the surface. This is in contrast to the β2 nAChR subunit which is predominantly intracellular, as described previously (Hill et al. 1993; Kuryatov et al. 2005). Furthermore, Lynx1 is preferentially localized to synaptic compartments in the FC and HIP. These findings are consistent with a role of Lynx1 in the modulation of synaptic neurotransmission. We further show that Lynx1 protein is predominantly expressed in the brain with some expression in the lung. This is in line with a previous report demonstrating Lynx1 mRNA in the mouse brain, but not in prostate, liver, or kidney (Miwa et al. 1999). To determine which cell types in the brain express Lynx1, we analyzed Lynx1 protein levels in primary cultures and were able to detect Lynx1 in neuronal, but not in micro- or astroglia cultures. This is consistent with the finding that more than 90 % of parvalbumin-containing interneurons express Lynx1 mRNA in the visual cortex (Morishita et al. 2010).

To our knowledge, the absolute amounts of Ly-6 proteins in the brain have never been determined. Using known amounts of human ws-Lynx1 we were able to estimate the absolute amount of Lynx1 to 1.0 and 0.13 μmol/kg total protein in the rat cortex and CSF, respectively. However, it should be noted that although human and rat Lynx1 protein have a high degree of sequence similarity, there are amino acid variations, which may cause differences in antibody affinity. Ws-Lynx1 has been shown to displace α-bungarotoxin binding to AChBPs and *Torpedo* nAChRs and alter the current response of nAChRs expressed in *Xenopus* oocytes to ACh in a dose-dependent and nAChR-type specific manner (Lyukmanova et al. 2011). Thus, 1 μM ws-Lynx1 enhanced the effect of ACh on the α7 nAChR, but 10 μM ws-Lynx1 decreased it, whereas ws-Lynx1 decreased α4β2-mediated responses at both doses (Lyukmanova et al. 2011). With the determined concentration of 0.5 μM Lynx1 in the CSF, and assuming that 1.0 μmol/kg in the FC corresponds roughly to 1 μM, this indicates that Lynx1 is present in the FC and CSF in sufficient concentrations to affect nAChR-mediated signaling. And with the preferential localization of Lynx1 to the cell surface and synaptic compartments, local concentrations of Lynx1 at synapses may be much higher.

Some Ly-6 proteins exist as soluble proteins in addition to the membrane-bound forms (Adermann et al. 1999). Whether or not soluble forms exist may have an impact on where and how these proteins can exert their function, since the soluble protein may diffuse across the synaptic cleft and the membrane-bound protein may be more restricted in its interaction with nAChRs (Miwa and Walz 2012). In line with this, transgenic mice overexpressing full-length or soluble Lynx1, respectively, display markedly different effects in terms of motor learning (Miwa and Walz 2012). We show that Lynx1 in the cortex is exclusively membrane bound and is not present in soluble forms. We did, however, detect Lynx1 in the CSF. This may come from a number of sources; Lynx1 could be expressed on immune cells in the CSF, although we did not find evidence of cell residue in our samples. And in healthy animals, the number of immune cells in the CSF is low (Wilson et al. 2010). Lynx1 could also be expressed as a soluble protein outside the CNS or in distinct cell types within the CNS and enter the CSF from these cells. It is thus possible that the CSF acts as a source of soluble Lynx1 for the brain. Finally, soluble Lynx1 may be concentrated in the CSF enabling a detection that is not possible in tissue, or Lynx1 in the CSF may represent a waste product from cells within the CNS.

Ly6H

Ly6H has been identified as a member of the Ly-6 family in humans and mice (Horie et al. 1998; Apostolopoulos et al. 1999), but unlike Lynx1 and Lynx2, Ly6H does not bind to the major nAChR subtypes in the brain, α7 and α4β2, when overexpressed in HEK293 cells (Tekinay et al. 2009). Here we show that endogenous Ly6H protein is expressed in the rat cortex where it is exclusively membrane bound. Ly6H demonstrated a restrictive expression profile since it was not detectable in the cerebellum, heart, lung, liver, kidney, or prostate. This is in agreement with the reported expression pattern of human and mouse Ly6H

mRNA (Horie et al. 1998; Apostolopoulos et al. 1999). We also demonstrate that a significant proportion of Ly6H in the HIP is located on the cell surface, and that Ly6H is predominantly localized to synaptosomes in the HIP and FC, suggesting a synaptic function of the protein. Furthermore, Ly6H was detected in cultured neurons, but not in microglia or astroglia. The similarities in distribution and synaptic localization between Ly6H and Lynx1, as well as the possibility of nAChR-mediated changes in Ly6H mRNA expression (Thomsen et al. 2011), suggest the possibility of a role for Ly6H in the modulation of membrane signaling. Although Ly6H does not seem to interact with α7 or α4β2 nAChRs, further studies are required to determine whether it can bind to other nAChR subtypes.

Developmental expression of nAChR subunits and Ly-6 proteins

We found that the developmental pattern of mRNA expression of Ly-6 family members and nAChR subunits differed between the FC and HIP. In the FC, the β2, α2, and α7 nAChR subunits displayed a marked peak in expression at P7. It has previously been shown that postnatal mRNA levels of α4, α7, and β2 in the rat cortex and HIP peaks at P7–14 (Broide et al. 1995; Shacka and Robinson 1998), although this is not found by all (Zhang et al. 1998). The expression of α4, α7, and β2 in the FC was paralleled by Ly6H although the latter had a more gradual decline, whereas Lynx2 peaked 1 week later. By contrast, Lynx1 and PSCA did not have peaks in mRNA expression, but displayed a gradual increase throughout postnatal development. These data are consistent with a previous report demonstrating an increase in Lynx1 and a decrease in Lynx2 mRNA in the V1 region from P18 to P60 in mice (Morishita et al. 2010). In the HIP, β2 and α4 displayed a peak at P7, which was paralleled by Ly6H, whereas Lynx1 peaked at P14. Lynx2 and PSCA showed broader peaks with high expression at P7, but did not reach maximum expression before P14. Contrarily, α2 and α7 did not display postnatal peaks in expression in the HIP. The expression of Ly6H and Lynx2, but not Lynx1 at P1 is in line with a previous report showing embryonic expression of Ly6H and Lynx2, but not Lynx1 in mice (Dessaud et al. 2006).

The mRNA expression was not entirely paralleled by protein levels for Ly6H or β2. In the FC, Lynx1 and Ly6H showed similar profiles with a gradual increase in protein levels reaching a plateau at P14–P26, whereas β2 protein levels increased gradually throughout postnatal development. In the HIP, Ly6H reached near maximum levels at P14, whereas Lynx1 levels reached a maximum a little later at P14–P26, and β2 levels were relatively constant. Thus, Lynx1 protein levels in the FC parallels mRNA, levels as has previously been shown in mice (Morishita et al. 2010), whereas this is not the case for Ly6H. This suggests that the two products are subject to differential post-transcriptional regulation during development. Protein data are not available for all the genes of interest since we could not get reliable staining for several of the proteins due to non-specific antibodies, as has been reported earlier for α7 (Herber et al. 2004; Moser et al. 2007).

These developmental data demonstrate for the first time a degree of coherence between the expression of Ly-6 family genes and nAChR subunits. The expression of Lynx1, Lynx2, and PSCA mRNA reached a maximum approximately 1 week later than the nAChR subunits. Notably, these three genes have all been implicated in regulation of nAChR function, and particularly Lynx1 has been proposed to be a dampener of cholinergic neurotransmission during development (Morishita et al. 2010). Our data invite the possibility that the expression of Ly-6 proteins may regulate the expression of nAChR subunits and thereby the developmental regulation of cholinergic signaling. The different patterns of expression of nAChRs and Ly-6 proteins in the FC and HIP, respectively, suggest that this putative regulation is may differ between brain regions. This is not surprising given that the distribution of nAChRs differs between the FC and HIP (Albuquerque et al. 2009).

Finally, our results from neuronal primary cultures suggest that Lynx1 and Ly6H protein levels follow similar temporal patterns in vivo and in vitro.

Conclusions

We demonstrate that Lynx1 and Ly6H are membrane-bound proteins in the brain, which are localized to the cell surface and in synaptosome fractions. These proteins are therefore well-situated to modulate synaptic signaling, e.g., via nAChRs to which several Ly-6 proteins have been shown to bind directly. However, it is possible that the intracellular pool of Ly-6 proteins has different functions, perhaps as molecular chaperones of nAChRs, as has previously been hypothesized (Lester et al. 2009). In addition, we show that several members of the Ly-6 protein family display similar expression patterns during postnatal development, and that they to some degree mirror nAChR expression. These data support a role for Ly-6 in the regulation of nAChR function during development. In line with this, we demonstrate that endogenous Lynx1 is present in the brain in concentrations, which have been demonstrated to modulate nAChR function (Lyukmanova et al. 2011).

Acknowledgments The authors would like to thank Dr. Cecilia Gotti for kindly providing the β2 antibody, Felix Eckenstein for providing the Lynx1 knock-out mouse tissue, and Imad Damaj for providing the α7 and β2 knock-out mouse tissue. This work was supported by the Danish Medical Research Council, the Danish Strategic Research Council, the Lundbeck Foundation, the NOVO Nordisk Foundation, the Danish Ministry of Science, Innovation and Higher Education, the Russian Academy of Sciences (Program "Molecular and Cell Biology"), the Ministry of Science and Education (contract No. 8268), and the Russian Foundation for Basic Research.

References

Adermann K, Wattler F, Wattler S, Heine G, Meyer M, Forssmann WG, Nehls M (1999) Structural and phylogenetic characterization of human SLURP-1, the first secreted mammalian member of the Ly-6/uPAR protein superfamily. Protein Sci 8:810–819

Albuquerque EX, Pereira EFR, Alkondon M, Rogers SW (2009) Mammalian nicotinic acetylcholine receptors: from structure to function. Physiol Rev 89:73–120

Apostolopoulos J, Chisholm LJ, Sandrin MS (1999) Identification of mouse Ly6H and its expression in normal tissue. Immunogenetics 49:987–990

Bamezai A (2004) Mouse Ly-6 proteins and their extended family: markers of cell differentiation and regulators of cell signaling. Arch Immunol Ther Exp (Warsz) 52:255–266

Broide RS, O'Connor LT, Smith MA, Smith JA, Leslie FM (1995) Developmental expression of alpha 7 neuronal nicotinic receptor messenger RNA in rat sensory cortex and thalamus. Neuroscience 67:83–94

Carino C, Fibuch EE, Mao L-M, Wang JQ (2012) Dynamic loss of surface-expressed AMPA receptors in mouse cortical and striatal neurons during anesthesia. J Neurosci Res 90:315–323

Chimienti F, Hogg RC, Plantard L, Lehmann C, Brakch N, Fischer J, Huber M, Bertrand D, Hohl D (2003) Identification of SLURP-1 as an epidermal neuromodulator explains the clinical phenotype of Mal de Meleda. Hum Mol Genet 12:3017–3024

Choo YM, Lee BH, Lee KS, Kim BY, Li J, Kim JG, Lee JH, Sohn HD, Nah SY, Jin BR (2008) Pr-lynx1, a modulator of nicotinic acetylcholine receptors in the insect. Mol Cell Neurosci 38:224–235

Darvas M, Morsch M, Racz I, Ahmadi S, Swandulla D, Zimmer A (2009) Modulation of the Ca2+ conductance of nicotinic acetylcholine receptors by Lypd6. Eur Neuropsychopharmacol 19:670–681

Dessaud E, Salaün D, Gayet O, Chabbert M, DeLapeyrière O (2006) Identification of lynx2, a novel member of the ly-6/neurotoxin superfamily, expressed in neuronal subpopulations during mouse development. Mol Cell Neurosci 31:232–242

Fu XW, Rekow SS, Spindel ER (2012) The Ly-6 protein, lynx1 is an endogenous inhibitor of nicotinic signaling in airway epithelium. Am J Physiol Lung Cell Mol Physiol 303(8):L661–L668

Grosshans DR, Clayton DA, Coultrap SJ, Browning MD (2002) LTP leads to rapid surface expression of NMDA but not AMPA receptors in adult rat CA1. Nat Neurosci 5:27–33

Herber DL, Severance EG, Cuevas J, Morgan D, Gordon MN (2004) Biochemical and histochemical evidence of nonspecific binding of alpha7 nAChR antibodies to mouse brain tissue. J Histochem Cytochem 52:1367–1376

Hill JA, Zoli M, Bourgeois JP, Changeux JP (1993) Immunocytochemical localization of a neuronal nicotinic receptor: the beta 2-subunit. J Neurosci 13:1551–1568

Horie M, Okutomi K, Taniguchi Y, Ohbuchi Y, Suzuki M, Takahashi E (1998) Isolation and characterization of a new member of the human Ly6 gene family (LY6H). Genomics 53:365–368

Hruska M, Keefe J, Wert D, Tekinay AB, Hulce JJ, Ibañez-Tallon I, Nishi R (2009) Prostate stem cell antigen is an endogenous Lynx1-like prototoxin that antagonizes alpha7-containing nicotinic receptors and prevents programmed cell death of parasympathetic neurons. J Neurosci 29:14847–14854

Ibañez-Tallon I, Miwa JM, Wang HL, Adams NC, Crabtree GW, Sine SM, Heintz N (2002) Novel modulation of neuronal nicotinic acetylcholine receptors by association with the endogenous prototoxin lynx1. Neuron 33:893–903

Kuryatov A, Luo J, Cooper J, Lindstrom J (2005) Nicotine acts as a pharmacological chaperone to up-regulate human alpha4beta2 acetylcholine receptors. Mol Pharmacol 68:1839–1851

Lester HA, Xiao C, Srinivasan R, Son CD, Miwa J, Pantoja R, Banghart MR, Dougherty DA, Goate AM, Wang JC (2009) Nicotine is a selective pharmacological chaperone of acetylcholine receptor number and stoichiometry. Implications for drug discovery. AAPS J 11:167–177

Liu Z, Cao G, Li J, Bao H, Zhang Y (2009) Identification of two Lynx proteins in Nilaparvata lugens and the modulation on insect nicotinic acetylcholine receptors. J Neurochem 110:1707–1714

Lozada AF, Wang X, Gounko NV, Massey KA, Duan J, Liu Z, Berg DK (2012a) Glutamatergic synapse formation is promoted by α7-containing nicotinic acetylcholine receptors. J Neurosci 32:7651–7661

Lozada AF, Wang X, Gounko NV, Massey KA, Duan J, Liu Z, Berg DK (2012b) Induction of dendritic spines by β2-containing nicotinic receptors. J Neurosci 32:8391–8400

Lyukmanova EN, Shenkarev ZO, Shulepko MA, Mineev KS, D'Hoedt D, Kasheverov IE, Filkin SY, Krivolapova AP, Janickova H, Dolezal V, Dolgikh DA, Arseniev AS, Bertrand D, Tsetlin VI, Kirpichnikov MP (2011) NMR structure and action on nicotinic acetylcholine receptors of water-soluble domain of human LYNX1. J Biol Chem 286:10618–10627

Mielke JG, Mealing GA (2009) Cellular distribution of the nicotinic acetylcholine receptor alpha7 subunit in rat hippocampus. Neurosci Res 65:296–306

Miwa JM, Walz A (2012) Enhancement in motor learning through genetic manipulation of the Lynx1 gene. PLoS One 7:e43302

Miwa JM, Ibanez-Tallon I, Crabtree GW, Sánchez R, Sali A, Role LW, Heintz N (1999) Lynx1, an endogenous toxin-like modulator of nicotinic acetylcholine receptors in the mammalian CNS. Neuron 23:105–114

Miwa JM, Stevens TR, King SL, Caldarone BJ, Ibanez-Tallon I, Xiao C, Fitzsimonds RM, Pavlides C, Lester HA, Picciotto MR, Heintz N (2006) The prototoxin lynx1 acts on nicotinic acetylcholine receptors to balance neuronal activity and survival in vivo. Neuron 51:587–600

Miwa JM, Freedman R, Lester HA (2011) Neural systems governed by nicotinic acetylcholine receptors: emerging hypotheses. Neuron 70:20–33

Miwa JM, Lester HA, Walz A (2012) Optimizing cholinergic tone through lynx modulators of nicotinic receptors: implications for plasticity and nicotine addiction. Physiology (Bethesda) 27:187–199

Morishita H, Miwa JM, Heintz N, Hensch TK (2010) Lynx1, a cholinergic brake, limits plasticity in adult visual cortex. Science 330:1238–1240

Moser N et al (2007) Evaluating the suitability of nicotinic acetylcholine receptor antibodies for standard immunodetection procedures. J Neurochem 102:479–492

Nirogi R, Kandikere V, Mudigonda K, Bhyrapuneni G, Muddana N, Saralaya R, Benade V (2009) A simple and rapid method to collect the cerebrospinal fluid of rats and its application for the

assessment of drug penetration into the central nervous system. J Neurosci Methods 178:116–119

Sarter M, Parikh V, Howe WM (2009) nAChR agonist-induced cognition enhancement: integration of cognitive and neuronal mechanisms. Biochem Pharmacol 78:658–667

Schmittgen TD, Livak KJ (2008) Analyzing real-time PCR data by the comparative CT method. Nat Protoc 3:1101–1108

Shacka JJ, Robinson SE (1998) Postnatal developmental regulation of neuronal nicotinic receptor subunit alpha 7 and multiple alpha 4 and beta 2 mRNA species in the rat. Brain Res Dev Brain Res 109:67–75

Soliakov L, Gallagher T, Wonnacott S (1995) Anatoxin-a-evoked [3H]dopamine release from rat striatal synaptosomes. Neuropharmacology 34:1535–1541

Srivastava S, Osten P, Vilim FS, Khatri L, Inman G, States B, Daly C, DeSouza S, Abagyan R, Valtschanoff JG, Weinberg RJ, Ziff EB (1998) Novel anchorage of GluR2/3 to the postsynaptic density by the AMPA receptor-binding protein ABP. Neuron 21:581–591

Tekinay AB, Nong Y, Miwa JM, Lieberam I, Ibanez-Tallon I, Greengard P, Heintz N (2009) A role for LYNX2 in anxiety-related behavior. Proc Natl Acad Sci USA 106:4477–4482

Thomsen MS, Mikkelsen JD (2012a) The α7 nicotinic acetylcholine receptor complex: one, two or multiple drug targets? Curr Drug Targets 13(5):707–720

Thomsen MS, Mikkelsen JD (2012b) The α7 nicotinic acetylcholine receptor ligands methyllycaconitine, NS6740 and GTS-21 reduce lipopolysaccharide-induced TNF-α release from microglia. J Neuroimmunol 251:65–72

Thomsen MS, Hansen HH, Timmermann DB, Mikkelsen JD (2010) Cognitive improvement by activation of alpha7 nicotinic acetylcholine receptors: from animal models to human pathophysiology. Curr Pharm Des 16:323–343

Thomsen MS, El-Sayed M, Mikkelsen JD (2011) Differential immediate and sustained memory enhancing effects of alpha7 nicotinic receptor agonists and allosteric modulators in rats. PLoS One 6:e27014

Tsetlin V (1999) Snake venom alpha-neurotoxins and other "three-finger" proteins. Eur J Biochem 264:281–286

Tsuji H, Okamoto K, Matsuzaka Y, Iizuka H, Tamiya G, Inoko H (2003) SLURP-2, a novel member of the human Ly-6 superfamily that is up-regulated in psoriasis vulgaris. Genomics 81:26–33

Wilson EH, Weninger W, Hunter CA (2010) Trafficking of immune cells in the central nervous system. J Clin Invest 120:1368–1379

Zhang X, Liu C, Miao H, Gong Z, Nordberg A (1998) Postnatal changes of nicotinic acetylcholine receptor 2, α3, α4, α7 and β2 subunits genes expression in rat brain. Int J Dev Neurosci 16:507–518

Supplementary material

Figure S1. Validation of antibodies used
(A) Anti-Lynx1 antibody (sc-23060) 1:1000 detected on cortical samples from wild-type (WT) and Lynx1 knock-out (KO) mice as well as rat. There is a clear band around 12 kDa, corresponding to the expected molecular weight of Lynx1, which is not present in Lynx1 KO mice. **(B)** Anti-β2 antibody (#834, provided by Cecilia Gotti) 1:1000 detected on cortical samples from rat and human samples as well as α7 and β2 WT and KO mice. There is a clear band around 50 kDa, corresponding to the expected molecular weight of β2, which is not present in β2 KO mice. **(C)** Anti-Ly6H antibody ((H00004062-M01) 1:1000 detected on 0.1 µg GST-tagged recombinantly expressed human Ly6H protein (Abnova #H00004062-P01) and 40 µg samples of rat cortex, rat cerebellum and human cortex. A clear band around 20 kDa is detected in rat and human cortex, but not in rat cerebellum. This is in line with the previous demonstration that Ly6H is expressed in human cortex, but not cerebellum (Horie et al., 1998). A clear band around 45 kDa is detected in the recombinant protein sample, which is in line with an extra 25 kDa being added due to the GST tag.

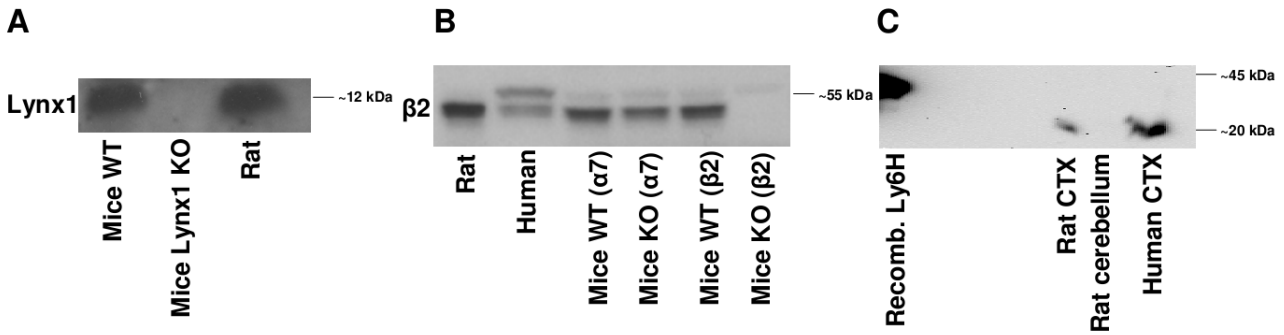

Figure S2. Validation of synaptosome preparation
Representative western blot images of frontal cortical and hippocampal tissue fractionated using differential centrifugation into a pellet 1 (P1, nuclear) and pellet 2 (P2, crude synaptosome) fraction. Enrichment of synaptosomes in P2 is confirmed by emrichment of the synaptic protein Syntaxin (Anti-Syntaxin, MAB336) in the P2 fraction compared to P1 and the total homogenate (Hom)

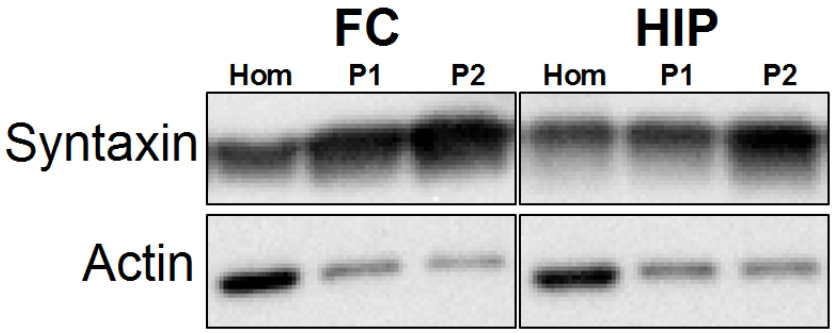

Figure S3. Validation of primary neuronal cultures

Protein levels in cortical tissue from an adult male rat (CTX), in rat cortical primary neurons cultured for 7 days in vitro (Neuron DIV7), in rat primary microglia cultured for 15 days in vitro, and in rat primary astroglia cultured for 18 days *in vitro*

Glial fibrillary acidic protein (GFAP) is an astrocyte-specific protein. There is clear staining of GFAP in adult cortex and astroglial cultures, but an almost complete lack of GFAP staining in neuronal and microglial cultures.

MAP2 is a neuron-specific protein. There are two MAP2 bands in adult cortex, corresponding to the high molecular weight isoforms MAP2a and c and the low molecular weight isoform MAP2c. There is clear MAP2c staining in neuronal cultures, and no MAP2 staining in astro- or microglial cultures. MAP2c has previously been shown to be expressed mainly in immature neurons (Chung, Kindler, Seidenbecher, & Garner, 1996), which is in line with our data.

Antibodies used for detection were Anti-GFAP (#G9269) 1:5000 and Anti-MAP2 (#MM03) 1:500.

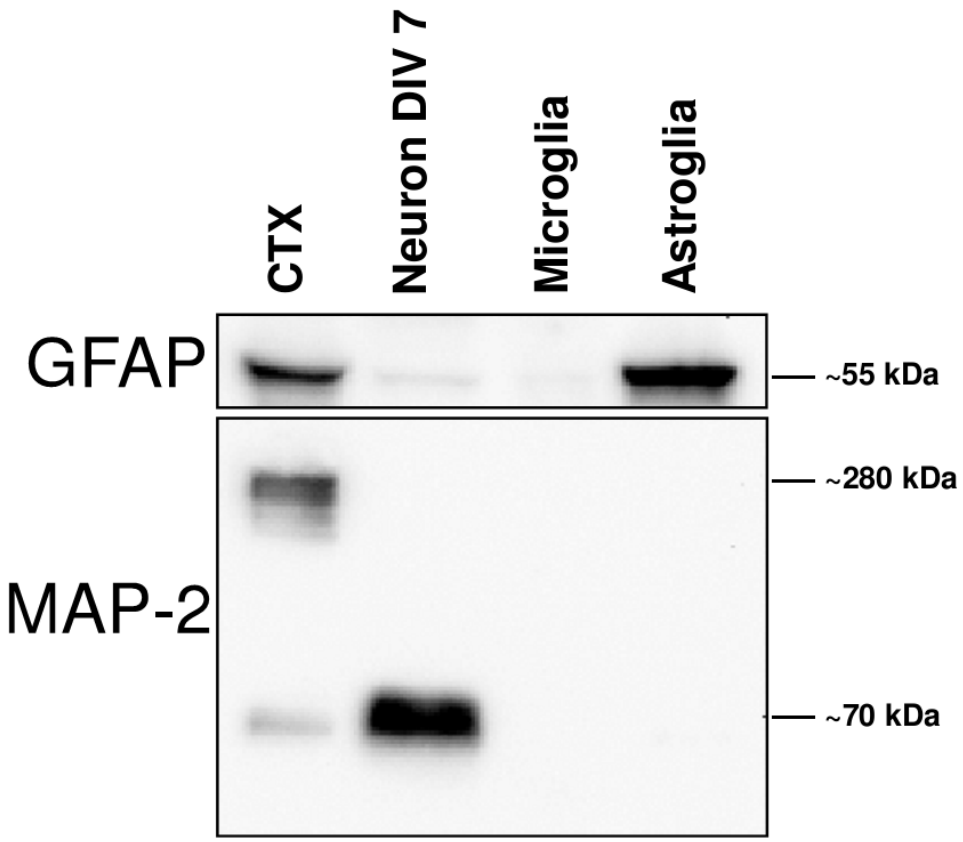

Figure S4. Validation of primary astroglia cultures
Rat primary astroglia stained with: **(A)** the microglia-specific protein OX-42 (mouse, BD#550299, 1:50) combined with AlexaFluor488 Donkey Anti-mouse 1:300 (green) and the astrocyte-specific protein glial fibrillary acidic protein GFAP (rabbit, Abcam#ab7260, 1:500) combined withAlexaFlour533 Goat Anti-rabbit 1:500 (red). The micrograph was taken at 10x magnification from a confluent culture, scale bar= 10 µm. Or **(B)** the neuron-specific protein MAP-2 (mouse, Sigma #4403, 1:500) combined with AlexaFluor488 Donkey Anti-mouse 1:500 (green) and GFAP (rabbit, Abcam#ab7260, 1:500) combined with AlexaFlour533 Goat Anti-rabbit 1:500 (red). The micrograph was taken at 20x magnification from a non-confluent culture, scale bar= 10 µm. Counting of immunopositive cells show that the astroglia cultures contain ≥99% GFAP-positive cells.

A B

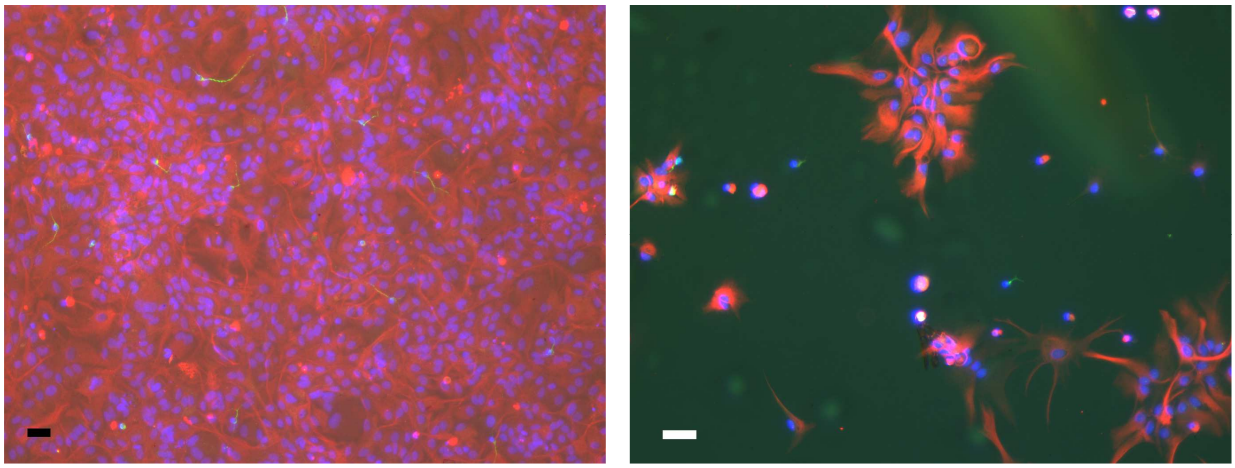

References

Chung, W. J., Kindler, S., Seidenbecher, C., & Garner, C. C. (1996). MAP2a, an alternatively spliced variant of microtubule-associated protein 2. *Journal of neurochemistry*, *66*(3), 1273–81.

Horie, M., Okutomi, K., Taniguchi, Y., Ohbuchi, Y., Suzuki, M., & Takahashi, E. (1998). Isolation and characterization of a new member of the human Ly6 gene family (LY6H). *Genomics*, *53*(3), 365–8.

Paper III

Jensen MM, Arvaniti M, Mikkelsen JD, Michalski D, Pinborg LH, Härtig W, Thomsen MS.

Prostate stem cell antigen interacts with nicotinic acetylcholine receptors and is affected in Alzheimer's disease.

Neurobiol Aging (2015), in press.

The article was accepted on January 3rd 2015.
The decision letter from Neurobiol Aging is included after the manuscript.

(Note in print: The manuscript is shown in online version)

Neurobiology of Aging xxx (2015) 1–10

Contents lists available at ScienceDirect

Neurobiology of Aging

journal homepage: www.elsevier.com/locate/neuaging

Prostate stem cell antigen interacts with nicotinic acetylcholine receptors and is affected in Alzheimer's disease

Majbrit M. Jensen [a], Maria Arvaniti [a], Jens D. Mikkelsen [a], Dominik Michalski [b], Lars H. Pinborg [a,c], Wolfgang Härtig [d], Morten S. Thomsen [a,*]

[a] Neurobiology Research Unit, Copenhagen University Hospital, Rigshospitalet, Copenhagen, Denmark
[b] Department of Neurology, University of Leipzig, Leipzig, Germany
[c] Epilepsy Clinic, Copenhagen University Hospital, Rigshospitalet, Copenhagen, Denmark
[d] Paul Flechsig Institute for Brain Research, University of Leipzig, Leipzig, Germany

ARTICLE INFO

Article history:
Received 2 July 2014
Received in revised form 8 December 2014
Accepted 3 January 2015

Keywords:
Alzheimer's disease
Nicotinic acetylcholine receptor
Frontal cortex
Lynx
PSCA
Lypd6

ABSTRACT

Alzheimer's disease (AD) is a neurodegenerative disorder involving impaired cholinergic neurotransmission and dysregulation of nicotinic acetylcholine receptors (nAChRs). Ly-6/neurotoxin (Lynx) proteins have been shown to modulate cognition and neural plasticity by binding to nAChR subtypes and modulating their function. Hence, changes in nAChR regulatory proteins such as Lynx proteins could underlie the dysregulation of nAChRs in AD. Using Western blotting, we detected bands corresponding to the Lynx proteins prostate stem cell antigen (PSCA) and Lypd6 in human cortex indicating that both proteins are present in the human brain. We further showed that PSCA forms stable complexes with the α4 nAChR subunit and decreases nicotine-induced extracellular-signal regulated kinase phosphorylation in PC12 cells. In addition, we analyzed protein levels of PSCA and Lypd6 in postmortem tissue of medial frontal gyrus from AD patients and found significantly increased PSCA levels (approximately 70%). In contrast, no changes in Lypd6 levels were detected. In concordance with our findings in AD patients, PSCA levels were increased in the frontal cortex of triple transgenic mice with an AD-like pathology harboring human transgenes that cause both age-dependent β-amyloidosis and tauopathy, whereas Tg2576 mice, which display β-amyloidosis only, had unchanged PSCA levels compared to wild-type animals. These findings identify PSCA as a nAChR-binding protein in the human brain that is affected in AD, suggesting that PSCA-nAChR interactions may be involved in the cognitive dysfunction observed in AD.

1. Introduction

Alzheimer's disease (AD) is the most common form of dementia in the elderly individuals. Characteristics of AD consist of accumulation of β-amyloid (Aβ) plaques and neurofibrillary tangles of hyperphosphorylated tau proteins (Querfurth and LaFerla, 2010). Another neuropathologic feature of AD is the selective degeneration of cholinergic neurons in the basal forebrain, which is associated with the cognitive decline in AD (reviewed in Auld et al., 2002).

The most abundant nicotinic acetylcholine receptors (nAChRs) in the brain, α7 and α4β2, are involved in cognitive performance, such as attention and memory function, as well as synaptic plasticity (reviewed in Sarter et al., 2009; Thomsen et al., 2010). Accordingly, they have been widely investigated for their involvement in the pathology of AD. Genetic analyses have demonstrated associations between single-nucleotide polymorphisms in the α7 nAChR gene and AD (Carson et al., 2008b) as well as the delusional symptoms in AD (Carson et al., 2008a). Single-nucleotide polymorphisms in the genes of α4 (Dorszewska et al., 2005; Kawamata and Shimohama, 2002) and β2 nAChR subunits (Cook et al., 2004; Laumet et al., 2010) have also shown to be associated with AD. Recent studies agree that α4β2 nAChR levels are decreased in AD. Thus, reduced [^{3}H]-nicotine binding was observed postmortem in frontal cortex of AD patients (Marutle et al., 2013), and binding of the α4β2 nAChR radioligand [^{18}F]-2FA-85380, by the use of PET, was decreased in several brain regions of AD patients and demonstrated significant correlations with both Aβ levels in the medial prefrontal cortex and cognitive performance of the AD patients (Okada et al., 2013). In contrast, there is currently no consensus on whether α7 nAChR levels in the brain are changed in AD, because binding

* Corresponding author at: Department of Drug Design and Pharmacology, Faculty of Health and Medical Sciences, University of Copenhagen, Universitetsparken 2, DK-2100 Copenhagen, Denmark. Tel.: +4535331717.
E-mail address: morten.s.thomsen@sund.ku.dk (M.S. Thomsen).

0197-4580/$ – see front matter © 2015 Elsevier Inc. All rights reserved.
http://dx.doi.org/10.1016/j.neurobiolaging.2015.01.001

studies have reported either downregulation or no change (Court et al., 2001; Davies and Feisullin, 1981; Hellstrom-Lindahl et al., 1999; Marutle et al., 2013).

$A\beta_{1-42}$ has been shown to bind both α7 and α4β2 nAChRs, the former with picomolar affinity, whereas its affinity for α4β2 was 5000 times lower (Wang et al., 2000). Furthermore, $A\beta_{1-42}$ is able to modulate the function of both α7 and α4β2 nAChRs with dose-dependent effects (reviewed in Buckingham et al., 2009; Jurgensen and Ferreira, 2010).

In addition to $A\beta_{1-42}$, several members of Ly-6/neurotoxins (Lynx) protein superfamily have been shown to modulate the function of nAChRs (reviewed in Miwa et al., 2011; Thomsen and Mikkelsen, 2012). Therefore, alterations in α7 and α4β2 nAChRs may be secondary to changes in Lynx protein levels.

The Lynx superfamily has structural similarities to snake venom toxins such as α-bungarotoxin and are characterized by a "three-fingered" loop motif (Tsetlin, 1999). The Lynx proteins Lynx1 and Lynx2 have been shown to form stable complexes with and negatively regulate both α7 and α4β2 nAChRs (Ibanez-Tallon et al., 2002; Miwa et al., 2006; Tekinay et al., 2009). In addition, mice with genetic deletions of Lynx1 or Lynx2 displayed increased associative learning and elevated anxiety-like behavior, respectively (Miwa et al., 2006; Tekinay et al., 2009). Moreover, it was recently shown that Lynx1 through a nAChR-dependent action had a crucial role in the loss of synaptic plasticity observed in adult visual cortex (Morishita et al., 2010). Furthermore, transgenic overexpression of the Lynx protein Lypd6 in mice resulted in increased pre-pulse inhibition indicating possible involvement in attention (Darvas et al., 2009). Thus, Lynx proteins are suggested to be involved in cognitive function.

Prostate stem cell antigen (PSCA), another Lynx protein, was found to suppress nicotine-induced Ca^{2+} influx via activation of α7 nAChRs, when retrovirally expressed in dissociated avian ciliary ganglion neurons (Hruska et al., 2009). In contrast, nicotine-induced Ca^{2+} currents were enhanced in dissociated murine trigeminal ganglia neurons from transgenic mice overexpressing Lypd6, suggesting that Lypd6 is a positive modulator of nAChR function (Darvas et al., 2009).

Because nAChRs and Lynx proteins can bind directly to each other to affect cognitive function and synaptic plasticity, it is pertinent to examine the involvement of Lynx proteins in AD. The purpose of this study was to (1) investigate PSCA and Lypd6 in the human brain in relation to expression and complex formations with nAChR subtypes; (2) examine the ability of PSCA to modulate a nicotine-mediated response in PC12 cells; and (3) reveal whether the levels of the two Lynx proteins were changed in AD in both human AD patients and transgenic AD mouse models.

2. Methods

2.1. Human tissue

Temporal cortical tissue was obtained from anterior temporal lobectomies in two patients (1 female, aged 30 years and 1 male, aged 57 years) with medically intractable temporal lobe epilepsy with hippocampal onset. Written informed consent was obtained from both patients before surgery. The study was approved by the Ethical Committee in the Capital Region of Denmark (H-2-2011-104) and performed in accordance with the Declaration of Helsinki. The tissue was dissected and immediately frozen on dry ice and stored at −80 °C until use. The neuropathologic examinations of the neocortex from both patients were normal.

Postmortem brain tissue from medial frontal gyrus of 7 AD subjects and 8 nondemented (non-AD) control subjects (see Table 1) were obtained from the Netherland's Brain Bank, Amsterdam, the Netherlands. Autopsies were performed on donors from whom written informed consent had been obtained either from the donor or direct next of kin. All AD subjects were confirmed by standard clinical (Dubois et al., 2007; McKhann et al., 1984) and neuropathologic (Braak and Braak, 1991, 1995) diagnosis criteria.

Table 1
Clinicopathologic data of the human brain material

Diagnosis	Age	Gender	pH	PMD (h:min)	Braak stage
Nondemented control	60	F	6.27	06:50	1
Nondemented control	60	F	6.80	07:30	1
Nondemented control	62	M	6.36	07:20	1
Nondemented control	78	M	6.52	<17:40	1
Nondemented control	87	M	7.11	08:00	1
Nondemented control	87	F	6.91	08:00	2
Nondemented control	97	F	—	10:00	2
Nondemented control	90	F	6.54	06:10	3
Alzheimer's disease	67	F	6.73	03:30	5
Alzheimer's disease	58	M	6.29	05:15	6
Alzheimer's disease	58	M	6.42	06:25	6
Alzheimer's disease	59	M	6.26	05:05	6
Alzheimer's disease	62	M	6.31	04:15	6
Alzheimer's disease	62	F	6.53	04:25	6
Alzheimer's disease	62	F	6.06	04:45	6

Key: F, female; M, male; PMD, postmortem delay.

2.2. Animals

Triple transgenic mice (3×Tg-AD), expressing mutant human transgenes (human amyloid precursor protein [APP] 695 with the Swedish double mutation K670N/M671L [hAPPSwe], tau P301L) mutation, and the presenilin-1 mutant M146V knock-in construct (Oddo et al., 2003), were studied in two different age groups: 6-month-old mice (n = 8) and 19- to 21-month-old mice (n = 8) with age-matched wild-type (WT) mice (Sv129/B6; n = 7–8) as controls. The mice were bred at the Medizinisch-Experimentelles Zentrum at Leipzig University. At the day of experiment, the mice were decapitated, frontal cortex and hippocampus dissected, and the tissue was immediately frozen on dry ice and stored at −80 °C until use.

Twelve male Tg2576 mice expressing the hAPPSwe mutations (Hsiao et al., 1996) and their WT littermates (n = 15) bred on an inbred 129S6 background were obtained from Taconic (Ry, Denmark). At the age of 9 months, in an unrelated set of experiments, the mice received bilateral intracerebroventricular phosphate-buffered saline (PBS) injections (Laursen et al., 2014) followed by electrophysiological testing. Mice were euthanized at the age of 15 months, and one hemisphere was dissected, snap frozen, and kept at −80 °C until further analysis. Frontal cortex was later separated from the frozen sample and used for Western blot analyses as described in the following.

Experiments with 3×Tg-AD were approved by the Animal Care and Use Committee of the University of Leipzig and local authorities (Regierungspräsidium Leipzig; T40/13) and conformed to the European Communities Council Directive (86/609/EEC). Experiments with Tg2576 mice were approved by the Danish National Committee for Ethics in Animal Experimentation.

2.3. Tissue fractionation

To fraction tissue into membrane and soluble fractions, human temporal cortical tissue from neurosurgery (150–170 mg, n = 2) was homogenized 2 × 30 seconds in Buffer1 (0.5 M NaCl, 50 mM Tris–HCl, 10 mM $MgCl_2$, 2 mM ethylenediaminetetraacetic acid (EDTA), 10 μL/mL protease inhibitor cocktail [Sigma-Aldrich, Brøndby, Denmark], pH 7.3) using a PT1200C polytron blender (Kinematica, Luzern, Switzerland) and centrifuged for 30 minutes

at 126,000*g* at 20 °C–22 °C using an air-driven ultracentrifuge (Airfuge, Copenhagen, Denmark). The supernatant containing the soluble fraction was transferred to a new tube, and the pellet containing the membrane fraction was washed twice in Buffer1, resuspended by blending 2 × 30 seconds in Buffer2 (4 M urea, 50 mM Tris–HCl, 1% SDS, 10 μL/mL protease inhibitor cocktail, pH 7.3), and sonicated 3 × 5 seconds on ice.

2.4. PSCA affinity purification

Recombinant human GST-tagged PSCA produced in *Escherichia coli* (purchased from MyBioSource Inc, San Diego, CA) and dissolved to 0.7 mg/mL in PBS, pH 7.4 was coupled to PureProteome NHS Flexibind magnetic beads (Millipore, Billerica, MA) in a ratio of 1:1.25 (vol/vol). In brief, beads were washed once in ice-cold 1 mM HCl before addition of the PSCA solution. Subsequently, beads were incubated overnight at 4 °C in a rotator (15 rpm). Unbound PSCA was removed, and the beads were resuspended and washed four times in Quench buffer (100 mM Tris-HCl, 150 mM NaCl, pH 8.0) followed by incubation for 1 hour at room temperature. A batch of beads without PSCA in the PBS was processed in parallel as a negative control. The beads were incubated in 0.1% bovine serum albumin in PBS, pH 7.4, for 1 hour at 4 °C before use.

The tissue was lysed in 1 mL lysis buffer (50 mM Tris, 50 mM NaCl, 5 mM EDTA, 5 mM EGTA, 10 μL/mL protease inhibitor cocktail [Sigma-Aldrich, pH 7.5]) using the PT1200C polytron blender for 20 seconds. The lysate was centrifuged for 30 minutes at 160,000*g* at 20 °C–22 °C using the air-driven ultracentrifuge and the supernatant discarded. The pellet was resuspended in 1 mL lysis buffer containing 2% Triton X-100 by blending for 20 seconds and incubated for 2 hours at 4 °C on a rotor (15 rpm). Thereafter, the sample was centrifuged as mentioned previously, and the resulting supernatant (input) was used for affinity purification. Total protein content was determined using the Pierce 660 nm Protein Assay (Thermo Scientific, Rockford, IL), and 1000 μg protein was incubated with 50 μL magnetic beads in a total volume of 1500 μL lysis buffer for 18–22 hours at 4 °C in a rotator (15 rpm). A sample of the homogenate after affinity purification was taken (output). Subsequently, the beads were washed twice in 1 M NaCl, 8 mM Na_2HPO_4, 2 mM NaH_2PO_4, 0.5% Triton X-100, pH 7.5 and three times in an identical buffer, where 1 M NaCl was substituted with 0.1 M NaCl, and thereafter, the samples were immediately processed for Western blotting.

2.5. ERK phosphorylation and β2 nAChR expression in PC12 cells

PC12 cells were maintained in 75 cm^2 flasks coated with 5 μg/mL poly-L-lysine (Sigma-Aldrich), in Dulbecco modified Eagle medium (DMEM, Gibco Life Technologies, NY) supplemented with 10% heat-inactivated horse serum, 5% fetal bovine serum, 25 U/mL penicillin, 25 μg/mL streptomycin, 1 mM sodium pyruvate, and 2 mM glutamine (complete culture medium) at 37 °C in a humidified incubator with 5% CO_2. Cells were subcultured every 3–4 days by detachment with 0.25% trypsin in EDTA solution (Gibco Life Technologies) and reseeded at 15% confluence.

For the extracellular-signal regulated kinase (ERK) phosphorylation assay, cells were seeded in 24-well plates at 12 × 10^4 cells/cm^2, in low serum medium (1% heat-inactivated horse serum, 0.5% fetal bovine serum) 24 hours before the experiments, which started by incubating cells for 10 minutes with recombinant human PSCA protein (MyBiosource) in the concentrations (0.1, 1, and 10 μM) diluted in DMEM, followed by stimulation with 25 μM nicotine (Sigma-Aldrich) for 5 minutes. For the β2 nAChR expression assay, PC12 cells were seeded in 96-well plates at 12 × 10^4 cells/cm^2 on the day of the experiment in complete culture medium. Subsequently, cells were stimulated for 24 hours with recombinant human PSCA protein (MyBiosource) in the concentrations (0.1, 1, and 10 μM) diluted in DMEM. Thereafter, cells were immediately lysed in 100 μL and 50 μL, respectively, ice-cold lysis buffer/well (100 mM NaCl, 25 mM EDTA, 10 mM Tris, 4 mM Na_3VO_4, 1 mM NaF, and 1% [vol/vol] Triton X-100, 1% [vol/vol] NP-40, 1 μL/mL protease inhibitor cocktail [Sigma-Aldrich], pH 7.4). To ensure complete lysis, lysates were then placed in −80 °C for 15 minutes, thawed, and sonicated for 5 seconds on ice. Lysates were stored at −80 °C until they were processed for Western blotting.

2.6. Small interfering RNA transfection and real-time quantitative reverse transcription polymerase chain reaction

FlexiTube small interfering RNA (siRNA) (Qiagen, Limburg, the Netherlands) against PSCA (TACAATCATCCTGTAATAAAT) and a scrumbled negative control were diluted in DMEM (Gibco Life Technologies) to a final concentration of 50 nM. The transfection reagent Lipofectamine 2000 (Life Technologies, Carlsbad, CA) was diluted in opti-MEM (Life Technologies) and incubated for 5 minutes at room temperature according to the manufacturer's instructions. siRNAs were mixed with the transfection reagent and incubated further for 15 minutes at room temperature to allow the formation of transfection complexes. Subsequently, 100 μL of transfection complexes were added into each well of a 24-well plate, and PC12 cells were seeded at 24 × 10^4 cells/cm^2 in complete culture medium without antibiotics. Cells were incubated at 37 °C in a humidified incubator with 5% CO_2. After 48 hours, the medium was removed, the plate was placed on ice, and RNA was immediately extracted using the RNeasy Mini Kit (Qiagen) according to the manufacturer's instructions.

RNA samples were dissolved in RNase-free water, and RNA content was quantified using a Nanodrop ND-1000 Spectrophotometer (Nanodrop Technologies, Wilmington, DE). Samples were diluted with RNase-free water to equal RNA concentrations and reverse transcribed into single-stranded complementary DNA (cDNA) with the ImProm-II Reverse Transcription System (Promega, Madison, WI) according to the manufacturer's directions using 0.5 g/reaction oligo$(dT)_{15}$ primers, 6 mM $MgCl_2$, and 20 units of RNase inhibitor. Real-time quantitative reverse transcription polymerase reactions (RT-qPCR) were performed in a total volume of 20 μL, containing 1 μL sample cDNA, 1× Brilliant II SYBR Green qPCR Master Mix (Stratagene, La Jolla, CA), and 15 pmol each of the forward and reverse primers (DNA Technology, Aarhus, Denmark). RT-qPCR was performed on a Light Cycler 480 Real-Time PCR System (Roche, Indianapolis, IN) with a 10-minute preincubation at 94 °C followed by 40 cycles of 30 seconds at 94 °C, 45 seconds at 60 °C, and 90 seconds at 72 °C. Primer pairs were validated by using serially diluted cDNA to establish a standard curve and by confirming the existence of a single product on a gel at the correct molecular weight. Quantification of messenger RNA (mRNA) expression was performed according to the comparative C_T method as described by (Schmittgen and Livak, 2008). For each sample, the amount of target mRNA was normalized to the amount of GAPDH.

The sequence of the designed primers were as follows: PSCA, forward 5′-GCCCTACCAGTTCTGATCAG-3′, reverse 5′-TCACACCCACCTAGCTTCAT-3′; β2 nAChR, forward 5′-ACGGTGTTCCTGCTGCTCATC-3′, reverse 5′-CACACTCTGGTCATCATCCTC-3′; and GAPDH, forward 5′-CATCAAGAAGGTGGTGAAGCA-3′, reverse 5′-CTGTTGAAGTCACAGGAGACA-3′.

2.7. Tissue preparation for Western blotting

Human postmortem cortical tissue was lysed in homogenization buffer (50 mM Tris, 100 nM NaCl, 25 mM EDTA, 1% [vol/vol] Triton-X, 1% [vol/vol] NP-40, 1 μL/mL protease inhibitor cocktail [Sigma-Aldrich], pH 7.4). Mouse cortical tissue was lysed in lysis buffer

(50 mM Tris-HCl, 4 M urea, 1% [wt/vol] SDS, 1 μL/mL protease inhibitor cocktail [Sigma-Aldrich], pH 7.4). All lysates were briefly sonicated 2 × 5 seconds and centrifuged at 1000*g* for 10 minutes at 4 °C. The resultant supernatant was used for detection of proteins using Western blotting as described in the following.

2.8. Western blotting

Total protein content was determined using the DC Protein Assay Kit (BioRad, Hercules, CA), and the samples were diluted in loading buffer (final concentration: 60 mM Tris, 10% [vol/vol] glycerol, 5% [vol/vol] mercaptoethanol, 2% [wt/vol] SDS, 0.025% [wt/vol] bromophenol blue, pH 6.8), incubated for 5 minutes at 95 °C, and submitted to gel electrophoresis using AnykD gels (BioRad). After blotting onto polyvinylidene difluoride membranes (BioRad), the membranes were washed in Tris-buffered saline with 0.1% Tween 20 (TBS-T), and blocked in TBS containing 5% (wt/vol) dry milk powder. Blots were incubated in primary antisera against PSCA (1:1,000, #NB100-91938, Novus Biologicals, Cambridge, UK), Lypd6 (1:1,000, #ARP53451_P050, Aviva Systems Biology, San Diego, CA), β2 nAChR subunit (1:1,000, kindly provided by Dr Cecilia Gotti, previously characterized in Thomsen et al., 2014), GluR2 (1:200, #MABN71, Millipore), α4 nAChR subunit (1:100, sc-5591, Santa Cruz Biotechnology), α7 nAChR subunit (1:1000 #ab23832, Abcam, Cambridge, UK), or actin (1:10,000, #A5060, Sigma-Aldrich) overnight at 4 °C. Subsequently, blots were washed in TBS-T 3 × 10 minutes followed by 1 hour incubation at room temperature with horseradish peroxidase-conjugated secondary antibodies (1:2000, Dako, Glostrup, Denmark). After thorough washing in TBS-T, blots were visualized by enhanced chemiluminescence reagents (Western Lightning ECL Pro, Perkin Elmer, Waltham, MA) using a Chemidoc XRS system with Quantity One software (BioRad). Data were quantified by measuring mean optical densities of bands and subtracting an adjacent background measurement.

Validation of PSCA antibody (1:1,000, Novus Biologicals) was done with co-incubation with the PSCA peptide, which had been used as immunogen (1:100, # NB100-91938PEP, Novus Biologicals). To determine the amount of endogenous PSCA in cortex, cortical samples from mouse and human cortex were loaded along with samples with known concentrations of the recombinant PSCA (0.5, 1, 2, 4, 8, and 16 ng). A standard curve was created based on the PSCA samples and used to determine the amount of PSCA in the cortical samples.

2.9. Immunofluorescence labeling

Age-matched 3×Tg-AD and WT mice (n = 8) were perfused transcardially with phosphate-buffered 4% paraformaldehyde after being euthanized with CO_2. Dissected brains were immersed in fixative overnight, dehydrated, and cut with a freezing microtome resulting in free-floating, 30-μm-thick coronal sections. Selected sections containing the frontal cortex or the hippocampal formation were used for phospho-tau and Aβ-immunolabeling according to an earlier protocol with minor modifications (Härtig et al., 2014). Tissues were incubated with a mixture of biotinylated mouse-anti-$Aβ_{17–24}$ (4G8; Covance, Emeryville, CA; 1:400 in TBS with 5% normal donkey serum) and rabbit-anti-phospho-tau205 (Invitrogen, Karlsruhe, Germany; 1:300) overnight. Subsequently, the sections were rinsed with TBS and incubated for 1 hour in a mixture of carbocyanine 2 (Cy2)-conjugated streptavidin and Cy3-tagged donkey anti-rabbit IgG (both from Dianova, Hamburg, Germany; 20 μg/mL TBS containing 2% bovine serum albumin). After washing with TBS, the sections were treated with Sudan Black B for 10 minutes (Schnell et al., 1999) and mounted onto glass slides. For data illustration, images were taken from selected sections using a 510 Meta confocal laser-scanning microscope (Zeiss, Jena, Germany) and processed with CorelDraw and/or Photo-Paint version 12.0 (Corel Corp, Ottawa, Canada).

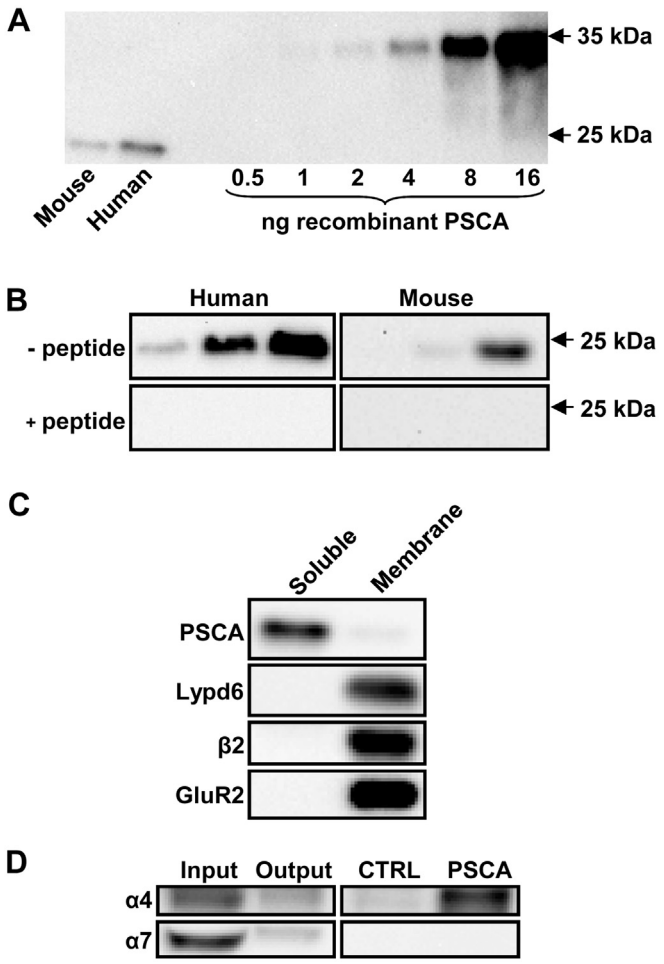

Fig. 1. Prostate stem cell antigen (PSCA) is soluble and co-purifies with the α4 nAChR subunit in human cortex. (A) The antiserum directed against PSCA recognizes the human recombinant GST-tagged PSCA protein (total molecular weight 34.2 kDa) from 1 to 16 ng/well at the expected band size. Endogenous PSCA from mouse and human cortical tissue (8 μg total protein/well) is detected at approximately 24 kDa, and the amount in the cortical samples was compared with the known concentrations of recombinant PSCA protein. (B) Images of Western blot showing PSCA protein levels in cortical tissue from human (protein concentration 4, 8, and 12 μg/well) and mouse (8, 15, and 30 μg/well) in the absence (−peptide) and the presence of PSCA peptide (+peptide). (C) Representative images of Western blots showing PSCA and Lypd6 protein levels in soluble and membrane fractions of human temporal cortical tissue. The membrane receptor proteins β2 nAChR and GluR2 are used as control. (D) Magnetic beads covalently coupled with PSCA recombinant protein were incubated with cortical homogenates from human temporal cortex followed by detection of nAChR subunits by Western blot. Homogenates before (input) and after affinity purification (output) as well as the negative control (CTRL) were loaded.

2.10. Statistical analyses

Data from PC12 cells were analyzed using one-way analysis of variance (ANOVA) with Dunnett multiple comparisons test. Correlation of age, postmortem delay, and pH with protein levels in human subjects was done using Pearson correlation analysis. Two-way ANOVA was applied to analyze effects of genotype and age in 3×Tg-AD mice. Unpaired multiple *t* tests using the Holm-Sidak method was used to compare groups. The statistical calculations were performed using GraphPad Prism version 6 for Windows (GraphPad Software, San Diego, CA). Data are presented as mean ±

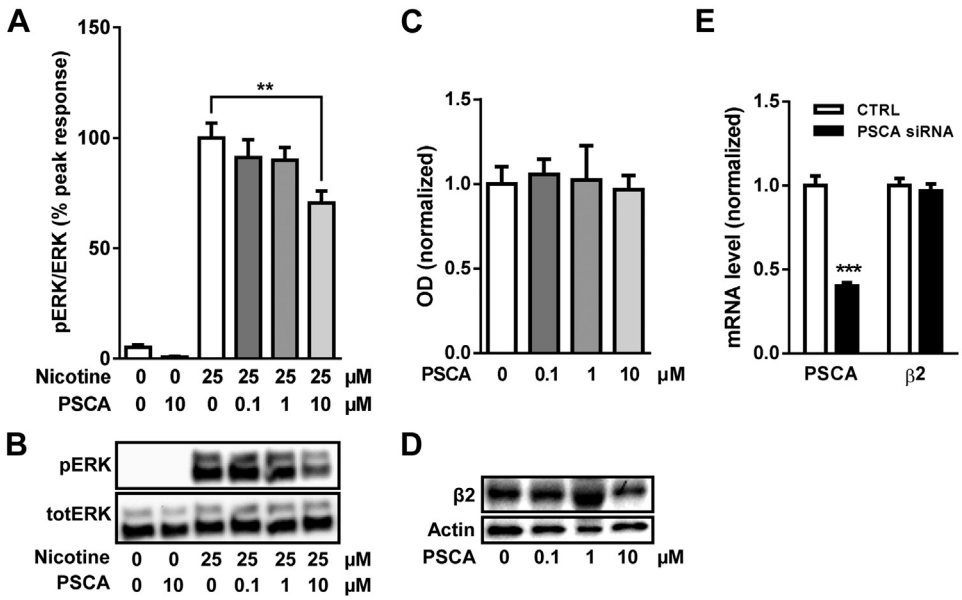

Fig. 2. Prostate stem cell antigen (PSCA) inhibits nicotine-induced ERK phosphorylation. (A) Preincubation with 10 µM recombinant human PSCA reduces nicotine-induced ERK phosphorylation in PC12 cells. Values are presented as the ratio between phosphorylated and total ERK protein and normalized to the 25 µM nicotine group. (B) Representative images of Western blots. (C) Protein levels of the β2 nAChR subunit are unchanged after 24 hours stimulation with PSCA in PC12 cells. (D) Representative images of Western blots. Data are normalized to actin levels, and the vehicle group is set to 1. (E) Silencing PSCA messenger RNA (mRNA) expression in PC12 cells with PSCA small interfering RNA (siRNA) has no effect on β2 nAChR mRNA levels. Data are normalized to GAPDH levels, and the control (CTRL) group is set to 1. $^{**}p < 0.01$ indicates statistical difference in a one-way analysis of variance with Dunnett multiple comparisons test (n = 4–6). Vehicles are not included in the statistical test in A. $^{***}p < 0.001$ indicates statistical difference in an unpaired *t* test.

standard error of the mean, and $p < 0.05$ was considered as statistically significant.

3. Results

3.1. PSCA is a soluble protein that binds to α4 nAChR subunits in the human cortex

The PSCA antiserum recognized recombinant human PSCA protein in the concentration range of 1–16 ng/well at molecular weight band of approximately 34 kDa (Fig. 1A). Recombinant PSCA protein consisted of 75 amino acids (immunogen sequence positions 21–95) with a calculated molecular weight of 8.2 kDa. However, this protein was GST-tagged (approximately 26 kDa) resulting in a total molecular weight of approximately 34 kDa, which correlated with the molecular weight of the identified protein (Fig. 1A). A band at a molecular weight of approximately 24 kDa was detected by Western blotting in extracts from both human frontal cortex (Fig. 1A), human temporal cortex (Fig. 1B), and mouse frontal cortex (Fig. 1A and B). To estimate protein levels of PSCA in cortical tissue, the intensity of PSCA staining in cortical samples was compared with that of recombinant PSCA with known concentrations (Fig. 1A). Based on the standard curve, cortical tissue was estimated to contain 0.3 and 0.5 ng/µg total protein for mouse and human cortex, respectively. Co-incubation of the diluted PSCA antiserum with the immunogen peptide prevented detection of bands in both human and mouse cortical extracts (Fig. 1B).

Human temporal cortical tissue was fractionated into soluble and membrane fractions by ultracentrifugation, and the resulting fractions were subjected to Western blotting (Fig. 1C). PSCA was detectable only in the soluble fraction. On the contrary, Lypd6 was detected only in the membrane fraction. To validate the fractionation method, we show that the two receptor units, β2 nAChR and GluR2, were only present in the membrane fraction (Fig. 1C).

Affinity purification from human temporal cortical homogenates using magnetic beads coupled to recombinant human PSCA demonstrated that PSCA was able to isolate the α4 nAChR subunit (Fig. 1D). Affinity purification using uncoupled beads yielded no isolation of α4 protein. By contrast, PSCA did not isolate the α7 nAChR subunit.

3.2. PSCA regulates nicotine-induced ERK phosphorylation in PC12 cells

Nicotine induces phosphorylation of the MAP kinase ERK in PC12 cells (Fig. 2A). Recombinant human PSCA at 10 µM significantly inhibited nicotine-induced ERK phosphorylation by approximately 30% in PC12 cells ($p < 0.01$), whereas 0.1 and 1 µM had no significant effects. PSCA alone did not affect basal levels of ERK phosphorylation.

Stimulation of PC12 cells with PSCA (0.1, 1, and 10 µM) for 24 hours did not alter β2 protein levels (Fig. 2C). In addition, β2 mRNA levels in PC12 cells were unchanged, when silencing PSCA levels using PSCA siRNA (Fig. 2E). The expression of PSCA was reduced to approximately 40% by PSCA siRNA, when compared with the expression in the presence of the negative control siRNA.

3.3. PSCA levels are increased in frontal cortex of AD patients

PSCA, Lypd6, and β2 protein levels were determined in human postmortem cortical tissue from medial frontal gyrus using Western blotting (Fig. 3). The levels of PSCA were increased by approximately 70% in AD postmortem tissue compared with nondemented (non-AD) control subjects (1.71 ± 0.16, $p = 0.0025$), whereas Lypd6 levels were unchanged (0.99 ± 0.12, $p = 0.97$). Levels of the β2 nAChR subunit were significantly decreased in AD patients (0.66 ± 0.06, $p = 0.014$).

Although AD subjects were noted to be slightly younger and have slightly shorter postmortem delay than the non-AD control subjects (see Table 1), we found no correlation between any of these parameters or pH with protein levels of PSCA, Lypd6, and β2 nAChR within the non-AD or AD groups.

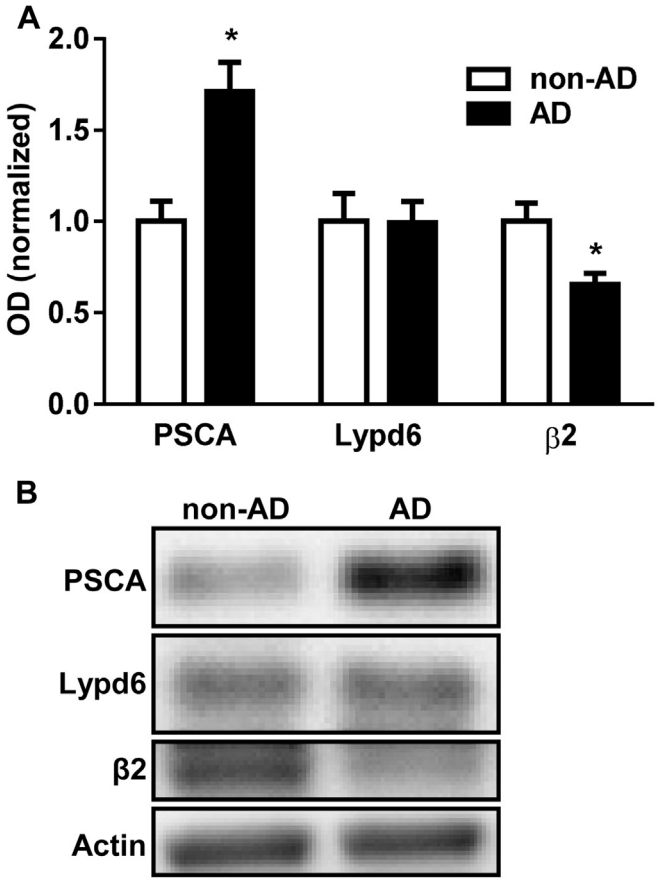

Fig. 3. Prostate stem cell antigen (PSCA) protein levels are increased in medial frontal gyrus in Alzheimer's disease (AD). (A) Quantification of PSCA and Lypd6 protein levels as well as the β2 nAChR subunit in homogenized postmortem tissue of medial frontal gyrus from AD patients and nondemented control subjects (non-AD). (B) Representative Western blot images of protein levels of non-AD and AD patients. Data are normalized to actin levels, and the non-AD control group is set to 1. $^{*}p < 0.05$ indicates statistical difference from non-AD control subjects in multiple *t* tests with Holm-Sidak multiple comparison test (n = 7–8).

3.4. PSCA levels are increased in frontal cortex of 3×Tg-AD mice

Protein levels of PSCA, Lypd6, and the β2 nAChR subunit were determined in frontal cortex and hippocampus from 6 to 19- to 21-month-old 3×Tg-AD mice and age-matched WT controls using Western blotting (Fig. 4). In frontal cortex using two-way ANOVA with age and genotype as independent variables, there was no interaction of the variables, but a significant main effect of genotype on PSCA and β2 nAChR levels in 3×Tg-AD mice in the two age groups ($p < 0.01$ and $p < 0.05$, respectively) compared with age-matched WT mice (Fig. 4A), whereas there was no significant main effect of age. Subsequent unpaired *t* tests revealed that the effect of genotype was driven primarily by the 6-month group, where 3×Tg-AD mice had significantly enhanced PSCA (1.46 ± 0.17, $p = 0.038$) and significant lower β2 nAChR levels (0.79 ± 0.04, $p < 0.01$) compared with age-matched WT animals. PSCA and β2 nAChR levels in 19- to 21-month-old 3×Tg-AD mice were not significantly altered in unpaired *t* tests ($p = 0.10$ and $p = 0.23$, respectively). In the hippocampus (Fig. 4A), there were no significant main effects on PSCA and β2 nAChR levels of genotype ($p = 0.05$ and $p = 0.06$, respectively) or age ($p = 0.19$ and $p = 0.35$, respectively) in a two-way ANOVA. A two-way ANOVA did not reveal any main effect of genotype or age in Lypd6 levels in frontal cortex ($p = 0.98$ and $p = 0.80$, respectively) or hippocampus ($p = 0.42$ and $p = 0.94$, respectively).

Immunofluorescence labeling was applied to sections of frontal cortex and hippocampus in 21-month-old 3×Tg-AD mice (Fig. 4C). Frontal cortex displayed extracellular amyloid plaques as well as intracellular deposits intermingled with phospho-tau-immunoreactivity. In hippocampus, tau hyperphosphorylation was present, and β-amyloidosis was more pronounced than in frontal cortex (Fig. 4C). In 6-month-old 3×Tg-AD mice, weak intracellular Aβ staining was displayed in both frontal cortex and hippocampus. The staining of tissues comprising frontal cortex and the hippocampus in age-matched WT mice revealed neither Aβ-immunoreactive senile plaques nor hyperphosphorylated tau (see Supplementary Fig. 1).

3.5. PSCA levels are unchanged in frontal cortex of Tg2576 mice

In frontal cortex of Tg2576 mice, there were no significant changes in the levels of PSCA, Lypd6, and β2 nAChR subunit (Fig. 5) compared with WT animals in unpaired *t* tests.

4. Discussion

Here, we show that the Lynx proteins PSCA and Lypd6 are present in the human brain and that PSCA forms stable complexes with the α4 nAChR subunit in the human temporal cortex and is able to decrease nicotine-induced ERK phosphorylation in PC12 cells. We further demonstrate that PSCA is increased in the frontal cortex of AD patients as well as in 3×Tg-AD mice. Because 3×Tg-AD display both age-dependent β-amyloidosis and tauopathy, this finding suggests that increased levels of PSCA are linked to the pathophysiology of AD.

PSCA was first identified as a protein that was upregulated in prostate cancer (Reiter et al., 1998). PSCA mRNA has previously been demonstrated in the central nervous system of adult mouse and chicken embryos (Hruska et al., 2009), and Lypd6 mRNA has been found in human and mouse brain tissue (Darvas et al., 2009; Zhang et al., 2010). We demonstrate that PSCA and Lypd6 proteins are present in the human cortex. Because these Lynx proteins have been associated with regulation of nAChR function in dissociated neurons from chicken and mouse (Darvas et al., 2009; Hruska et al., 2009), it is pertinent to study their function in the healthy and diseased human brain.

Lynx proteins can exist as either glycosylphosphatidylinositol (GPI)-anchored membrane proteins or soluble proteins (Adermann et al., 1999; Bamezai, 2004). PSCA mRNA contains a GPI anchor signaling site (Hruska et al., 2009; Reiter et al., 1998), and PSCA protein is both secreted and cell-associated in PSCA-transfected 293T cells (Reiter et al., 1998). We detected native PSCA in the human brain exclusively as a soluble protein. Lypd6 was found to be membrane-bound in the human cortex, which is in line with previous data on rat cortical tissue (Thomsen et al., 2013). Some GPI-anchored proteins have been shown to have both membrane bound and secreted forms, for example, CD59, another member of the Lynx superfamily (Fritz and Lowe, 1996; Meri et al., 1996). Soluble Lynx can diffuse to sites not available to the membrane-bound GPI-anchored proteins. This may have an impact on how Lynx proteins exert their function, for example, it was reported that transgenic mice expressing secreted or full-length Lynx1, respectively, show different effects in terms of motor learning (Miwa and Walz, 2012).

We demonstrate that PSCA and the α4 nAChR subunit form stable complexes in human cortex using affinity purification with recombinant PSCA. We have recently shown that Lypd6 binds to multiple nAChR subtypes in the human cortex (Thomsen et al., 2013), and Lynx1 and Lynx2 have been shown to co-immunoprecipitate with α7 and α4β2 nAChR subunits in

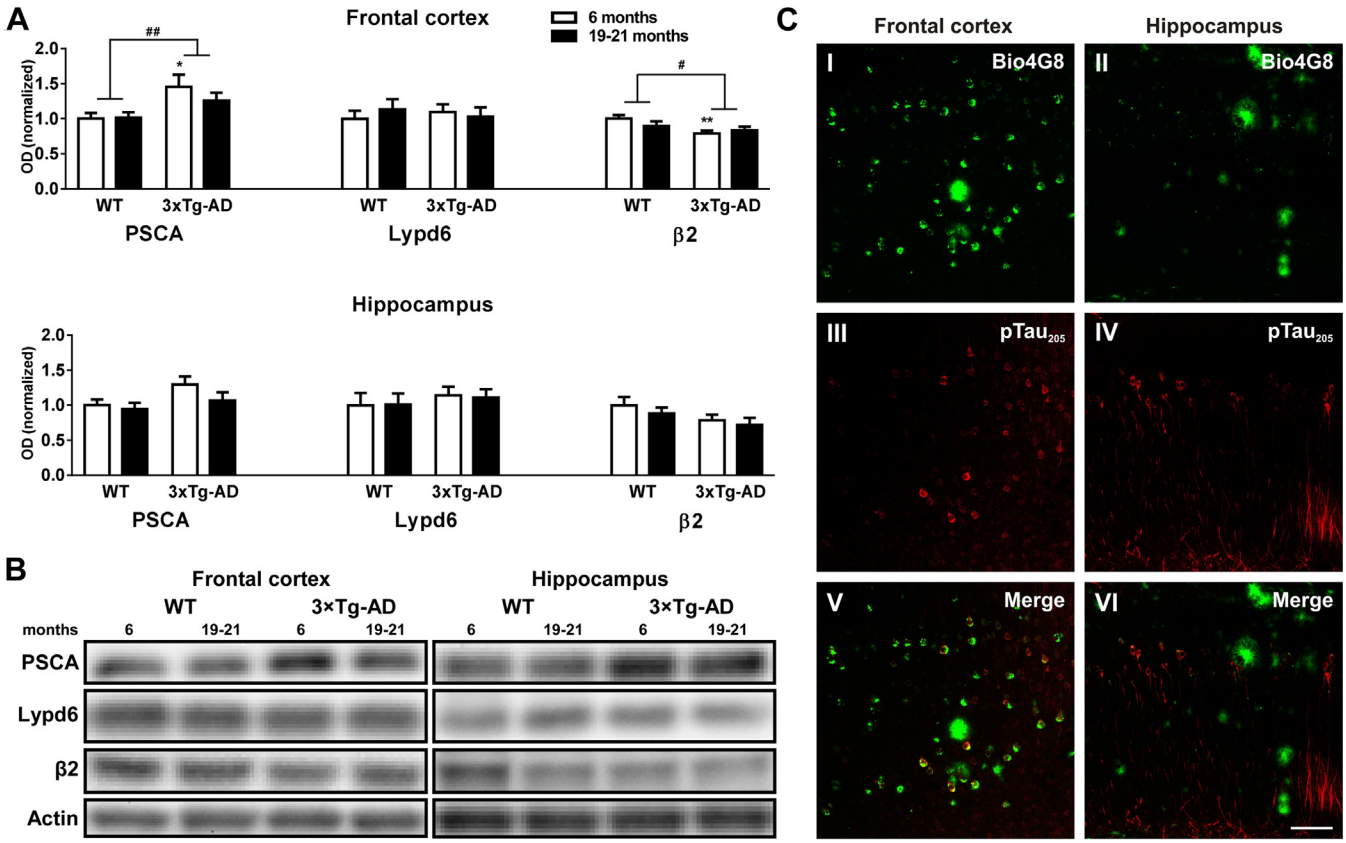

Fig. 4. Prostate stem cell antigen (PSCA) levels are increased in frontal cortex of 3×Tg-AD mice. (A) Frontal cortex and hippocampus were dissected from triple transgenic (3×Tg-AD) mice and age-matched wild-type (WT) animals, homogenized, and protein analysis was performed using Western blotting. Data are normalized to actin levels, and the 6-month-old WT group is set to 1 (n = 7–8 per group). $^{\#}p < 0.05$, $^{\#\#}p < 0.01$ indicates significant main effect of genotype in two-way analysis of variance, $^{*}p < 0.05$, $^{**}p < 0.01$ indicates statistical difference between 6-month-old 3×Tg-AD and age-matched WT mice in unpaired *t* tests. (B) Representative Western blot images of protein levels in frontal cortex and hippocampus. (C) Immunofluorescence labeling and confocal laser-scanning microscopy of neuropathologic alterations in the frontal cortex (I, III, V) and the hippocampal formation (II, IV, VI) from a 21-month-old 3×Tg-AD mouse. Biotinylated 4G8 visualized by green fluorescent Cy2-streptavidin reveals both extracellular plaques and intracellular deposits in the frontal cortex (I), whereas indirect immunolabeling with rabbit-anti-phospho-tau (Cy3, red) shows hyperphosphorylation in the same neocortical area (III). In the hippocampus, several 4G8-immunopositive plaques are detectable (II), and abnormally phosphorylated tau is found in numerous cells including pyramidal neurons (IV). Merged pictures (V, VI) indicate the allocation of the neuropathologic alterations. Scale bar = 75 μm. (For interpretation of the references to color in this figure, the reader is referred to the Web version of this article.)

heterologous expression systems (Ibanez-Tallon et al., 2002; Tekinay et al., 2009). These studies suggest that there may be an entire subfamily of Lynx proteins that bind to nAChRs in the brain.

It has previously been suggested that PSCA may be a negative modulator of α7 nAChRs in chicken ciliary ganglion neurons (Hruska et al., 2009). We did not detect co-purification of the α7 nAChR subunit using PSCA affinity purification on human cortical extracts. Possibly, the binding between PSCA and the α7 nAChR subunit is not strong enough to be detected in our assay. Alternatively, the binding of PSCA to nAChR subunits differs between species, as it has been shown for Lynx1. Human Lynx1 competes with binding of the α7 nAChR antagonist α-bungarotoxin to acetylcholine-binding proteins and *Torpedo* nAChRs with an IC_{50} of approximately 10 μM, suggesting that it binds to the orthosteric site, whereas it does not compete with α-bungarotoxin binding to human α7 nAChRs or with [^{3}H]-epibatidine binding to human α4β2 nAChRs (Lyukmanova et al., 2011).

To investigate the potential effect of PSCA on nAChR function, we determined the effect of PSCA on nicotine-induced phosphorylation of the MAP kinase ERK. Activation of the intracellular MAPK/ERK signaling pathway by phosphorylation plays a crucial role in the formation of long-term potentiation and memory in hippocampus (Adams and Sweatt, 2002). Nicotine has been suggested to induce ERK phosphorylation in PC12 cells through α3β4 (Nakayama et al., 2006) and to some extent α7 nAChRs (El Kouhen et al., 2009; Gubbins et al., 2010). We show that 10 μM PSCA inhibits nicotine-induced ERK phosphorylation in PC12 cells with no effect on basal levels of ERK phosphorylation indicating that the inhibitory effect is unique to nAChR signaling. The concentration of PSCA corresponds to studies with Lynx1, which showed that 10 μM Lynx1 was able to inhibit ACh-induced currents in *Xenopus* oocytes expressing human α7, α4β2, and α3β2, whereas 1 μM Lynx1 was not (Lyukmanova et al., 2011). These data suggest that PSCA could bind to α7 nAChRs, although we were not able to detect it and possibly also to α3β4 nAChRs. Thus, PSCA may function as a modulator of nAChR function in the brain. That PSCA affects a signaling pathway known to be important for neural plasticity and memory, makes it an interesting target for future studies.

With the demonstration that PSCA and Lypd6 bind to and modulate nAChRs, it is pertinent to investigate the function of PSCA and Lypd6 in diseases, where nAChRs are dysregulated, such as AD. nAChRs are important for normal cognitive function, and some studies suggest a correlation between nAChR levels and cognitive deficits in AD (Nordberg et al., 1995; Okada et al., 2013; Perry et al., 2000). Recent studies suggest that Lynx1, Lynx2, and Lypd6 are involved in cognitive processes in rodents (Darvas et al., 2009;

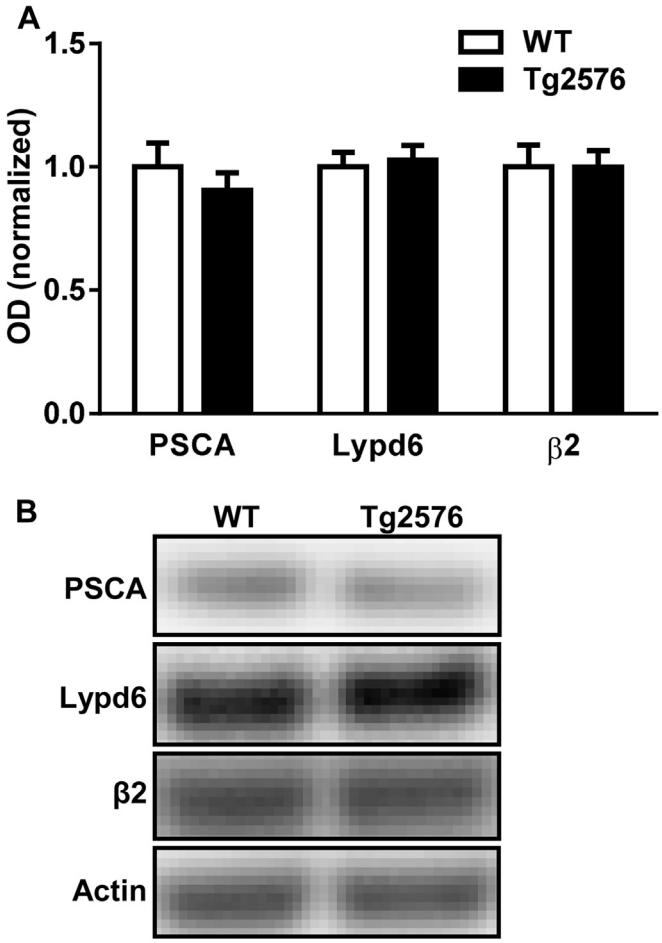

Fig. 5. No changes in prostate stem cell antigen (PSCA) levels in frontal cortex of Tg2576 mice over-expressing β-amyloid. (A) Frontal cortical extracts dissected from 15-month-old male Tg2576 mice and age-matched wild-type (WT) controls were homogenized and followed by Western blotting for protein analysis. (B) Representative images of Western blots. Data are normalized to actin levels, and the WT group is set to 1 (n = 12–14 per group).

Miwa et al., 2006; Tekinay et al., 2009). However, whether cognitive disturbances seen in AD patients are caused by alterations in Lynx protein function and/or expression is unknown. Here, we show that the level of PSCA protein is increased in the frontal cortex of AD patients. Combined with our finding that PSCA binds to the α4 nAChR subunit and inhibits nAChR signaling, increased PSCA levels may decrease nAChR function in patients with AD. If PSCA is able to inhibit the function of α4β2 nAChRs similar to Lynx1 (Ibanez-Tallon et al., 2002), the dysfunction of the receptor may have negative impact on the cognitive performance of the AD patients especially on attention and executive function as has been described previously (Okada et al., 2013; Sarter et al., 2009). Lypd6 also binds to nAChRs in human cortex (Thomsen et al., 2013) and is suggested as a nAChR neuromodulator (Darvas et al., 2009; Thomsen et al., 2013), but we found no change in Lypd6 levels in AD. Another member of the Lynx superfamily CD59, which is involved in the innate immune system as inhibitor of the membrane attack complex (Davies et al., 1989), has been demonstrated to be down-regulated in AD (Yang et al., 2000). Alterations of both PSCA and CD59 in AD suggest that some Lynx proteins may be involved in the disease.

Therefore, we asked whether altered protein levels of PSCA are related to AD pathophysiology. We found increased PSCA protein levels in frontal cortex of 3×Tg-AD animals that overexpress Aβ and hyperphosphorylated tau, the hallmarks of AD pathology. This indicates that the combination of increased Aβ and hyperphosphorylated tau are sufficient to increase in PSCA protein and suggest that the increase in PSCA levels found in AD patients is linked to the pathophysiology of AD. PSCA levels were not altered in transgenic Tg2576 mice that overexpress the Aβ precursor APP and display increased Aβ levels (Hsiao et al., 1996). This suggests that increased Aβ levels are not sufficient to increase PSCA levels. However, it should be noted that APP transgene animal models, such as the Tg2576 mice, show a slower accumulation of Aβ plaques than the 3×Tg-AD mouse model (reviewed by Lee and Han, 2013), so the lack of effect in the model may reflect lower Aβ load. Furthermore, the progression and dynamics of AD pathology in 3×Tg-AD mice are rather similar to the pathogenesis in AD patients (Bilkei-Gorzo, 2014), where Aβ deposition begins first in cortical regions and later in hippocampus, whereas tau pathology initiates in limbic regions and then progresses to cortical regions (Oddo et al., 2003). Here, we demonstrate by immunofluorescence labeling of frontal cortex and hippocampus from 3×Tg-AD mice a pronounced AD-like pathology in 21-month-old animals, whereas 6-month-old animals are displaying intracellular Aβ immunoreactivity but are devoid of amyloid plaques or apparent tau pathology suggesting that the changes in PSCA are not driven by tau pathology alone. Intracellular immunoreactivity in the young animals could indicate cross-reactivity of the applied antibody 4G8 for APP as previously reported (Härtig et al., 2014; Winton et al., 2011). Because we show the strongest increase of PSCA levels in 6-month-old 3×Tg-AD mice, our data indicate that the regulation of PSCA levels occurs before Aβ plaque and neurofibrillary tangle formation, although this does not preclude an involvement of soluble Aβ forms in the regulation of PSCA levels. Because both Aβ and PSCA can bind to nAChRs, they may share the same nAChR-binding site. However, it has been proposed that binding of Aβ to different nAChR subtypes may involve different binding sites (Nery et al., 2013). Our data suggest that increase in PSCA may be a precursor to stages of plaque overload in the 3×Tg-AD mice, suggesting that the regulation of PSCA is an early event in the progression of AD pathology in this animal model.

Because PSCA binds to α4-containing nAChRs, the altered expression of nAChRs in AD could be a consequence of changes in PSCA or vice versa. We demonstrate that β2 nAChR levels are decreased in frontal cortex of AD patients and 3×Tg-AD mice, whereas they are not changed in Tg2576 animals and in the hippocampus of 3×Tg-AD mice, where we do not observe increased PSCA levels. However, when we investigated PSCA in PC12 cells, we did not find alterations of β2 expression at both mRNA and protein levels in the absence or presence of PSCA, respectively. It should be noted that these findings do not exclude that PSCA is able to change β2 expression in native tissue and/or under pathologic conditions. The finding that PSCA and β2 nAChR levels are not increased in hippocampus of the 3×Tg-AD mice could be because of different origin of the cholinergic input to frontal cortex and hippocampus, respectively. Pathologic changes in the nuclei of the basal forebrain may therefore influence the expression of PSCA and β2 nAChRs more prominently in the frontal cortex. Regulation of frontal cortical α4β2 nAChR expression in early-stage AD has previously been demonstrated in humans, for example, a significant reduction in α4β2 binding in vivo in frontal cortex of patients with mild cognitive impairment (Kendziorra et al., 2011) and early-stage AD, which correlated with high [^{11}C]-PiB uptake as a measure of amyloid deposits (Okada et al., 2013). In addition, [^{3}H]-nicotine autoradiography in postmortem frontal cortical tissue showed a significantly reduced binding in AD patients (Marutle et al., 2013). Given our data that PSCA binds to the α4 nAChR subunit, and the fact that α4 and β2 nAChR subunits form heteromers, increased PSCA expression may influence α4β2 nAChR levels in AD.

In summary, our findings have identified PSCA as a nAChR-binding protein in the human brain. PSCA inhibits nAChR signaling in vitro and is dysregulated in the frontal cortex of AD patients as well as animal models with AD pathology. Therefore, PSCA-nAChR interactions may affect cognitive function particularly in the context of AD pathology.

Disclosure statement

The authors have no conflicts of interest to disclose.

Acknowledgements

The authors would like to thank Dr Cecilia Gotti (University of Milan, Milan, Italy) for kindly providing the β2 antiserum, Drs Frank M. LaFerla and Salvatore Oddo (University of California, Irvine, CA) for breeding pairs of 3×Tg-AD and WT mice, Dr Carsten Hobohm (University of Leipzig, Germany) for funding the breeding of mice, Jesper F. Bastlund (H. Lundbeck A/S, Valby, Denmark) for providing tissue from Tg2576 and WT mice, and Dr Jens Grosche (Effigos, Leipzig) and Maria Nørnberg (NRU, Copenhagen, Denmark) for technical assistance. This work was supported by the Danish Strategic Research Council (COGNITO) and the Lundbeck Foundation.

Appendix A. Supplementary data

Supplementary data associated with this article can be found, in the online version, at http://dx.doi.org/10.1016/j.neurobiolaging.2015.01.001.

References

Adams, J.P., Sweatt, J.D., 2002. Molecular psychology: roles for the ERK MAP kinase cascade in memory. Annu. Rev. Pharmacol. Toxicol. 42, 135–163.
Adermann, K., Wattler, F., Wattler, S., Heine, G., Meyer, M., Forssmann, W.G., Nehls, M., 1999. Structural and phylogenetic characterization of human SLURP-1, the first secreted mammalian member of the Ly-6/uPAR protein superfamily. Protein Sci. 8, 810–819.
Auld, D.S., Kornecook, T.J., Bastianetto, S., Quirion, R., 2002. Alzheimer's disease and the basal forebrain cholinergic system: relations to beta-amyloid peptides, cognition, and treatment strategies. Prog. Neurobiol. 68, 209–245.
Bamezai, A., 2004. Mouse Ly-6 proteins and their extended family: markers of cell differentiation and regulators of cell signaling. Arch. Immunol. Ther. Exp. (Warsz) 52, 255–266.
Bilkei-Gorzo, A., 2014. Genetic mouse models of brain ageing and Alzheimer's disease. Pharmacol. Ther. 142, 244–257.
Braak, H., Braak, E., 1991. Neuropathological stageing of Alzheimer-related changes. Acta Neuropathol. 82, 239–259.
Braak, H., Braak, E., 1995. Staging of Alzheimer's disease-related neurofibrillary changes. Neurobiol. Aging 16, 271–278 discussion 278–284.
Buckingham, S.D., Jones, A.K., Brown, L.A., Sattelle, D.B., 2009. Nicotinic acetylcholine receptor signalling: roles in Alzheimer's disease and amyloid neuroprotection. Pharmacol. Rev. 61, 39–61.
Carson, R., Craig, D., Hart, D., Todd, S., McGuinness, B., Johnston, J.A., O'Neill, F.A., Ritchie, C.W., Passmore, A.P., 2008a. Genetic variation in the alpha 7 nicotinic acetylcholine receptor is associated with delusional symptoms in Alzheimer's disease. Neuromolecular Med. 10, 377–384.
Carson, R., Craig, D., McGuinness, B., Johnston, J.A., O'Neill, F.A., Passmore, A.P., Ritchie, C.W., 2008b. Alpha7 nicotinic acetylcholine receptor gene and reduced risk of Alzheimer's disease. J. Med. Genet. 45, 244–248.
Cook, L.J., Ho, L.W., Taylor, A.E., Brayne, C., Evans, J.G., Xuereb, J., Cairns, N.J., Pritchard, A., Lemmon, H., Mann, D., St Clair, D., Turic, D., Hollingworth, P., Moore, P.J., Jehu, L., Archer, N., Walter, S., Foy, C., Edmondson, A., Powell, J., Lovestone, S., Owen, M.J., Williams, J., Lendon, C., Rubinsztein, D.C., 2004. Candidate gene association studies of the alpha 4 (CHRNA4) and beta 2 (CHRNB2) neuronal nicotinic acetylcholine receptor subunit genes in Alzheimer's disease. Neurosci. Lett. 358, 142–146.
Court, J., Martin-Ruiz, C., Piggott, M., Spurden, D., Griffiths, M., Perry, E., 2001. Nicotinic receptor abnormalities in Alzheimer's disease. Biol. Psychiatry 49, 175–184.
Darvas, M., Morsch, M., Racz, I., Ahmadi, S., Swandulla, D., Zimmer, A., 2009. Modulation of the Ca2+ conductance of nicotinic acetylcholine receptors by Lypd6. Eur. Neuropsychopharmacol. 19, 670–681.
Davies, A., Simmons, D.L., Hale, G., Harrison, R.A., Tighe, H., Lachmann, P.J., Waldmann, H., 1989. CD59, an LY-6-like protein expressed in human lymphoid cells, regulates the action of the complement membrane attack complex on homologous cells. J. Exp. Med. 170, 637–654.
Davies, P., Feisullin, S., 1981. Postmortem stability of alpha-bungarotoxin binding sites in mouse and human brain. Brain Res. 216, 449–454.
Dorszewska, J., Florczak, J., Rozycka, A., Jaroszewska-Kolecka, J., Trzeciak, W.H., Kozubski, W., 2005. Polymorphisms of the CHRNA4 gene encoding the alpha4 subunit of nicotinic acetylcholine receptor as related to the oxidative DNA damage and the level of apoptotic proteins in lymphocytes of the patients with Alzheimer's disease. DNA Cell Biol. 24, 786–794.
Dubois, B., Feldman, H.H., Jacova, C., Dekosky, S.T., Barberger-Gateau, P., Cummings, J., Delacourte, A., Galasko, D., Gauthier, S., Jicha, G., Meguro, K., O'Brien, J., Pasquier, F., Robert, P., Rossor, M., Salloway, S., Stern, Y., Visser, P.J., Scheltens, P., 2007. Research criteria for the diagnosis of Alzheimer's disease: revising the NINCDS-ADRDA criteria. Lancet Neurol. 6, 734–746.
El Kouhen, R., Hu, M., Anderson, D.J., Li, J., Gopalakrishnan, M., 2009. Pharmacology of alpha7 nicotinic acetylcholine receptor mediated extracellular signal-regulated kinase signalling in PC12 cells. Br. J. Pharmacol. 156, 638–648.
Fritz, B.A., Lowe, A.W., 1996. Polarized GP2 secretion in MDCK cells via GPI targeting and apical membrane-restricted proteolysis. Am. J. Physiol. 270, 176–183.
Gubbins, E.J., Gopalakrishnan, M., Li, J., 2010. Alpha7 nAChR-mediated activation of MAP kinase pathways in PC12 cells. Brain Res. 1328, 1–11.
Härtig, W., Saul, A., Kacza, J., Grosche, J., Goldhammer, S., Michalski, D., Wirths, O., 2014. Immunolesion-induced loss of cholinergic projection neurones promotes beta-amyloidosis and tau hyperphosphorylation in the hippocampus of triple-transgenic mice. Neuropathol. Appl. Neurobiol. 40, 106–120.
Hellstrom-Lindahl, E., Mousavi, M., Zhang, X., Ravid, R., Nordberg, A., 1999. Regional distribution of nicotinic receptor subunit mRNAs in human brain: comparison between Alzheimer and normal brain. Brain Res. Mol. Brain Res. 66, 94–103.
Hruska, M., Keefe, J., Wert, D., Tekinay, A.B., Hulce, J.J., Ibanez-Tallon, I., Nishi, R., 2009. Prostate stem cell antigen is an endogenous lynx1-like prototoxin that antagonizes alpha7-containing nicotinic receptors and prevents programmed cell death of parasympathetic neurons. J. Neurosci. 29, 14847–14854.
Hsiao, K., Chapman, P., Nilsen, S., Eckman, C., Harigaya, Y., Younkin, S., Yang, F., Cole, G., 1996. Correlative memory deficits, Abeta elevation, and amyloid plaques in transgenic mice. Science 274, 99–102.
Ibanez-Tallon, I., Miwa, J.M., Wang, H.L., Adams, N.C., Crabtree, G.W., Sine, S.M., Heintz, N., 2002. Novel modulation of neuronal nicotinic acetylcholine receptors by association with the endogenous prototoxin lynx1. Neuron 33, 893–903.
Jurgensen, S., Ferreira, S.T., 2010. Nicotinic receptors, amyloid-beta, and synaptic failure in Alzheimer's disease. J. Mol. Neurosci. 40, 221–229.
Kawamata, J., Shimohama, S., 2002. Association of novel and established polymorphisms in neuronal nicotinic acetylcholine receptors with sporadic Alzheimer's disease. J. Alzheimers Dis. 4, 71–76.
Kendziorra, K., Wolf, H., Meyer, P.M., Barthel, H., Hesse, S., Becker, G.A., Luthardt, J., Schildan, A., Patt, M., Sorger, D., Seese, A., Gertz, H.J., Sabri, O., 2011. Decreased cerebral alpha4beta2* nicotinic acetylcholine receptor availability in patients with mild cognitive impairment and Alzheimer's disease assessed with positron emission tomography. Eur. J. Nucl. Med. Mol. Imaging 38, 515–525.
Laumet, G., Chouraki, V., Grenier-Boley, B., Legry, V., Heath, S., Zelenika, D., Fievet, N., Hannequin, D., Delepine, M., Pasquier, F., Hanon, O., Brice, A., Epelbaum, J., Berr, C., Dartigues, J.F., Tzourio, C., Campion, D., Lathrop, M., Bertram, L., Amouyel, P., Lambert, J.C., 2010. Systematic analysis of candidate genes for Alzheimer's disease in a French, genome-wide association study. J. Alzheimers Dis. 20, 1181–1188.
Laursen, B., Mork, A., Plath, N., Kristiansen, U., Bastlund, J.F., 2014. Impaired hippocampal acetylcholine release parallels spatial memory deficits in Tg2576 mice subjected to basal forebrain cholinergic degeneration. Brain Res. 1543, 253–262.
Lee, J.E., Han, P.L., 2013. An update of animal models of Alzheimer disease with a reevaluation of plaque depositions. Exp. Neurobiol. 22, 84–95.
Lyukmanova, E.N., Shenkarev, Z.O., Shulepko, M.A., Mineev, K.S., D'Hoedt, D., Kasheverov, I.E., Filkin, S.Y., Krivolapova, A.P., Janickova, H., Dolezal, V., Dolgikh, D.A., Arseniev, A.S., Bertrand, D., Tsetlin, V.I., Kirpichnikov, M.P., 2011. NMR structure and action on nicotinic acetylcholine receptors of water-soluble domain of human LYNX1. J. Biol. Chem. 286, 10618–10627.
Marutle, A., Gillberg, P.G., Bergfors, A., Yu, W., Ni, R., Nennesmo, I., Voytenko, L., Nordberg, A., 2013. (3)H-deprenyl and (3)H-PIB autoradiography show different laminar distributions of astroglia and fibrillar beta-amyloid in Alzheimer brain. J. Neuroinflammation 10, 90.
McKhann, G., Drachman, D., Folstein, M., Katzman, R., Price, D., Stadlan, E.M., 1984. Clinical diagnosis of Alzheimer's disease: report of the NINCDS-ADRDA Work Group under the auspices of Department of Health and Human Services Task Force on Alzheimer's Disease. Neurology 34, 939–944.
Meri, S., Lehto, T., Sutton, C.W., Tyynela, J., Baumann, M., 1996. Structural composition and functional characterization of soluble CD59: heterogeneity of the oligosaccharide and glycophosphoinositol (GPI) anchor revealed by laser-desorption mass spectrometric analysis. Biochem. J. 316 (Pt 3), 923–935.
Miwa, J.M., Freedman, R., Lester, H.A., 2011. Neural systems governed by nicotinic acetylcholine receptors: emerging hypotheses. Neuron 70, 20–33.
Miwa, J.M., Stevens, T.R., King, S.L., Caldarone, B.J., Ibanez-Tallon, I., Xiao, C., Fitzsimonds, R.M., Pavlides, C., Lester, H.A., Picciotto, M.R., Heintz, N., 2006. The prototoxin lynx1 acts on nicotinic acetylcholine receptors to balance neuronal activity and survival in vivo. Neuron 51, 587–600.
Miwa, J.M., Walz, A., 2012. Enhancement in motor learning through genetic manipulation of the Lynx1 gene. PLoS One 7, e43302.
Morishita, H., Miwa, J.M., Heintz, N., Hensch, T.K., 2010. Lynx1, a cholinergic brake, limits plasticity in adult visual cortex. Science 330, 1238–1240.

Nakayama, H., Shimoke, K., Isosaki, M., Satoh, H., Yoshizumi, M., Ikeuchi, T., 2006. Subtypes of neuronal nicotinic acetylcholine receptors involved in nicotine-induced phosphorylation of extracellular signal-regulated protein kinase in PC12h cells. Neurosci. Lett. 392, 101–104.

Nery, A.A., Magdesian, M.H., Trujillo, C.A., Sathler, L.B., Juliano, M.A., Juliano, L., Ulrich, H., Ferreira, S.T., 2013. Rescue of amyloid-beta-induced inhibition of nicotinic acetylcholine receptors by a peptide homologous to the nicotine binding domain of the alpha 7 subtype. PLoS One 8, e67194.

Nordberg, A., Lundqvist, H., Hartvig, P., Lilja, A., Langstrom, B., 1995. Kinetic analysis of regional (S)(-)11C-nicotine binding in normal and Alzheimer brains–in vivo assessment using positron emission tomography. Alzheimer Dis. Assoc. Disord. 9, 21–27.

Oddo, S., Caccamo, A., Shepherd, J.D., Murphy, M.P., Golde, T.E., Kayed, R., Metherate, R., Mattson, M.P., Akbari, Y., LaFerla, F.M., 2003. Triple-transgenic model of Alzheimer's disease with plaques and tangles: intracellular abeta and synaptic dysfunction. Neuron 39, 409–421.

Okada, H., Ouchi, Y., Ogawa, M., Futatsubashi, M., Saito, Y., Yoshikawa, E., Terada, T., Oboshi, Y., Tsukada, H., Ueki, T., Watanabe, M., Yamashita, T., Magata, Y., 2013. Alterations in alpha4beta2 nicotinic receptors in cognitive decline in Alzheimer's aetiopathology. Brain 136, 3004–3017.

Perry, E., Martin-Ruiz, C., Lee, M., Griffiths, M., Johnson, M., Piggott, M., Haroutunian, V., Buxbaum, J.D., Nasland, J., Davis, K., Gotti, C., Clementi, F., Tzartos, S., Cohen, O., Soreq, H., Jaros, E., Perry, R., Ballard, C., McKeith, I., Court, J., 2000. Nicotinic receptor subtypes in human brain ageing, Alzheimer and Lewy body diseases. Eur. J. Pharmacol. 393, 215–222.

Querfurth, H.W., LaFerla, F.M., 2010. Alzheimer's disease. N. Engl. J. Med. 362, 329–344.

Reiter, R.E., Gu, Z., Watabe, T., Thomas, G., Szigeti, K., Davis, E., Wahl, M., Nisitani, S., Yamashiro, J., Le Beau, M.M., Loda, M., Witte, O.N., 1998. Prostate stem cell antigen: a cell surface marker overexpressed in prostate cancer. Proc. Natl. Acad. Sci. U. S. A. 95, 1735–1740.

Sarter, M., Parikh, V., Howe, W.M., 2009. nAChR agonist-induced cognition enhancement: integration of cognitive and neuronal mechanisms. Biochem. Pharmacol. 78, 658–667.

Schmittgen, T.D., Livak, K.J., 2008. Analyzing real-time PCR data by the comparative C(T) method. Nat Protoc 3, 1101–1108.

Schnell, S.A., Staines, W.A., Wessendorf, M.W., 1999. Reduction of lipofuscin-like autofluorescence in fluorescently labeled tissue. J. Histochem. Cytochem. 47, 719–730.

Tekinay, A.B., Nong, Y., Miwa, J.M., Lieberam, I., Ibanez-Tallon, I., Greengard, P., Heintz, N., 2009. A role for LYNX2 in anxiety-related behavior. Proc. Natl. Acad. Sci. U. S. A. 106, 4477–4482.

Thomsen, M.S., Cinar, B., Jensen, M.M., Lyukmanova, E.N., Shulepko, M.A., Tsetlin, V., Klein, A.B., Mikkelsen, J.D., 2014. Expression of the Ly-6 family proteins Lynx1 and Ly6H in the rat brain is compartmentalized, cell-type specific, and developmentally regulated. Brain Struct. Funct. 219, 1923–1934.

Thomsen, M.S., Hansen, H.H., Timmerman, D.B., Mikkelsen, J.D., 2010. Cognitive improvement by activation of alpha7 nicotinic acetylcholine receptors: from animal models to human pathophysiology. Curr. Pharm. Des. 16, 323–343.

Thomsen, M.S., Jensen, M.M., Cinar, B., Wang, H., Gondré-Lewis, M.C., Klein, A.B., Mikkelsen, J.D., 2013. Perinatal Nicotine Administration Increases Hippocampal Lypd6 Levels in Adulthood Program No. 702.09. 2013 Neuroscience Meeting Planner. Society for Neuroscience, San Diego, CA. Online.

Thomsen, M.S., Mikkelsen, J.D., 2012. The alpha7 nicotinic acetylcholine receptor complex: one, two or multiple drug targets? Curr. Drug Targets 13, 707–720.

Tsetlin, V., 1999. Snake venom alpha-neurotoxins and other 'three-finger' proteins. Eur. J. Biochem. 264, 281–286.

Wang, H.Y., Lee, D.H., Davis, C.B., Shank, R.P., 2000. Amyloid peptide abeta(1-42) binds selectively and with picomolar affinity to alpha7 nicotinic acetylcholine receptors. J. Neurochem. 75, 1155–1161.

Winton, M.J., Lee, E.B., Sun, E., Wong, M.M., Leight, S., Zhang, B., Trojanowski, J.Q., Lee, V.M., 2011. Intraneuronal APP, not free abeta peptides in 3xTg-AD mice: implications for tau versus abeta-mediated Alzheimer neurodegeneration. J. Neurosci. 31, 7691–7699.

Yang, L.B., Li, R., Meri, S., Rogers, J., Shen, Y., 2000. Deficiency of complement defense protein CD59 may contribute to neurodegeneration in Alzheimer's disease. J. Neurosci. 20, 7505–7509.

Zhang, Y., Lang, Q., Li, J., Xie, F., Wan, B., Yu, L., 2010. Identification and characterization of human LYPD6, a new member of the Ly-6 superfamily. Mol. Biol. Rep. 37, 2055–2062.

Supplementary material

Figure S1 Age- and transgene-dependent double fluorescence labeling of AD-like alterations

Confocal laser-canning micrographs of immunoreactivities for 4G8 (Cy2, green) and tau-phospho-threonine 205 in the frontal cortex (I-IV) and in the subiculum as part of the hippocampal formation (V-VIII). Comparative analysis of staining patterns reveals predominant intracellular 4G8-immunoreactivity in the frontal cortex (I), but considerably stronger β-amyloidosis as well as tau hyperphosphorylation in the subiculum of a 21-month-old 3×Tg-AD mouse (V). In parallel, these signs are completely lacking in an age-matched wild-type animal (II, VI). The 6-month-old transgenic mouse displays weak intracellular 4G8-immunoreactivity also indicating overexpressed APP in both investigated regions, which are devoid of extracellular plaques and phospho-tau (III, VII). The age-matched animal expectedly displays no immunolabeling at all (IV, VIII). Scale bar = 75 µm.